ORIGINAL ARTICLE

Oxidation of carcinogenic benzo[a] pyrene by human and rat cytochrome P450 1A1 and its influencing by cytochrome b_5 – a comparative study

Radek Indra [1], Michaela Moserova [1], Miroslav Sulc [1], Eva Frei [2], Marie Stiborova [1]

1 Department of Biochemistry, Faculty of Science, Charles University, Prague, Czech Republic
2 Division of Preventive Oncology, National Center for Tumor Diseases, German Cancer Research Center (DKFZ), Heidelberg, Germany

Correspondence to: Prof. RNDr. Marie Stiborova, DSc.
Department of Biochemistry, Faculty of Science, Charles University
Albertov 2030, 128 40 Prague 2, Czech Republic
TEL: +420 221951285; FAX: +420 221951283; E-MAIL: stiborov@natur.cuni.cz

Submitted: 2013-06-21 Accepted: 2013-08-30 Published online: 2013-11-10

Key words: **benzo[a]pyrene; human carcinogen; metabolism; human and rat cytochrome P450 1A1; NADPH:cytochrome P450 reductase; cytochrome b_5**

Neuroendocrinol Lett 2013; **34**(Suppl.2):55–63 **PMID:** 24362093 NEL341013A08

Abstract

OBJECTIVES: Cytochrome P450 (CYP) 1A1 is the most important enzyme in both activation and detoxification of carcinogenic benzo[a]pyrene (BaP), in combination with microsomal epoxide hydrolase (mEH). To evaluate metabolism of BaP in human, identification of a suitable animal model that mimics the metabolic fate of BaP in human is of great importance. The aim of this work was to compare BaP oxidation by human CYP1A1 and CYP1A1 of one animal model, rat. Investigation of the effect of cytochrome b_5 on BaP oxidation by CYP1A1 was another target of this study.

METHODS: High performance liquid chromatography (HPLC) was employed for separation of BaP metabolites formed by enzymatic systems. Their structures were identified by mass- and NMR-spectrometry.

RESULTS: Human hepatic microsomes oxidized BaP to BaP-9,10-dihydrodiol, BaP-4,5-dihydrodiol, BaP-7,8-dihydrodiol, BaP-1,6-dione, BaP-3,6-dione and BaP-3-ol. The same metabolites were generated by rat liver microsomes, but BaP-9-ol and a metabolite Mx, the structure of which has not been identified as yet, were also formed in these microsomes. Human CYP1A1 expressed with NADPH:CYP reductase (POR) in Supersomes™ oxidized BaP to the same metabolites as microsomes, but BaP-4,5-dihydrodiol has not been detected. Rat recombinant CYP1A1 in this SupersomesTM system oxidized BaP to BaP-9,10-dihydrodiol, a metabolite Mx, BaP-4,5-dihydrodiol, BaP-7,8-dihydrodiol, BaP-1,6-dione, BaP-3,6-dione, BaP-9-ol and BaP-3-ol. Addition of cytochrome b_5 to rat and human recombinant CYP1A1 systems led to a more than 2-fold increase in BaP oxidation.

CONCLUSION: The results show similarities between human and rat CYP1A1 in BaP oxidation and demonstrate rats as a suitable model mimicking BaP oxidation in human.

Abbreviations:

BaP	- benzo[a]pyrene
BPDE	- BaP-7,8-dihydrodiol-9,10-epoxide
COSY	- correlation spectroscopy
CYP	- cytochrome P450
dG-N^2-BPDE	- 10-(deoxyguanosin-N^2-yl)-7,8,9-trihydroxy-7,8,9,10-tetrahydrobenzo-[a]pyrene
DMSO	- dimethyl sulfoxide
HMBC	- heteronuclear multiple-bond correlation spectroscopy
HPLC	- high performance liquid chromatography
HSQC	- heteronuclear single-quantum correlation spectroscopy
IARC	- International Agency for Research on Cancer
MALDI-TOF	- matrix-assisted laser desorption/ionization time-of-flight
mEH	- epoxide hydrolase
NADPH	- nicotinamidadeninedinucleotide phosphate (reduced)
NMR	- nuclear magnetic resonance
PAH	- polycyclic aromatic hydrocarbon
POR	- NADPH:cytochrome P450 reductase
r. t.	- retention time
UV	- ultraviolet

INTRODUCTION

Benzo[*a*]pyrene (BaP) is a polycyclic aromatic hydrocarbon (PAH) that has been classified as human carcinogen (Group 1) by the International Agency for Research on Cancer (IARC 2010). BaP requires metabolic activation catalyzed by cytochrome P450 (CYP) enzymes prior to reaction with DNA (Baird *et al.* 2005). Of the CYP enzymes, CYP1A1 is one of the most important CYP enzymes in metabolic activation of BaP to species forming DNA adducts (Baird *et al.* 2005; Hamouchene *et al.* 2011), in combination with microsomal epoxide hydrolase (mEH). First, CYP1A1 oxidizes BaP to an epoxide that is then converted to a dihydrodiol by mEH (*i.e.* BaP-7,8-dihydrodiol); then further bio-activation by CYP1A1 leads to the ultimately reactive species, BaP-7,8-dihydrodiol-9,10-epoxide (BPDE) that can react with DNA, forming adducts preferentially at guanine residues. The 10-(deoxyguanosin-N^2-yl)-7,8,9-trihydroxy-7,8,9,10-tetrahydrobenzo[*a*]pyrene (dG-N^2-BPDE) adduct is the major product of the reaction of BPDE with DNA *in vitro* and *in vivo* (Fig. 1) (Phillips & Venitt 2012).

BaP is, however, oxidized also to other metabolites such as the other dihydrodiols, BaP-diones and hydroxylated metabolites (Bauer *et al.* 1995; Chun *et al.* 1996; Kim *et al.* 1998; Jiang *et al.* 2007; Zhu *et al.* 2008). Even though most of these metabolites are the detoxification products, BaP-9-ol is a precursor of 9-hydroxy-BaP-4,5-epoxide, which can form another adduct with deoxyguanosine in DNA (Schoket *et al.* 1989; Nesnow *et al.* 1993; Fang *et al.* 2001). Therefore, regulation of CYP1A1-mediated oxidation of BaP leading to either metabolites forming BPDE, 9-hydroxy-BaP-4,5-epoxide or the BaP metabolites that are the detoxification products is of major importance.

In order to modulate CYP1A1-catalyzed oxidation of BaP in human, knowledge on such modulation of the CYP1A1 enzyme from suitable animal models that might mimic oxidation of BaP in human should be investigated and the results found applied to regulation of BaP oxidation by human CYP1A1. In fact, the first step of such investigations is to find which of the animal model CYP1A1 enzyme oxidizes BaP similarly to human CYP1A1. In addition, there are still not clearly explained how an electron transfer mediated by another component of the microsomal enzymatic system, NADPH:CYP reductase (POR), on CYP1A1 during BaP oxidation occurs, and whether microsomal cytochrome b_5 might influence this electron transfer. Namely, the oxygen needed for BaP oxidation is activated in the active center of CYPs by two electrons transferred from NADPH and/or NADH by means of POR and cytochrome b_5, respectively (Coon 1978). Whereas POR is an essential constituent of the electron transport chain towards CYP, the role of cytochrome b_5 is still quite enigmatic (Porter 2002; Stiborova *et al.* 2006, 2012b; Kotrbova *et al.* 2011; Koberova *et al.* 2013). Indeed, in the case of CYP1A1, the influencing of the POR-mediated electron transfer from NADPH to this CYP, which dictates a velocity of BaP oxidation, by cytochrome b_5 is not known.

Therefore, this study is focused on two major targets: (i) evaluation of a suitability of rat CYP1A1 enzymatic systems to mimic BaP oxidation by human CYP1A1, and (ii) investigation of the effect of cytochrome b_5 on oxidation of CYP1A1 by these CYP1A1 enzymes. Human and rat CYP1A1 expressed with POR in microsomes of insect cells (Supersomes^{TM}) and these enzyme

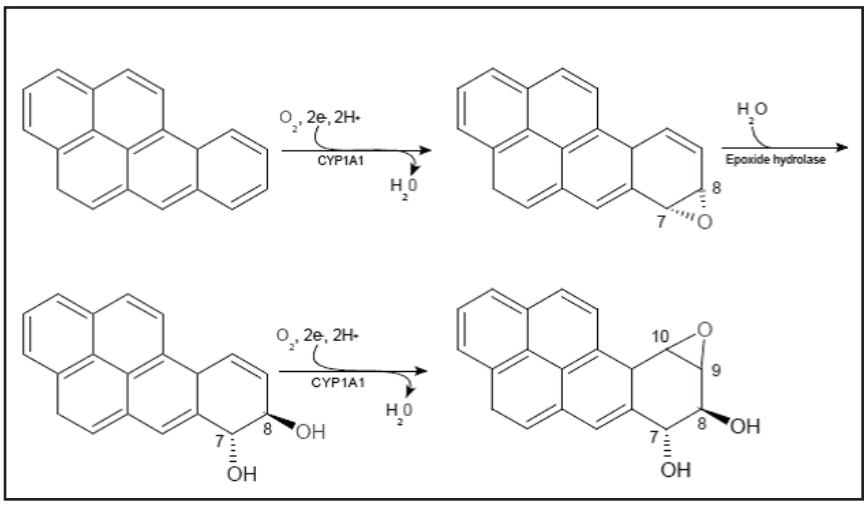

Fig. 1. Metabolic activation of benzo[a]pyrene

systems reconstituted with purified cytochrome b_5 were utilized for such a study. Human and rat hepatic microsomes containing a natural spectrum of CYPs and other enzymes located in a membrane of endoplasmic reticulum were used as positive controls.

MATERIAL AND METHODS

Chemicals and enzymes

Male human hepatic microsomes (pooled sample; cat. no. 452172), Supersomes™, microsomes isolated from insect cells transfected with a baculovirus construct containing cDNA of human or rat CYP1A1 and expressing POR were purchased from Gentest Corp. (Woburn, MI, USA). Microsomes from rat livers were isolated and characterized for CYP activities as described (Stiborova *et al.* 2011, 2012a). Cytochrome b_5 was isolated from rabbit liver microsomes by the procedure described by Roos (1996). This protein was used for the reconstitution experiments. There were no problems with CYP1A1 enzyme activity when this enzyme was reconstituted with other enzymes that were isolated from rabbit. As shown in our previous works, the enzymatic activity of rat (and/or human) CYP1A1 reconstituted with rabbit POR and cytochrome b_5 was essentially the same as that of the enzyme reconstituted with rat orthologs of these enzymes (Stiborova *et al.* 2002, 2006, 2012b; Kotrbova *et al.* 2009, 2011).

$NADP^+$, D-glucose-6-phosphate, D-glucose-6-phosphate dehydrogenase, dimethylsulfoxide (DMSO) were obtained from Sigma Chemical Co (St Louis, MO, USA). All these and other chemicals were reagent grade or better.

Preparation of rat microsomes and assays

The study was conducted in accordance with the Regulations for the Care and Use of Laboratory Animals (311/1997, Ministry of Agriculture, Czech Republic), which complies with the Declaration of Helsinki. Microsomes from livers of ten male untreated Wistar rats and those of ten male rats pre-treated with Sudan I were prepared by the procedure described previously (Stiborova *et al.* 2003, 2011; 2013). Protein concentrations in the microsomal fractions were assessed using the bicinchoninic acid protein assay with the bovine serum albumin as a standard (Weichelman *et al.* 1988). The concentration of CYP was estimated according to Omura and Sato (1964) based on absorption of the complex of reduced CYP with carbon monoxide. Hepatic microsomes of control (uninduced) rats and rats induced with Sudan I contained 0.6 and 1.8 nmol CYP/mg protein, respectively.

Microsomal and CYP1A1 enzymatic incubations

Rat hepatic microsomes of control (untreated) rats and rats treated with Sudan I, and human hepatic microsomes (pooled sample; cat. no. 452172), Supersomes™, microsomes isolated from insect cells transfected with a baculovirus construct containing cDNA of human or rat CYP1A1 and expressing POR were used to study BaP oxidation. Human and rat CYP1A1 expressed in these microsomes oxidized a CYP1A1-marker substrate, Sudan I (Stiborova *et al.* 2002; 2005). However, rat CYP1A1 exhibited ~2-fold lower efficiencies in Sudan I oxidation than human CYP1A1 (data not shown). Incubation mixtures used for studying BaP metabolism in human and rat hepatic microsomes or in Supersomes™ contained 100 mM potassium phosphate buffer (pH 7.4), NADPH-generating system (1 mM $NADP^+$, 10 mM D-glucose-6-phosphate, 1 U/ml D-glucose-6-phosphate dehydrogenase), 0.5 mg of microsomal protein or 100 nM human or rat CYP1A1 in Supersomes™ and 50 μM BaP (dissolved in 5 μl dimethyl sulfoxide, DMSO) in a final volume of 500 μl. In additional experiments, the Supersomal CYP1A1 systems were reconstituted with cytochrome b_5. The enzyme reconstitution utilizing the above systems (Supersomes™ containing human or rat CYP1A1 and expressing POR) with cytochrome b_5 were performed as described (Stiborova *et al.* 2002; 2006; 2012b). The reaction was initiated by adding 50 μl of the NADPH-generating system. Control incubations were carried out either without enzymatic system (microsomes or the CYP1A1 systems), or without NADPH-generating system, or without BaP. After incubation (37 °C, 20 min), 5 μl of 1 mM phenacetin (PA) in methanol was added as an internal standard. BaP metabolites were extracted twice with ethyl acetate (2×1 ml), solvent evaporated to dryness, residues dissolved in 25 μl methanol and BaP metabolites separated by HPLC.

HPLC analysis of BaP metabolites

HPLC analysis of BaP metabolites was performed on a Nucleosil® C18 reverse phase column, (250×4 mm, 5 μm; Macherey Nagel, Düren, Germany) using a Dionex system consisting of a pump P580, a UV/VIS Detector UVD 170S/340S, an ASI-100 Automated Sample Injector, a termobox COLUMN OVEN LCO 101 and an In-Line Mobile Phase Degasser Degasys DG-1210 Dionex controlled with Chromeleon™ 6.11 build 490 software. The conditions used for the chromatographic separation of BaP metabolites were as follows: 50% acetonitrile in water; (*v/v*), with a linear gradient to 85% acetonitrile in 35 min, then an isocratic elution with 85% acetonitrile for 5 min, a linear gradient from 85% acetonitrile to 50% acetonitrile in 5 min, followed by an isocratic elution of 50% acetonitrile for 5 min, flow rate of 0.6 ml/min. Application of samples (20 μl) at ambient temperature) and HPLC were carried out at 35 °C (Moserova *et al.* 2009). Detection was by UV at 254 nm. BaP metabolite peaks (Figure 2) were collected and analyzed by NMR and/or mass spectrometry. The peak areas at 254 nm were calculated relative to the peak area of the internal standard PA, and expressed as relative peak areas.

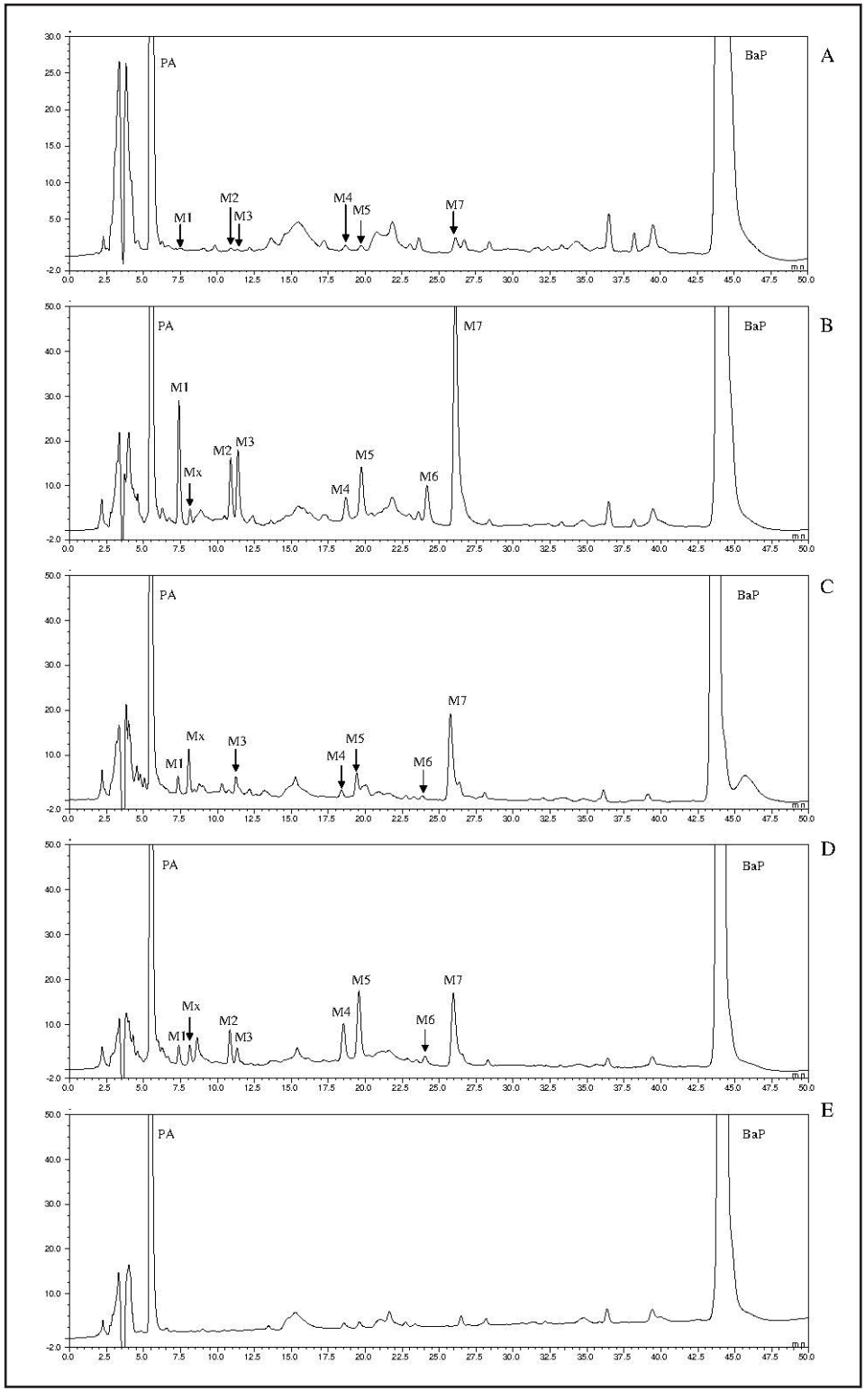

Fig. 2. High performance liquid chromatography (HPLC) of benzo[a]pyrene (BaP) metabolites formed by human hepatic microsomes (A), hepatic microsomes of rats treated with Sudan I (B), human recombinant cytochrome P450 (CYP) 1A1 (C), and rat recombinant CYP1A1 (D). (E) HPLC of control incubation mixture containing BaP and human recombinant CYP1A1, but without the NADPH (reduced nicotinamidadeninedinucleotide phosphate)-generating system. For BaP metabolites M1–M7 and Mx, see Fig. 3.

NMR spectrometry

NMR spectra (δ, ppm; *J*, Hz) of BaP and its metabolites M1, M4, M5 and M7 were measured on a Bruker Avance II-600 and/or Bruker Avance II-500 instruments equipped with a cryoprobe (600.1 or 500.0 MHz for ^{1}H and 150.9 or 125.7 MHz for ^{13}C) in hexadeuterated acetone and $CDCl_3$ and referenced to the solvent signals (δ 2.05 and 7.27, respectively). Due to the low amounts of metabolites it was not possible to acquire ^{13}C NMR spectra or perform heteronuclear correlation experiments.

1) BaP. ^{1}H NMR spectrum of BaP contains five isolated spin systems: one three-spin system of hydrogens H-1, H-2 and H-3, one four-spin system of H-7,

H-8, H-9 and H-10, one isolated spin of H-6 and two two-spin systems of H-4, H-5 and of H-11, H-12. The assignment of signals in the spectrum could be done with the help of homonuclear correlation spectroscopy (COSY) spectrum (data not shown), where strong cross-peaks corresponding to three-bond couplings were observed. However, the signals of the two two-spin systems (H-4,H-5 and H-11, H-12) could not be assigned with the use of COSY spectrum only and heteronuclear correlation spectra [heteronuclear multiple-bond correlation spectroscopy (HSQC) and heteronuclear multiple-bond correlation spectroscopy (HMBC)] had to be used.

2) M1. Two signals of the four-spin system of M1 were shifted upfield (to 4.5 and 5.7 ppm). These values are too low for the fully aromatic BaP skeleton. The structure of M1 was identified as *trans*-9,10-dihydro-BaP-9,10-diol (BaP-9,10-dihydrodiol) by comparison with previously reported NMR data of this compound (Platt & Oesch 1983). The *trans* arrangement of the two hydroxy groups was supported by the inspection of the vicinal coupling constant between hydrogen atoms H-9 and H-10. The torsion angle between these two hydrogen atoms calculated using the generalized Karplus type equation (Haasnoot *et al.* 1980) was predicted to be 48°. This value is very close to the torsion angle observed in the molecular model of the *trans*-derivative with the two hydroxyl groups in pseudo-axial positions. The molecular model of the *cis*-derivative predicts the torsion angle between the two hydrogen atoms to be close to −75°. We were not able to determine the absolute configuration on the new asymmetric centers (C-9 and C-10). It is possible that both enantiomers are present in metabolite M1.

3) M4 and M5. In the spectra of both compounds M4 and M5, we observed the four-spin system of H-7, H-8, H-9 and H-10 and three two-spin systems. Two substituents are therefore attached to the BaP skeleton: one in the position 6 and the second one in position 1 or 3. Furthermore, the unusually shielded H-2 proton at 6.7 ppm was characteristic of the α-proton (next to carbonyl) in phenalones (Prinzbach *et al.* 1967) suggesting that the structures of M4 and M5 could be BaP-1,6-dione and -3,6-dione, respectively. Because these two compounds were synthesized previously and their ^{1}H NMR spectra reported (Leeruff *et al.* 1986; Xu *et al.* 2009), spectra in $CDCl_3$ could be compared and the metabolites identified as BaP-1,6-dione (M4) and BaP-3,6-dione (M5).

4) M7. In the spectrum of M7, the three-spin system was replaced with a two-spin system suggesting that one substituent is attached to the position 1 or 3 of the BaP. The structure of M7 was confirmed to be BaP-3-ol by comparison of the chemical shifts and coupling constants with those reported previously (Xu *et al.* 2009).

5) M2, M3 and M6. Because the amounts of M2, M3 and M6 samples were insufficient for NMR spectroscopy, these metabolites were analyzed by mass spectrometry only as described below.

Mass spectrometry

Mass spectra of BaP and its metabolites M2, M3 and M6 were measured on a matrix-assisted laser desorption/ionisation reflectron time-of-flight (MALDI-TOF) mass spectrometer ultraFLEX III (Bruker-Daltonics, Bremen, Germany). Positive spectra were calibrated externally using the monoisotopic $[M+H]^+$ ion of MRFA peptide 524.26 m/z and CCA matrix peaks 190.05, 379.09 *m/z*. A 10 mg/ml solution of α-cyano-4-hydroxy-cinnamic acid or 2,5-dihydrobenzoic acid in 50% acetonitrile/0.3% acetic acid was used as MALDI matrix. A 0.5 µl of sample dissolved in acetonitrile was premixed with 0.5 µl of the matrix solution on the target and allowed to dry at ambient temperature. The MALDI-TOF positive spectra were collected in reflectron mode. Positive $[M^+]$ of BaP corresponded to this compound (*m/z* 252.1). The metabolites with retention times of 11.9 (M2) and 12.9 min (M3) gave a positive molecular ion at *m/z* 286.1 that is indicative of BaP-dihydrodiol metabolites. The metabolite eluted at 24.6 min (M6) gave a positive molecular ion at *m/z* 268.1, which is indicative of a hydroxylated BaP metabolite. These results are consistent with previous studies on the metabolism of BaP by human CYP1A1 (Bauer *et al.* 1995; Kim *et al.* 1998), in which these metabolites were identified as BaP-4,5-dihydrodiol (M2), BaP-7,8-dihydrodiol (M3), and BaP-9-ol (M6).

Statistical analyses

For statistical data analysis we used Student's *t*-test. All *p*-values are two-tailed and considered significant at the 0.05 level.

RESULTS

Oxidation of BaP by rat and human hepatic microsomes

Human and rat hepatic microsomes are natural systems containing all components of a monooxygenase system located in a membrane of endoplasmic reticulum, CYPs, POR, cytochrome b_5, and its reductase NADH:cytochrome b_5 reductase, in addition to mEH. Human hepatic microsomes oxidized BaP to six metabolites that were separated by HPLC (Figure 2A). These BaP metabolites and those formed by other enzyme systems used in this work were collected and subsequently characterized by NMR and/or mass spectrometry. The BaP metabolites formed by human hepatic microsomes were identified to be BaP-9,10-dihydrodiol (M1), BaP-4,5-dihydrodiol (M2), BaP-7,8-dihydrodiol (M3), BaP-1,6-dione (M4), BaP-3,6-dione (M5) and BaP-3-ol (M7) (see Figures 2A and 3), all corresponding to the metabolites that were formed by CYP1A1 in combination with mEH in other studies (Bauer *et al.* 1995; Kim *et al.* 1998; Baird *et al.* 2005).

Rat liver microsomes, in which CYP1A was induced by Sudan I, generated beside all these metabolites also BaP-9-ol (M6) and a metabolite Mx, the structure of which has not been identified as yet (Figures 2B and 3).

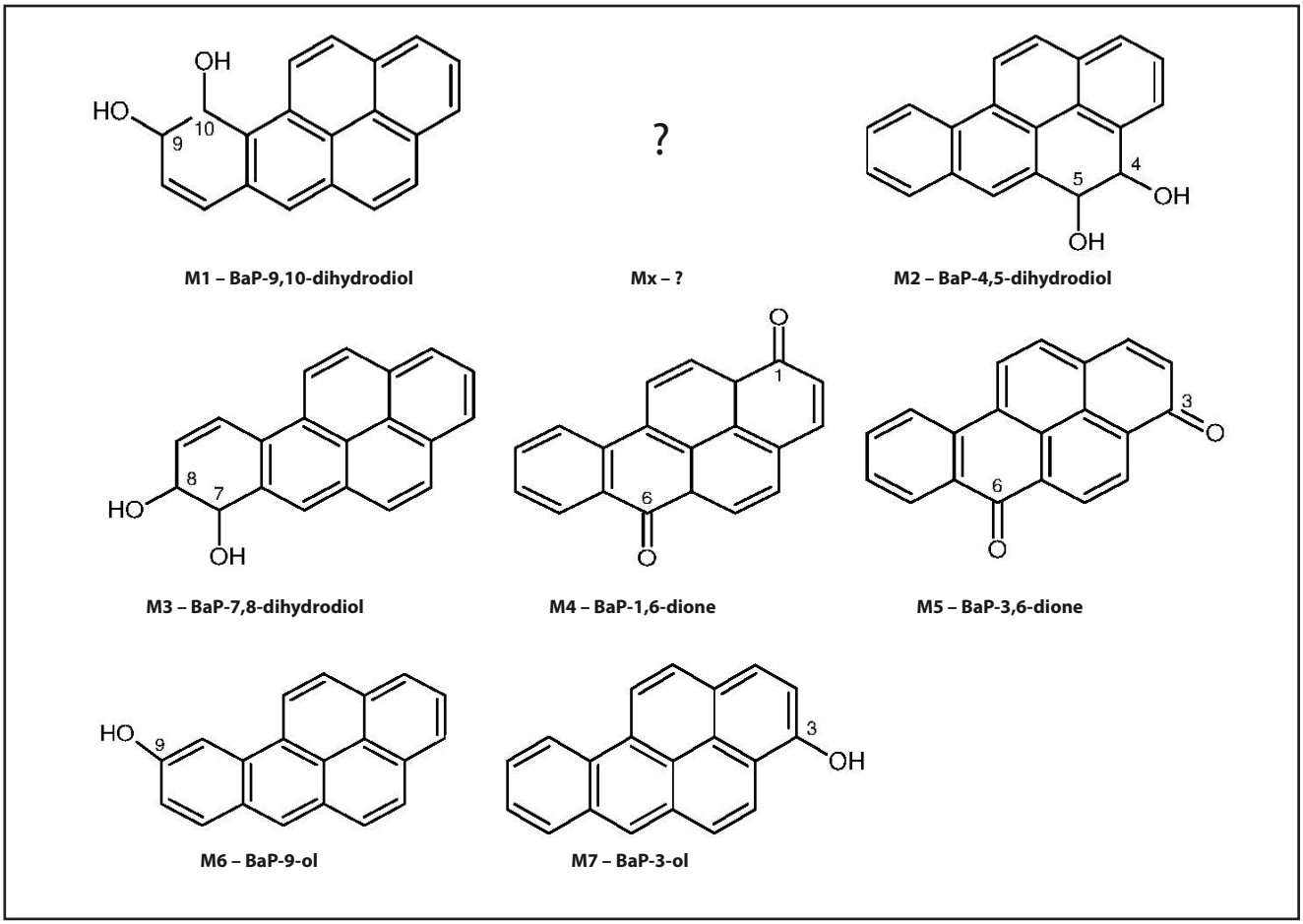

Fig. 3. Benzo[a]pyrene (BaP) metabolites formed by human and rat hepatic microsomes and human and rat cytochrome P450 1A1.

The same BaP metabolites were also formed by hepatic microsomes of control (untreated) rats, but to a more than 3.5-fold lower extent (data not shown).

The BaP-3-ol, considered as a detoxification BaP metabolite, was the major oxidation product generated both by human and rat hepatic microsomes (Figure 2B). Essentially no BaP metabolites were found when NADPH-generating system was not present in the incubation mixtures containing human and rat hepatic microsomes (data not shown).

Oxidation of BaP by human and rat CYP1A1 in Supersomes™

Human CYP1A1 expressed with POR in a microsomal system of Supersomes™ oxidized BaP to seven metabolites, BaP-9,10-dihydrodiol, a metabolite Mx, BaP-7,8-dihydrodiol, BaP-1,6-dione, BaP-3,6-dione, BaP-9-ol and BaP-3-ol (Figures 2C and 3). One of the dihydrodiols formed by human and rat hepatic microsomes, BaP-4,5-dihydrodiol (M2), has not been detected in the system containing human CYP1A1.

Rat recombinant CYP1A1 expressed with POR in Supersomes™ oxidized BaP to the analogous spectrum of metabolites as human CYP1A1, but rat CYP1A1 generated also BaP-4,5-dihydrodiol (Figure 2D). In addition, lower amounts of most BaP metabolites were formed by human than by rat CYP1A1, mainly the amount of BaP-3-ol (Figures 2 and 4). Such a lower efficacy of rat CYP1A1 corresponded to lower activity of this enzyme with a CYP1A1 marker substrate, Sudan I (data not shown).

The results found using these human and rat CYP1A1 systems indicate that BaP is metabolized not only by CYP1A1 present in these systems, but also by mEH, which is important for the hydration of BaP epoxides to produce dihydrodiols. Indeed, BaP dihydrodiols were formed in these human and rat CYP1A1 systems. Therefore, mEH is expressed in microsomes of the Supersomal system.

Essentially no BaP metabolites were found when the NADPH-generating system was deleted from the incubation mixtures containing human and rat CYP1A1 (see Figure 2E for human CYP1A1).

The effect of cytochrome b_5 on BaP oxidation by human and rat CYP1A1

Addition of cytochrome b_5 to human and rat CYP1A1 in Supersomes™ led to up to a more than 2-fold increase in BaP oxidation to its metabolites. The highest stimulation effect of cytochrome b_5 on human

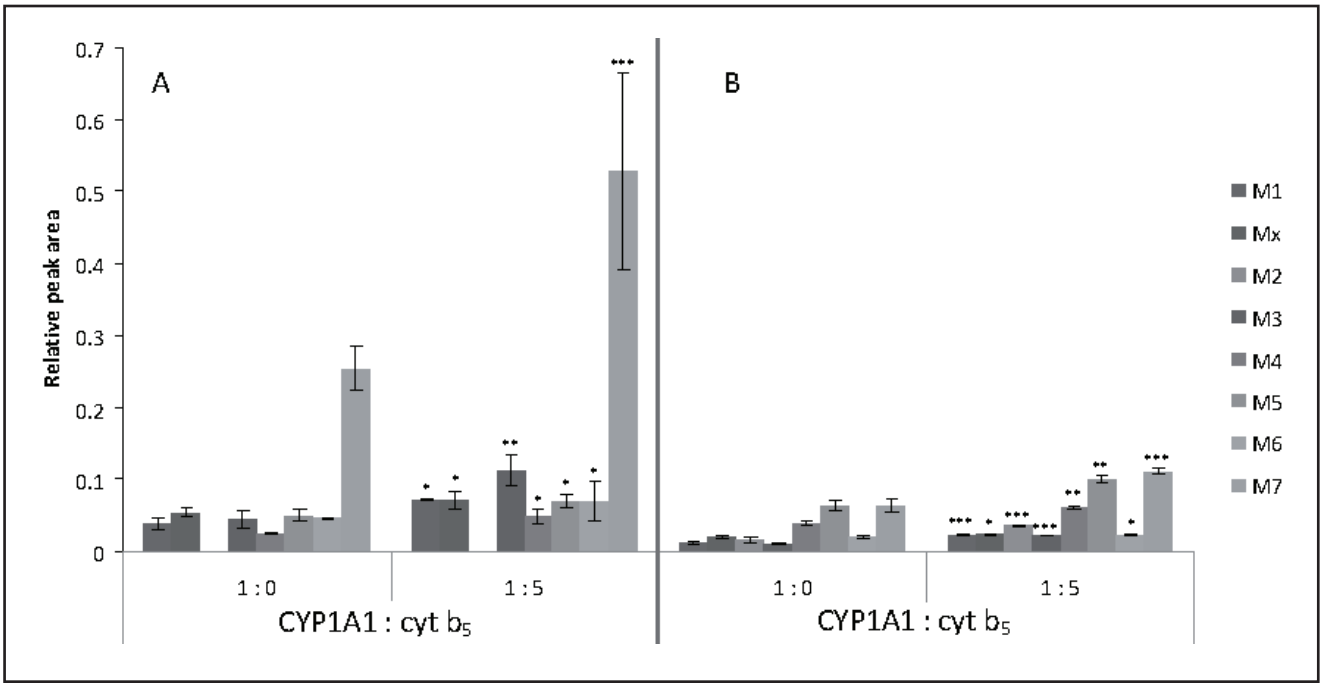

Fig. 4. Oxidation of benzo[a]pyrene (BaP) by human (A) and rat (B) cytochrome P450 (CYP) 1A1 and the effect of cytochrome b_5 (cyt b_5) on this oxidation. All values are given as means and standard deviations of triplicate incubations (n=3). Comparison was performed by *t*-test analysis; **p*<0.05, ***p*<0.01, ****p*<0.001, different from CYP1A1-mediated oxidation of BaP without cytochrome b_5. For BaP metabolites M1–M7 and Mx, see Fig. 3.

CYP1A1 has been found on formation of BaP-3-ol and BaP-7,8-dihydrodiol, followed by the effect on generation of BaP-9,10-dihydrodiol, BaP-1,6-dione, BaP-9-ol, a metabolite Mx, and BaP-3,6-dione. In the case of rat CYP1A1, the highest increase in formation of BaP-7,8,dihydrodiol, BaP-9,10-dihydrodiol and BaP-3-ol was found (Figure 4).

DISCUSSION

The results found in this work demonstrate that oxidation of BaP by human CYP1A1 is similar to that catalyzed by rat CYP1A1; the only one difference has been found. Whereas BaP-9,10-dihydrodiol, a metabolite Mx, BaP-4,5-dihydrodiol, BaP-7,8-dihydrodiol, BaP-1,6-dione, BaP-3,6-dione, BaP-9-ol and BaP-3-ol were formed both by human and rat CYP1A1, BaP-4,5-dihydrodiol was not detectable in the system containing human CYP1A1. Similar results were found in experiments where human bronchoalveolar H358 cells expressing CYP1A1 were treated with BaP; no BaP-4,5-dihydrodiol was detectable as a BaP metabolic product (Jiang *et al.* 2007). Also in the case of human and rat hepatic microsomes, where a spectrum of analogous BaP metabolites such as BaP-phenols, BaP-diones and BaP-dihydrodiols was generated, one difference in metabolic products was found; BaP-9-ol has not been detectable in human hepatic microsomes. Low levels of CYP1A1 expressed in human livers (Stiborova *et al.* 2002, 2005), resulting in low efficiencies of this subcellular system, might be responsible for no detectable amounts of BaP-9-ol.

The structure of one BaP metabolite, a metabolite Mx, that has been formed by human and rat CYP1A1 remains to be explored. Nevertheless, its chromatographic properties on HPLC indicate its polarity; it is eluted from a HPLC column with a retention time between that of BaP-9,10-dihydrodiol and BaP-4,5-dihydrodiol. All results found in this work indicate that rat CYP1A1 enzymatic systems are appropriate models that might be utilized to investigate BaP oxidation by human CYP1A1 and, therefore, to be used to evaluate risk of BaP carcinogenicity for human.

The pattern of BaP metabolites found to be formed by human and rat CYP1A1 in Supersomes™ demonstrate that not only human and rat CYP1A1, but also POR and mEH enzymes, necessary to metabolize BaP to the metabolites found, are expressed in the Supersomal microsomes. However, cytochrome b_5, which is a natural component of insect microsomes (Supersomes™), seems to be present in this system in the amounts which is not sufficient to mediate oxidation of BaP by CYP1A1 to its highest catalytic efficiencies. Namely, the addition of cytochrome b_5 to the human and rat CYP1A1 in Supersomes™ resulted in an increase in formation of BaP metabolites. This is an important finding that was shown in this study for the first time. A stimulation of CYP1A1-mediated catalysis by cytochrome b_5 has already been found in oxidation of its marker substrate Sudan I (Stiborova *et al.* 2005, 2006)

and an anticancer drug ellipticine (Kotrbova *et al.* 2011), but not in that of 7-ethoxyresorufin (Stiborova *et al.* 2005). Two mechanisms of cytochrome b_5-mediated modulation of CYP catalysis have been suggested previously: it can affect the CYP catalytic activities by donating the second electron to CYP in a CYP catalytic cycle and/or act as an allosteric modifier of the oxygenase (Yamazaki *et al.* 1997; 2001; Loughran *et al.* 2001; Porter 2002; Schenkman & Jansson 2003; Guengerich 2005; Zhang *et al.* 2005; Kotrbova *et al.* 2009, 2011; Stiborova *et al.* 2012b). The mechanism(s) underlying such allosteric effects, based on reports that apo-cytochrome b_5 can stimulate CYP catalysis, remains uncertain. It does seem clear, however, that cytochrome b_5 binding can cause conformational changes to the substrate access channel and binding pocket in the CYP enzyme (Yamazaki *et al.* 1997, 2001; Loughran *et al.* 2001; Porter 2002; Schenkman & Jansson 2003; Guengerich 2005; Zhang *et al.* 2005; Kotrbova *et al.* 2009, 2011; Stiborova *et al.* 2012b). Because addition of cytochrome b_5 changed the levels of all BaP metabolites formed by human and rat CYP1A1, the effect of this protein on an electron transfer to CYP1A1 seems to be the predominant mechanism responsible for the observed increase in oxidation of BaP. Nevertheless, the allosteric effects due to cytochrome b_5 cannot be excluded. Namely, an increase in formation of individual BaP metabolites was not the same for all these metabolites. Therefore, the mechanism responsible for the effects of cytochrome b_5 on CYP1A1-mediated oxidation of a variety of substrates needs to be explored in further investigations.

CONCLUSION

The results found in this study demonstrate that the enzymatic system of rat CYP1A1 is a suitable enzyme model that might be utilized for investigation of BaP metabolism by human CYP1A1. In addition, the results also show for the fist time that cytochrome b_5 modulate BaP metabolism catalyzed by human and rat CYP1A1, stimulating formation of all its metabolic products. All these findings demonstrate that rats seem to be a suitable animal model that might mimic BaP oxidation in human.

ACKNOWLEDGEMENTS

This work was supported by the Grant Agency of the Czech Republic (grant P301/10/0356), Charles University in Prague (grants 640712 and UNCE 204025/2012).

REFERENCES

1 Baird WM, Hooven LA, Mahadevan B (2005). Carcinogenic polycyclic aromatic hydrocarbon-DNA adducts and mechanism of action. Environ Mol Mutagen. **45**: 106–114.
2 Bauer E, Guo Z, Ueng YF, Bell LC, Zeldin D, Guengerich FP (1995). Oxidation of benzo[a]pyrene by recombinant human cytochrome P450 enzymes. Chem Res Toxicol **8**: 136–142.
3 Coon MJ (1978). Oxygen activation in the metabolism of lipids, drugs and carcinogens. Nutr Rev. **36**: 319–328.
4 Chun YJ, Shimada T, Guengerich FP (1996). Construction of a human cytochrome P450 1A1: rat NADPH-cytochrome P450 reductase fusion protein cDNA and expression in Escherichia coli, purification, and catalytic properties of the enzyme in bacterial cells and after purification. Arch Biochem Biophys. **330**: 48–58.
5 Fang AH, Smith WA, Vouros P, Gupta RC (2001). Identification and characterization of a novel benzo[a]pyrene-derived DNA adduct. Biochem Biophys Res Commun. **281**: 383–389.
6 Hamouchene H, Arlt VM, Giddings I, Phillips DH (2011). Influence of cell cycle on responses of MCF-7 cells to benzo[a]pyrene. BMC Genomics. **12**: 333.
7 Haasnoot CAG, Deleeuw FAAM, Altona C (1980). The relationship between proton-proton NMR coupling-constants and substituent electronegativies. 1. An empirical generalization of the Karplus equation. Tetrahedron. **36**: 2783–2792.
8 Guengerich FP (2005). Reduction of cytochrome b5 by NADPH-cytochrome P450 reductase. Arch Biochem Biophys. **440**: 204–211.
9 International Agency for Research on Cancer (IARC) (2010). Some non-heterocyclic polycyclic aromatic hydrocarbons and some related exposures. In: IARC Monogr Eval Carcinog Risks Hum. **92**: 1–853.
10 Jiang H, Gelhaus SL, Mangal D, Harvey RG, Blair IA, Penning TM (2007). Metabolism of benzo[a]pyrene in human bronchoalveolar H358 cells using liquid chromatography-mass spectrometry. Chem Res Toxicol. **20**: 1331–1341.
11 Kim JH, Stansbury KH, Walker NJ, Trush MA, Strickland PT, Sutter TR (1998). Metabolism of benzo[a]pyrene and benzo[a]pyrene-7,8-diol by human cytochrome P450 1B1. Carcinogenesis. 19: 1847–1853.Koberova M, Jecmen T, Sulc M, Cerna V, Hudeček J, Stiborova M. et al (2013). Photo-cytochrome b_5 – A new tool to study the cytochrome P450 electron-transport chain. Int J Electrochem Sci. **8**: 125–134.
12 Kotrbova V, Aimova D, Ingr M, Borek-Dohalska L, Martinek V, Stiborova M (2009). Preparation of a biologically active apocytochrome b_5 *via* heterologous expression in *Escherichia coli*. Protein Expr Purif. **66**: 203–209.
13 Kotrbova V, Mrazová B, Moserova M, Martinek V, Hodek P, Hudecek J, et al (2011). Cytochrome b_5 shifts oxidation of the anticancer drug ellipticine by cytochromes P450 1A1 and 1A2 from its detoxication to activation, thereby modulating its pharmacological efficacy. Biochem Pharmacol. **82**: 669–680.
14 Leeruff E, Kazarianmoghaddam H, Katz M (1986). Controlled oxidations of bezo[a]pyrene. Can J Chem. **64**: 1297–1303.
15 Loughran PA, Roman LJ, Miller RT, Masters BS (2001). The kinetic and spectral characterization of the E. coli-expressed mammalian CYP4A7: cytochrome b_5 effects vary with substrate. Arch Biochem Biophys. **385**: 311–321.
16 Moserova M, Kotrbova V, Aimova D, Sulc M, Frei E, Stiborova M (2009). Analysis of benzo[a]pyrene metabolites formed by rat hepatic microsomes using high pressure liquid chromatography: optimization of the method. Interdisc Toxicol. **2**: 239–244.
17 Nesnow S, Ross J, Nelson G, Holden K, Erexson G, Kligerman A, *et al.* (1993). Quantitative and temporal relationships between DNA adduct formation in target and surrogate tissues: implications for biomonitoring. Environ Health Perspect. **101(**Suppl 3): 37–42.
18 Omura T and Sato R (1964). The carbon monoxide-binding pigment of liver microsomes. I. Evidence for its hemoprotein nature. J Biol Chem. **239**: 2370–2378
19 Phillips DH and Venitt S (2012). DNA and protein adducts in human tissues resulting from exposure to tobacco smoke. Int J Cancer. **131**: 2733–2753.
20 Platt KL and Oesch F (1983). Efficient synthesis of non-K-region trans-dihydro diol sof polycyclic aromatic-hydrocarbons from ortho-quinones and catechols. J Org Chem. **48**: 265–268.
21 Porter TD (2002). The roles of cytochrome b_5 in cytochrome P450 reactions. J Biochem Mol Toxicol. **16**: 311–316.
22 Prinzbach H, Freudenberger V, Scheidegger U (1967). Cyclische gekreutz-konjugierte bindungssysteme. 13. NMR-untersuchungen am phenafulven-system. Helv Chim Acta. **50**: 1087–1107.

23 Roos PH (1996). Chromatographic separation and behavior of microsomal cytochrome P450 and cytochrome b_5. J Chromatogr B Biomed Appl. **684**: 107–131.

24 Schenkman JB and Jansson I (2003). The many roles of cytochrome b_5. Pharmacol Ther. **97**: 139–152.

25 Schoket B, Lévay K, Philips DH, Vincze I (1989). ^{32}P-postlabelling analysis of DNA adducts of benzo[a]pyrene formed in complex metabolic activation systems *in vitro*. Cancer Lett. **48**: 67–75.

26 Stiborova M, Martinek V, Rydlova H, Hodek P, Frei E (2002). Sudan I is a potential carcinogen for humans: Evidence for its metabolic activation and detoxication by human recombinant cytochrome P450 1A1 and liver microsomes. Cancer Res. **62**: 5678–5684.

27 Stiborova M, Stiborova-Rupertova M, Borek-Dohalska L, Wiessler M, Frei E (2003). Rat microsomes activating the anticancer drug ellipticine to species covalently binding to deoxyguanosine in DNA are a suitable model mimicking ellipticine bioactivation in humans. Chem Res Toxicol. **16**: 38–47.

28 Stiborova M, Martinek V, Rydlova H, Koblas T, Hodek P (2005). Expression of cytochrome P450 1A1 and its contribution to oxidation of a potential human carcinogen 1-phenylazo-2-naphthol (Sudan I) in human livers. Cancer Lett. **220**: 145–154.

29 Stiborova M, Martinek V, Schmeiser HH, Frei E (2006). Modulation of CYP1A1-mediated oxidation of carcinogenic azo dye Sudan I and its binding to DNA by cytochrome b_5. Neuroendocrinol Lett. **27(**Suppl 2): 35–39.

30 Stiborova M, Mares J, Levova K, Pavlickova J, Barta F, Hodek P, et al (2011). Role of cytochromes P450 in metabolism of carcinogenic aristolochic acid I: evidence of their contribution to aristolochic acid I detoxication and activation in rat liver. Neuroendocrinol Lett. **32**(Suppl 1): 121–130.

31 Stiborova M, Cechova T, Borek-Dohalska L, Moserova M, Frei E, Schmeiser HH, et al (2012a). Activation and detoxification metabolism of urban air pollutants 2-nitrobenzanthrone and carcinogenic 3-nitrobenzanthrone by rat and mouse hepatic microsomes. Neuroendocrinol Lett. **33** (Suppl 3): 8–15.

32 Stiborova M, Indra R, Moserova M, Cerna V, Rupertova M, Martinek V, et al (2012b). Cytochrome b_5 increases cytochrome P450 3A4-mediated activation of anticancer drug ellipticine to 13-hydroxyellipticine whose covalent binding to DNA is elevated by sulfotransferases and *N,O*-acetyltransferases. Chem Res Toxicol. **25**: 1075–1085.

33 Stiborova M, Dracinska H, Martinek V, Svaskova D, Hodek P, Milichovsky J, et al (2013). Induced expression of cytochrome P450 1A and NAD(P)H:quinone oxidoreductase determined at mRNA, protein and enzyme activity levels in rats exposed to the carcinogenic azo dye 1-phenylazo-2-naphthol (Sudan I). Chem Res Toxicol. **26**: 290–299.

34 Weichelman KJ, Braun RD, Fitzpatrick JD (1988). Investigation of the bicinchoninic acid protein assay: identification of the groups responsible for color formation. Anal Biochem. **175**: 231–237.

35 Xu DW, Penning TM, Blair IA, Harvey RG (2009). Synthesis of phenol and quinone metabolites of benzo[a]pyrene, a carcinogenic component of tobacco smoke implicated in lung cancer. J Org Chem. **74**: 597–604.

36 Yamazaki H, Gillam EM, Dong MS, Johnson WW, Guengerich FP, Shimada T (1997). Reconstitution of recombinant cytochrome P450 2C10(2C9) and comparison with cytochrome P450 3A4 and other forms: effects of cytochrome P450-P450 and cytochrome P450-b_5 interactions. Arch Biochem Biophys. **342**: 329–337.

37 Yamazaki H, Shimada T, Martin MV, Guengerich FP (2001). Stimulation of cytochrome P450 reactions by apo-cytochrome b_5: evidence against transfer of heme from cytochrome P450 3A4 to apo-cytochrome b_5 or heme oxygenase. J Biol Chem. **276**: 30885–30891.

38 Zhu S, Li L, Thornton C, Carvalho P, Avery BA, Willett KL (2008). Simultaneous determination of benzo[a]pyrene and eight of its metabolites in *Fundulus heteroclitus* bile using ultra-performance liquid chromatography with mass spectrometry. J Chromatogr B Analyt Technol Biomed Life Sci. **863**: 141–149.

39 Zhang H, Myshkin E, Waskell L (2005). Role of cytochrome b_5 in catalysis by cytochrome P450 2B4. Biochem Biophys Res Commun. **338**: 499–506.

The impact of p53 on DNA damage and metabolic activation of the environmental carcinogen benzo[*a*]pyrene: effects in *Trp53(+/+)*, *Trp53(+/-)* and *Trp53(-/-)* mice

Annette M. Krais[1], Ewoud N. Speksnijder[2,3], Joost P.M. Melis[2,3], Radek Indra[4], Michaela Moserova[4], Roger W. Godschalk[5], Frederik-J. van Schooten[5], Albrecht Seidel[6], Klaus Kopka[7], Heinz H. Schmeiser[7], Marie Stiborova[4], David H. Phillips[1], Mirjam Luijten[2,3] and Volker M. Arlt[1,*]

[1]*Analytical and Environmental Sciences Division, MRC-PHE Centre for Environment & Health, King's College London, London SE1 9NH, United Kingdom*

[2]*Center for Health Protection, National Institute for Public Health and the Environment (RIVM), Bilthoven 3721 MA, The Netherlands*

[3]*Department of Human Genetics, Leiden University Medical Center, Leiden 2300 RC, The Netherlands*

[4]*Department of Biochemistry, Faculty of Science, Charles University, 12840 Prague 2, Czech Republic*

[5]*Department of Toxicology, School for Nutrition, Toxicology and Metabolism (NUTRIM), Maastricht University Medical Centre, 6200 MD Maastricht, The Netherlands*

[6]*Biochemical Institute for Environmental Carcinogens, Prof. Dr. Gernot Grimmer-Foundation, 22927 Grosshansdorf, Germany*

[7]*Division of Radiopharmaceutical Chemistry, German Cancer Research Center (DKFZ), Im Neuenheimer Feld 280, 69120 Heidelberg, Germany*

Correspondence to: Volker M. Arlt, Analytical and Environmental Sciences Division, MRC-PHE Centre for Environment & Health, King's College London, Franklin-Wilkins Building, 150 Stamford Street, London SE1 9NH, United Kingdom, Tel: +44-207-848-3781, E-mail: volker.arlt@kcl.ac.uk

Keywords: benzo[*a*]pyrene, tumour suppressor p53, mouse models, cytochrome P450, carcinogen metabolism, DNA adducts.

Abstract

The tumour suppressor p53 is one of the most important cancer genes. Previous findings have shown that p53 expression can influence DNA adduct formation of the environmental carcinogen benzo[*a*]pyrene (BaP) in human cells, indicating a role for p53 in the cytochrome P450 (CYP) 1A1-mediated biotransformation of BaP *in vitro*. We investigated the potential role of p53 in xenobiotic metabolism *in vivo* by treating *Trp53(+/+)*, *Trp53(+/-)* and *Trp53(-/-)* mice with BaP. BaP-DNA adduct levels, as measured by ^{32}P-postlabelling analysis, were significantly higher in liver and kidney of *Trp53(-/-)* mice than *Trp53(+/+)* mice. Complementarily, significantly higher amounts of BaP metabolites were also formed *ex vivo* in hepatic microsomes from BaP-pretreated *Trp53(-/-)* mice. Bypass of the need for metabolic activation by treating mice with BaP-7,8-dihydrodiol-9,10-epoxide (BPDE) resulted in similar adduct levels in liver and kidney in all mouse lines confirming that the influence of p53 is on the biotransformation of the parent compound. Indeed, nucleotide excision repair capacity did not contribute to the higher BaP-DNA adduct levels observed in *Trp53(-/-)* mice. Higher BaP-DNA adduct levels in the livers of *Trp53(-/-)* mice correlated with higher Cyp1a protein levels and increased Cyp1a enzyme activity in these animals. Our study demonstrates a role for p53 in the metabolism of BaP *in vivo* confirming previous *in-vitro* results on a novel role for p53 in CYP1A1-mediated BaP metabolism. However, our results also suggest that the mechanisms involved in the altered expression and activity of the CYP1A1 enzyme by p53 *in vitro* and *in vivo* are different.

Introduction

The *TP53* tumour suppressor gene, which encodes the protein p53, is often described as the guardian of the genome and is the most commonly mutated gene in human tumours (Olivier et al. 2010). As gatekeeper p53 regulates cell growth by inhibiting proliferation or promoting apoptosis (Taneja et al. 2011). As caretaker it controls cellular processes to maintain genomic integrity, including repair to remove DNA damage (Taneja et al. 2011). Disruption of the normal p53 response by *TP53* mutation leads to increased risks of tumour development. *TP53* is mutated in over 50% of sporadic tumours and various environmental carcinogens have been found to be associated with characteristic mutational signatures in *TP53* (Olivier et al. 2010). In addition to somatic mutations in the *TP53* gene, germline mutations have been found to cause predisposition to cancer and *TP53* polymorphisms have been shown to increase cancer susceptibility (Whibley et al. 2009). Besides its role in DNA damage response, p53 has also been found to regulate metabolic pathways, thereby linking p53 not only to cancer, but also to other diseases such as diabetes and obesity (Maddocks and Vousden 2011).

Previously, we used a panel of isogenic human colorectal carcinoma HCT116 cell lines that differed only with respect to their endogenous *TP53* status in order to investigate the metabolism and DNA damage induced by the environmental carcinogens benzo[*a*]pyrene (BaP) and 3-nitrobenzanthrone (3-NBA) (Hockley et al. 2008; Wohak et al. 2014). We found that HCT116 *TP53(-/-)* and *TP53(+/-)* cells formed significantly lower BaP-DNA adduct levels than *TP53(+/+)* cells. In contrast, no difference in adduct formation was observed in HCT116 cells exposed to BaP-7,8-diol-9,10-epoxide (BPDE), the activated metabolite of BaP, indicating that p53 expression is linked to the cytochrome P450 (CYP)-mediated metabolic activation of BaP. There were also significantly lower levels of BaP metabolites detected in the culture media of HCT116 *TP53(-/-)* and *TP53(+/-)* cells relative to *TP53(+/+)* cells, which was accompanied by a greater induction of CYP1A1 protein and *CYP1A1* mRNA in *TP53(+/+)* cells than in the other cell lines (Wohak et al. 2014). We found that BaP-induced CYP1A1 expression was regulated through a p53 response element (p53RE) in the *CYP1A1* promoter region thereby providing a novel pathway for the induction of CYP1A1 by polycyclic aromatic hydrocarbons (PAHs) like BaP (Wohak et al. 2014). Interestingly, DNA adduct formation by 3-NBA was not different in HCT116 *TP53(+/+)* and *TP53(-/-)* cells (Hockley et al. 2008), suggesting that NAD(P)H:quinone oxidoreductase (NQO1), which is the principal enzyme activating 3-NBA (Arlt et al. 2005; Stiborova et al. 2010), is not regulated by p53.

Transgenic and knock-out mouse models have been used to study tumour suppressor function through phenotypic analysis of the whole organism and by examining a variety of primary cell types (Taneja et al. 2011). The opportunity to study multiple tissues is particularly useful for *Trp53* because p53 function is highly cell type-specific (Donehower 2014; Kenzelmann Broz and Attardi 2010; Kucab et al. 2010; Lozano 2010). Much of the work carried out on the role of CYP enzymes in xenobiotic metabolism has been done *in vitro* (Nebert 2006; Nebert and Dalton 2006). However, extrapolation from *in vitro* data to *in vivo* pharmacokinetics requires additional factors to be considered such as route of administration, absorption, renal clearance and tissue-specific CYP expression (Nebert 2006; Nebert et al. 2013). For example, previous studies have revealed an apparent paradox, whereby hepatic CYP enzymes appear to be more important for detoxification of BaP *in vivo*, despite being involved in its metabolic activation *in vitro* (Arlt et al. 2012; Arlt et al. 2008; Nebert et al. 2013).

To evaluate the impact of the cellular *Trp53* status on the metabolic activation of BaP and 3-NBA we have compared metabolism and DNA adduct formation of BaP and 3-NBA in *Trp53(+/+)*, *Trp(+/-)* and *Trp53(-/-)* mice. DNA adduct formation *in vivo* and *in vitro* was investigated by ^{32}P-postlabelling analysis. Tissue-specific expression and activity of xenobiotic-metabolising enzymes (XMEs) involved in BaP and 3-NBA metabolism were compared with DNA adduct formation in the same tissue. Nucleotide excision repair (NER) capacity was assessed phenotypically in selected tissues using a modified comet assay. Urinary BaP metabolites and the Cyp-mediated formation of BaP metabolites *ex vivo* in hepatic microsomes were measured by high performance liquid chromatography (HPLC).

Materials and methods

Carcinogens

Benzo[*a*]pyrene (BaP; CAS number 50-32-8; purity ≥96%) was obtained from Sigma Aldrich. 3-Nitrobenzanthrone (3-NBA; CAS number 17117-34-9) was prepared as previously reported (Arlt et al. 2002). (±)-*Anti*-benzo[*a*]pyrene-*trans*-7,8-dihydrodiol-9,10-epoxide (BPDE) was synthesized at the Biochemical Institute for Environmental Carcinogens, Prof. Dr. Gernot Grimmer-Foundation, Germany.

Carcinogen treatment of Trp53(+/+), Trp53(+/-) and Trp53(-/-) mice

Trp53(+/+), *Trp53(+/-)* and *Trp53(-/-)* male C57BL/6 mice were generated as reported (Jacks et al. 1994). All animal experiments were conducted in accordance with the law at the Leiden University Medical Center, Leiden, The Netherlands, after approval by the institutional ethics committee. Animals were kept under controlled specific pathogen-free conditions (23ºC, 40-50% humidity) under a 12-h light-dark cycle. Food and water were available *ad libitum*. Genotyping of the animals was performed as described (Jacks et al. 1994). Groups of male *Trp53(+/+)*, *Trp53(+/-)* and *Trp53(-/-)* mice (3 months old; 25-30 g; *n* = 4/group) were treated with a single dose of 125 mg/kg body weight (bw) of BaP by intraperitoneal (i.p.) injection according to treatment protocols used previously to study BaP metabolism (Arlt et al. 2012; Arlt et al. 2008). We chose i.p. injection as the administration route to achieve a high induction of hepatic CYP-mediated BaP metabolism. Similarly, groups (*n* = 4) of *Trp53(+/+)*, *Trp53(+/-)* and *Trp53(-/-)* mice were injected i.p. with a single dose of 2 mg/kg bw of 3-NBA according to a previous study investigating 3-NBA metabolism (Arlt et al. 2005). Based on dose-finding experiments in *Trp53(+/+)* mice using single i.p. injections of 1.25, 6.25 or 12.5 mg/kg bw of BPDE, groups (*n* = 4) of *Trp53(+/+)*, *Trp53(+/-)* and *Trp53(-/-)* mice were treated i.p. with 1.25 mg/kg bw of BPDE. Control mice (*n* = 4) received solvent (corn oil) only. Animals were killed 24 hours after treatment and their liver, lung, kidney, colon, small intestine, bladder, glandular stomach, forestomach and spleen were removed, snap-frozen in liquid nitrogen and stored at −80°C until further analysis. Urine was collected for the preceding 24 hours.

Detection of DNA adducts by ^{32}P-postlabelling

DNA was isolated from tissues by a standard phenol-chloroform extraction method. DNA adduct analysis was performed by thin-layer chromatography ^{32}P-postlabelling analysis (Phillips and Arlt 2007; Phillips and Arlt 2014). For DNA from BaP- and BPDE-treated animals the nuclease P1 digestion enrichment method was used (Arlt et al. 2008) while for DNA from 3-NBA-treated animals, the butanol extraction method was employed (Arlt et al. 2002). DNA samples (4 μg) were digested with micrococcal nuclease (288 mU; Sigma) and calf spleen phosphodiesterase (1.2 mU; MP Biomedical), and then enriched and labelled as reported.

Measurement of nucleotide excision repair (NER) capacity

The ability of NER-related enzymes present in isolated tissue extracts to detect and incise substrate DNA containing BPDE-DNA adducts was measured using a modified comet assay (Langie et al. 2006). Tissue protein extracts were prepared as described previously (Gungor et al. 2010), and protein concentrations were optimised for analysis of liver and kidney samples (0.2 mg/mL). The *ex vivo* repair incubation and electrophoresis was performed according to the published protocol (Langie et al. 2006). Dried slides stained with ethidium bromide (10 μg/mL) were viewed with a Zeiss Axioskop fluorescence microscope. Comets were scored using the Comet III system (Perceptive Instruments, UK). Fifty nucleoids were assessed per slide and each sample was analysed in duplicate. All samples were measured blindly. Tail intensity (% tail DNA), defined as the percentage of DNA migrated from the head of the comet into the tail, was used to calculate repair capacity of the tissue extracts as reported previously (Langie et al. 2006).

Preparation of microsomal and cytosolic samples

Microsomal and cytosolic fractions were isolated from the livers and lungs of *Trp53(+/+)*, *Trp53(+/-)* and *Trp53(-/-)* mice. Tissue frozen in liquid nitrogen was ground up in a Teflon container with a steel ball in a dismembrator to a frozen powder. This was transferred into a Potter-Elvehejm homogenizer and the Teflon receptacle rinsed with 1/15 M sodium phosphate buffer with 0.5% potassium chloride pH 7.4. The powder was homogenized, transferred to a centrifuge tube and the potter rinsed with phosphate buffer. The homogenates were spun for 30 min at 18,000 × g. Supernatant were transferred to an ultracentrifuge tube and spun at 100,000 × g for 60 min at 4ºC. The resulting supernatants formed the cytosols, which was levered off the sediment gently while the sediments (microsomes) were taken up in phosphate buffer. Protein concentration in the fractions were measured using bicinchoninic

acid protein assay (Wiechelman et al. 1988) with bovine serum albumin and stored in small aliquots at − 80°C until analysis.

Microsomal BaP-DNA adduct formation

Incubation mixtures in a final volume of 750 µL consisted of 50 mM potassium phosphate buffer (pH 7.4), 1 mM NADPH, 0.5 mg of microsomal protein, 0.5 mg calf thymus DNA, and 0.1 mM BaP (dissolved in 7.5 µL dimethylsulfoxide [DMSO]). The reaction was initiated by adding NADPH. Microsomal incubations were carried out at 37ºC for 90 min. Microsomal-mediated BaP-DNA adduct formation was linear up to 120 min as reported previously (Arlt et al. 2008). Control incubations were carried out (*i*) without microsomes; (*ii*) without NADPH; (*iii*) without DNA; and (*iv*) without BaP. After incubation, DNA was isolated by a standard phenol/chloroform extraction method.

Microsomal BaP metabolite formation

In a final volume of 500 µL the incubation mixture contained 100 mM potassium phosphate buffer (pH 7.4), NADPH-generating system (1 mM $NADP^+$, 10 mM D-glucose-6-phosphate, 1 U/mL D-glucose-6-phosphate dehydrogenase), 0.5 mg microsomal protein and 50 µM BaP (dissolved in 5 µL DMSO). The reaction was initiated by adding 50 µL of the NADPH-generating system. Microsomal incubations were carried out at 37ºC for 20 min. Control incubations were carried out (*i*) without microsomes; (*ii*) without NADPH-generating system; and (*iii*) without BaP. After incubation, 5 µL of 1 mM phenacetin in methanol was added as internal standard. The BaP mixtures were extracted with ethyl acetate (2× 1 mL), the solvent was evaporated to dryness and the residue was dissolved in 25 µL methanol for HPLC analysis.

HPLC analysis of BaP metabolites

HPLC analysis was performed on a Nucleosil® C18 reversed phase column, (250 × 4 mm, 5 µm; Macherey Nagel, Germany) using a Dionex system consisting of a pump P580, a UV/VIS Detector UVD 170S/340S, an ASI-100 Automated Sample Injector, a termobox COLUMN OVEN LCO 101 and an In-Line Mobile Phase Degasser Degasys DG-1210 Dionex controlled with ChromeleonTM 6.11 build 490 software. HPLC conditions were: 50% acetonitrile in HPLC water (*v*/*v*), with a linear gradient to 85% acetonitrile in 35 min, then an isocratic elution with 85% acetonitrile for 5 min, a linear gradient from 85%

acetonitrile to 50% acetonitrile in 5 min, followed by an isocratic elution of 50% acetonitrile for 5 min. Detection was by UV at 254 nm. BaP metabolite peaks were collected and analysed by NMR and/or mass spectrometry as described (Stiborova et al. 2014). The structures of BaP metabolites analysed are given in Supplementary Figure 6C. The metabolite peak areas were calculated relative to the peak area of the internal standard.

BaP metabolites in urine

Urine samples (0.4-1.7 mL) collected from *Trp53(+/+)* and *Trp53(-/-)* mice treated with BaP were mixed with 4 volumes of methanol, centrifuged for 4 min at 1,000 rpm, and the supernatants were then evaporated to dryness. The residues were dissolved in 100 μL of methanol and analysed by HPLC as described above. Urine samples for *Trp53(+/-)* mice were lost during analysis.

Expression of Cyp1a1 and Nqo1 by Western blotting

Microsomal and cytosolic proteins were separated using NuPage 4-12% Bis-Tris sodium-dodecyl sulphate (SDS)-polyacrylamide gels (Life Technologies), and Western blotted as previously reported (Hockley et al. 2006). Chicken polyclonal antibody raised against recombinant rat CYP1A1 protein (Arlt et al. 2008) has been shown to recognise murine Cyp1a1. In microsomal samples Cyp1a was probed with chicken anti-rat CYP1A1 at 1:5,000 and peroxidase-conjugated goat-anti chicken (ab6877, Abcam, 1:10,000) was used as secondary antibody. Rat recombinant CYP1A1 and CYP1A2 (in Supersomes™, Gentest Corp.) were used as positive controls to identify protein bands in microsomal samples. In cytosolic samples an affinity purified rabbit antibody was used to detect Nqo1 (N5288, rabbit pAb, 1:10,000; Sigma) and peroxidase-conjugated goat anti-rabbit antibody (CST7076, Cell Signalling Technology, 1:10,000) was used as secondary antibody. Human recombinant NQO1 (Sigma) was used as positive control to identify the Nqo1 band in cytosols.

Measurement of Cyp1a enzyme activity

Microsomal samples were characterised for Cyp1a activity using 7-ethoxyresorufin *O*-deethylation (EROD) activity (Mizerovska et al. 2011). Enzyme activity was determined by following the conversion of 7-ethoxyresorufin into resorufin using fluorescent measurement on a Synergy HT Plate Reader (Bio-TEK) using an excitation wavelength of 530 nm and an emission wavelength of 580 nm.

Measurement of Nqo1 enzyme activity

Nqo1 enzyme activity in cytosolic samples was measured with menadione (2-methyl-1,4-naphthoquinone) as substrate as described previously (Mizerovska et al. 2011). Enzyme activity was determined by following the conversion of cytochrome *c* at 550 nm on a Synergy HT Plate Reader (Bio-TEK).

Results

DNA adduct formation in vivo

In the majority of tissues, the BaP-DNA adduct pattern consisted of a single adduct spot (spot 1), previously identified as 10-(deoxyguanosin-N^2-yl)-7,8,9-trihydroxy-7,8,9,10-tetrahydro-BaP (dG-N^2-BPDE) (Supporting Figure 2A). For lung, colon and small intestine additional adduct spots were detected. In all three tissues a minor adduct (spot 2) was detected that was previously suggested to be derived from reaction of 9-hydroxy-BaP-4,5-epoxide with guanine (Stiborova et al. 2014), while for colon and small intestine an additional major adduct (spot 3) was found that has not yet been structurally identified. The same adduct profiles were observed in all three mouse lines. A scheme showing the formation of adducts 1 and 2 is given in Supporting Figure 4. No DNA adducts were detected in control animals (data not shown).

BaP-DNA adduct levels ranged from 25-100 adducts per 10^8 nucleotides (Figure 1A). Adduct levels were significantly higher (~2-fold) in livers of *Trp53(-/-)* compared to *Trp53(+/+)* mice (106 ± 25 *versus* 48 ± 27 adducts per 10^8 nucleotides; $p<0.05$), while adduct formation in kidney was significantly higher (~2-fold) both in *Trp53(+/-)* and *Trp53(-/-)* relative to *Trp53(+/+)* mice (73 ± 31 and 70 ± 20 *versus* 27 ± 6 adducts per 10^8 nucleotides, respectively; $p<0.05$). A similar trend was observed in lung, fore stomach, and spleen, although the difference in adduct levels did not reach statistical significance. In contrast, adduct levels in liver, lung, and kidney did not significantly change after treatment with BPDE in all mouse lines (Figure 1B). In these tissues the adduct pattern consisted of adduct spot 1 only (see Supporting Figure 2B). As BPDE does not require CYP-mediated metabolic activation to bind to DNA, these findings suggest that the differences in DNA adduct formation observed in liver and kidney with the parent compound BaP are the consequence of the different capacities of the *Trp53* mouse lines to metabolically activate BaP.

The adduct pattern induced by 3-NBA consisted of up to four adduct spots (spots 1-4; Supporting Figure 3). These were characterised previously as 2-(2'-deoxyadenosin-N^6-yl)-3-aminobenzanthrone (dA-N^6-3-ABA; spot 1), 2-(2'-deoxyguanosin-N^2-yl)-3-aminobenzanthrone (dG-N^2-3-ABA; spot 3) and *N*-(2'-deoxyguanosin-8-yl)-3-aminobenzanthrone (dG-C8-*N*-3-ABA; spot 4), while spot 2 is an as-yet-uncharacterised deoxyadenosine adduct (Arlt et al. 2001; Arlt et al. 2006). Adduct levels ranged from 2-40 adducts per 10^8 nucleotides, but there were no significant differences between mouse lines in

DNA adduct formation in any of the tissues investigated (Figure 2). These results suggest that, in contrast to BaP metabolism, *Trp53* status has no impact on 3-NBA metabolism *in vivo*, which is in accord with experiments on human cells *in vitro* (Hockley et al. 2008; Simoes et al. 2008).

DNA repair capacity in liver and kidney

As p53-dependent pathways affecting global NER have been identified (Ford 2005; Sengupta and Harris 2005), we assessed whether mouse *Trp53* status influences NER activity. Tissue extracts from liver and kidney were examined for their ability to repair BPDE-induced DNA adducts using a modified comet assay (Langie et al. 2006). We found that in the liver the repair capacity was ~50% higher in *Trp53(-/-)* than in *Trp53(+/+)* mice, while no difference in the repair capacity between mouse lines was observed in kidney (Supporting Figure 5). These results indicate that NER capacity does not contribute to the higher BaP-DNA adduct levels observed in *Trp53(-/-)* relative to *Trp53(+/+)* mice, both in liver and kidney, which is in line with the finding that treatment of mice with BPDE resulted in similar adduct levels in the three mouse lines.

DNA adduct formation of BaP ex vivo

We investigated the ability of hepatic microsomes isolated both from control and BaP-treated animals to catalyse BaP-DNA adduct formation *ex vivo* (Figure 3). While *Trp53* status had no influence on DNA adduct formation by BaP with hepatic microsomes isolated from untreated animals (Figure 3A), BaP-induced adduct levels were significantly higher with microsomal samples from *Trp53(+/-)* and *Trp53(-/-)* relative to *Trp53(+/+)* mice pretreated with BaP (Figure 3B). The adduct pattern induced by BaP *ex vivo* consisted of adduct spots 1 and 2 (see inserts Figure 3 and Supporting Figure 4). Interestingly, adduct levels of adduct 2 were higher than adduct 1, the dG-N^2-BPDE adduct, and, in addition, adduct 2 was significantly higher in experiments with *Trp53(+/-)* and *Trp53(-/-)* microsomes than with *Trp53(+/+)* microsomes.

BaP metabolite profile ex vivo

As our data suggested that *Trp53* status affects the NADPH-dependent metabolic activation of BaP in hepatic microsomes, metabolite profiles were determined by HPLC analysis. A representative HPLC chromatogram of BaP metabolites is shown in Supporting Figure 6A. Hydroxylated BaP metabolites, BaP-dihydrodiols, as well as BaP-diones, were identified.

Previous studies have shown that many of these BaP metabolites are formed by CYP1A1 in combination with microsomal epoxide hydrolase (Bauer et al. 1995; Kim et al. 1998; Luch and Baird 2005). No BaP metabolites were detected in control incubations without microsomes, without NADPH-generating system or without BaP (data not shown). With hepatic microsomes isolated from untreated mice *Trp53* status had no influence on the BaP metabolite profile and the amounts of BaP metabolites formed (Figure 4, *left panels*). However, pretreating mice with BaP led to a significant increase in BaP metabolite formation *ex vivo* (Figure 4, *right panels*). Moreover, amounts of BaP-7,8-dihydrodiol, BaP-1,6-dione, BaP-3,6-dione, BaP-9-ol and BaP-3-ol were significantly higher in microsomes of pretreated *Trp53(+/-)* and *Trp53(-/-)* mice compared with pretreated *Trp53(+/+)* mice. These findings correlated with *ex vivo* BaP-DNA adduct formation using the same hepatic microsomes (compare Figure 3B).

Urine analysis of Trp53(+/+) and Trp53(-/-) mice treated with BaP

A representative HPLC chromatogram of urinary BaP metabolites is shown in Supporting Figure 6B. The amounts of BaP-4,5-dihydrodiol, BaP-7,8-dihydrodiol, BaP-3,6-dione, and BaP-3-ol were significantly lower in urine of *Trp53(-/-)* compared to *Trp53(+/+)* mice (Supporting Figure 7), although most of the differences were small (~15-20% reduction). BaP metabolites can be conjugated to glucuronides and sulphates (Luch and Baird 2005), which are excreted in the urine and feces, but only unconjugated BaP metabolites (see Supporting Figure 6B) were determined in the present work.

Influence of Trp53 status on xenobiotic-metabolising enzymes

We next studied the expression and activity of enzymes metabolising BaP. Metabolic activation of BaP is catalysed mainly by CYP1A1, but also CYP1B1 (Supporting Figure 1A), which leads via BPDE to the formation of dG-N^2-BPDE, the major BaP-derived DNA adduct detected *in vivo*. For these investigations we selected liver, as *Trp53* status impacted on hepatic BaP-DNA adduct formation (see Figure 1A), and also lung, because it is the main target organ of 3-NBA genotoxicity (Arlt 2005).

Treatment of mice with BaP led to a large induction of Cyp1a1 protein levels in liver (Figure 5A). However, induction was much greater in hepatic microsomes of BaP-treated *Trp53(+/-)* and *Trp53(-/-)* mice than in *Trp53(+/+)* mice, which correlates with the levels of BaP-DNA adducts in the livers of these animals. The increase in Cyp1a1 protein levels was associated with a significant increase in EROD activity (up to ~2-fold; $p<0.05$), a measure of

CYP1A enzyme activity, in BaP-treated *Trp53(+/-)* and *Trp53(-/-)* compared with *Trp53(+/+)* mice (Figure 6A). In contrast, *Trp53* status had no effect on EROD activity in hepatic microsomes isolated from control (untreated) mice (see Figure 6A), which was in line with no changes being observed in *ex vivo* BaP-DNA adduct formation (compare Figure 3) and BaP metabolite formation *ex vivo* using the same microsomes (compare Figure 4, *left panels*). Cyp1a1 protein levels were increased in pulmonary microsomes isolated from BaP-treated *Trp53(-/-)* compared to *Trp53(+/+)* (Figure 5A), but no significant change in EROD activity was observed (Figure 6B). Lung microsomes isolated from control (untreated) mice showed variability in EROD activity between preparations and/or experiments (compare Figure 6B and 6D) which may also be linked to low basal activity in these microsomes. No changes for Cyp1a1 protein levels, which were close to background levels (Figure 5B), or enzyme activity (Figure 6C and D) were observed in hepatic and pulmonary microsomes isolated from mice treated with 3-NBA between *Trp53* genotypes.

The principal enzyme that activates 3-NBA by nitroreduction is NQO1 (Supporting Figure 1B) (Arlt et al. 2005; Stiborova et al. 2010). The resulting *N*-hydroxy-3-aminobenzanthrone (*N*-OH-3-ABA) can spontaneously form reactive nitrenium ions capable of forming DNA adducts. Alternatively, *N*-OH-3-ABA can be further activated by *N*-acetyltransferases or sulfotransferases leading to the formation of the same reactive nitrenium ions (Arlt 2005). It has been shown that *in vivo* cytosolic nitroreduction of 3-NBA is more important than nitroreduction by microsomal NAD(P)H:cytochrome P450 oxidoreductase (Arlt et al. 2005; Arlt et al. 2003). As we did not observe any differences in DNA adduct formation with 3-NBA, we measured the expression and activity of Nqo1 in hepatic and pulmonary cytosols. In addition, as BaP-derivatives can also be metabolised by NQO1 (Luch and Baird 2005), we also determined expression and activity of Nqo1 in mice exposed to BaP.

All cytosolic samples contained Nqo1 (Figure 5C and D). In both liver and lung, BaP treatment led to an induction of Nqo1 (Figure 5C) that was independent of the *Trp53* genotype of the animals. These findings were in line with increased Nqo1 enzyme activity in these animals after BaP treatment (compare Figure 6E and F); however, *Trp53* status had no effect on Nqo1 enzyme activity in either organ, with or without BaP pretreatment of the animals. In hepatic cytosols Nqo1 protein levels were unchanged in 3-NBA-treated mice (Figure 5D). Nqo1 protein levels were increased in the lungs of 3-NBA-treated *Trp53(+/+)* mice, which is in concordance with previous studies showing that 3-NBA exposure can induce NQO1 (Stiborova et al. 2006; Stiborova et al. 2008), but not in 3-NBA-treated

Trp53(+/-) and *Trp53(-/-)* mice. Exposure to 3-NBA and *Trp53* genotype had no impact on Nqo1 enzyme activity in hepatic and pulmonary cytosols (Figure 6G and H); however, strong variability in Nqo1 activity was seen in lung cytosols isolated from 3-NBA-treated *Trp53(+/+)* mice (Figure 6H). Collectively, these results suggest that p53 expression has no impact on Nqo1-mediated bioactivation of 3-NBA, which correlates with the lack of influence of *Trp53* genotype on 3-NBA-DNA adduct formation *in vivo* (Figure 2).

Discussion

We used *Trp53(+/+)*, *Trp53(+/-)* and *Trp53(-/-)* mice to investigate the effect of p53 on BaP metabolism and DNA adduct formation induced by BaP *in vivo*. The BaP dose used in this study, 125 mg/kg bw, has been shown to be carcinogenic and able to induce mutagenicity in multiple organs after repeated administration (Hakura et al. 1998). We found that BaP-induced DNA adduct formation in liver and kidney was significantly higher in *Trp53(-/-)* mice than in *Trp53 (+/+)* mice after acute BaP treatment. Similar trends in DNA adduct formation were seen in other tissues (*e.g.* lung), although the difference in adduct formation did not reach statistical significance. This is in contrast to another study examining the effect of pentachlorophenol on DNA adduct formation in *Trp53(+/+)* and *Trp53(-/-)* mice exposed to BaP (Ress et al. 2002). In that study no influence of *Trp53* status on BaP-DNA adduct formation was evident in the tissues investigated, namely liver and lung. The discrepancy between the two studies could be attributable to the different dosing regimens (*i.e.* a higher BaP dose was used in our study) but otherwise remains unexplained at present. CYP1A1 is considered to be one of the key enzymes responsible for the metabolic activation of BaP in organisms (Luch and Baird 2005). Our data showed that higher BaP-DNA adduct levels in the livers of *Trp53(-/-)* mice relative to *Trp53(+/+)* mice correlated with higher hepatic Cyp1a protein levels and increased Cyp1a enzyme activity in these animals. The amounts of BaP metabolites formed in incubations using hepatic microsomes isolated from BaP-pretreated *Trp53(-/-)* and *Trp53(+/-)* mice were higher than when using those from BaP-pretreated *Trp53(+/+)* mice. This indicates again that Cyp activity was induced in *Trp53(-/-)* mice which correlated with higher BaP-DNA adduct formation in this mouse line.

Studies investigating xenobiotic metabolism and/or carcinogen-DNA adduct formation in transgenic mice with altered *Trp53* status are sparse and have mainly used *Trp53(+/-)* mice (Ariyoshi et al. 2001; Carmichael et al. 2001; Mori et al. 2001; Sanders et al. 2001). In one study DNA adduct levels induced by diethylstilbestrol (DES) were ~2-fold higher in *Trp53(+/-)* mice than in *Trp53(+/+)* mice (Carmichael et al. 2001). Small differences in the protein expression of several Cyp enzymes including Cyp1a1/2, Cyp1b1, Cyp2b9 and Cyp3a11 were observed and it was concluded that these differences in the expression of XMEs between *Trp53(+/-)* and *Trp53(+/+)* mice could have contributed to the higher DES-induced DNA adduct levels seen in *Trp53(+/-)* mice. In this context it is noteworthy that we also found higher DNA adduct levels in *Trp53(+/-)* mice relative to *Trp53(+/+)* mice after BaP exposure. Another study found that hepatic Cyp1a protein induction was higher in female *Trp53(+/-)* mice than in *Trp53(+/+)* mice after treatment with

another PAH, 3-methylcholanthrene (Ariyoshi et al. 2001). This finding is in line with our results showing that Cyp1a protein levels and Cyp1a enzyme activity are increased in the livers of *Trp53(+/-)* animals after BaP exposure. Other studies found no difference in the Cyp-mediated metabolism of *N*-butyl-*N*-(4-hydroxy-butyl)nitrosamine, benzene, ethoxyquin or methacrylonitrile between *Trp53(+/+)* and *Trp53(+/-)* mice (Mori et al. 2001; Sanders et al. 2001).

Haploinsufficiency in *TP53* has been shown to promote tumour development (Berger and Pandolfi 2011) as reduction in p53 dosage can impact on a cell's ability to respond to DNA damage (Berger et al. 2011). As such, survival of *Trp53(+/-)* mice show an intermediate survival to that of *Trp53(-/-)* and *Trp53(+/+)* mice, and tumours that develop in *Trp53(+/-)* mice do not always display loss of the remaining wild-type allele (Berger et al. 2011). Interestingly, in kidney *Trp53(+/-)* mice behaved like *Trp53(-/-)* showing higher BaP-DNA adduct levels relative to *Trp53(+/+)* mice while adduct formation in the livers of *Trp53(+/-)* and *Trp53(+/+)* mice was similar but lower compared to *Trp53(-/-)* mice. However, hepatic Cyp1a protein levels as well as Cyp1a enzyme activity was both higher in BaP-treated *Trp53(+/-)* and *Trp53(-/-)* mice than *Trp53(+/+)* mice suggesting that in *Trp53(+/-)* animals other factors besides Cyp1a expression may influence BaP-DNA adduct formation in the liver.

NER is considered to be the main DNA repair pathway for bulky DNA adducts and p53-dependent pathways affecting global genomic NER have been identified (Ford 2005; Sengupta and Harris 2005). Using a modified comet assay we showed that tissue-specific NER capacity did not contribute to the higher BaP-DNA adduct levels observed in *Trp53(-/-)* mice than in *Trp53(+/+)* mice, both in liver and kidney. This conclusion was strengthened by the fact that DNA adduct formation in livers and kidneys of *Trp53(+/+)*, *Trp53(+/-)* and *Trp53(-/-)* mice exposed to the corresponding reactive metabolite of BaP, BPDE, resulted in similar adduct levels in all mouse lines. As treatment with BPDE bypasses the need for metabolic activation, these results again indicated that the level of p53 expression impacts on the metabolic activation of the parent compound, BaP, but not on DNA repair.

Previous studies conducted in a panel of isogenic human cells differing only with respect to their endogenous *TP53* status showed that complete loss of p53 function (i.e. *TP53(-/-)* cells) resulted in considerably lower BaP-DNA adduct levels compared to *TP53(+/+)* cells after BaP exposure (Hockley et al. 2008; Wohak et al. 2014). CYP1A1 protein expression was induced to a much greater extent in *TP53(+/+)* cells than in *TP53(+/-)* and *TP53(-/-)* cells. There were also significantly lower levels of BaP metabolites in the

culture medium of *TP53(+/-)* and *TP53(-/-)* cells correlating with lower BaP-DNA adduct formation in these cell lines. It was also shown that exposure to BPDE resulted in similar adduct levels in all cell lines and that NER capacity did not contribute to the observed differences in BaP-DNA adduct formation as the repair capacity was the same in all cell lines (Wohak et al. 2014). Collectively, these results demonstrate the role of p53 in the CYP1A1-mediated metabolism of BaP in human cells.

However, the impact of p53 function on BaP metabolism is different *in vitro* and *in vivo*. Whereas loss of p53 function results in a decrease in BaP-DNA adduct formation *in vitro*, loss of p53 function *in vivo* leads to an increase in BaP-DNA adduct formation. Other studies (Arlt et al. 2008; Nebert et al. 2013) have revealed a paradox, whereby CYP enzymes (particularly CYP1A1) appear to be more important for detoxification of BaP *in vivo*, despite being involved in its metabolic activation *in vitro*, demonstrating that XMEs can have different effects on carcinogen metabolism *in vitro* and *in vivo*. Nevertheless, the mechanism involved in the altered expression and activity of Cyp1a enzymes by p53 function in mice is presently unclear. Additionally, it will be necessary to examine whether there are species-dependent differences between cultured human and mouse cells in the p53-dependent BaP metabolism *in vitro*.

Many studies have shown that BaP can induce CYP1A1 through binding to the aryl hydrocarbon receptor (AhR), a transcription factor that also regulates the expression of a number of phase I and phase II XME genes (Shimizu et al. 2000; Wang et al. 2011). However, when BaP was administered i.p. to *Ahr(-/-)* mice, total BaP-DNA adduct levels were similar to those in *Ahr(+/+)* mice, although the formation of individual adduct spots determined by ^{32}P-postlabelling varied (Kondraganti et al. 2003). In contrast, in other studies BaP-induced adduct levels in the livers of *Ahr(-/-)* mice were significantly higher than those in *Ahr(+/+)* mice after oral administration (Sagredo et al. 2009; Sagredo et al. 2006). Thus these studies provide evidence of a mechanism of BaP biotransformation that is Ahr-independent. Whether this mechanism involves p53 function *in vivo* is currently untested and would require the creation of a *Ahr(-/-)*/*Trp53(-/-)* double knockout mouse line.

We recently found that BaP-induced CYP1A1 expression in human cells can be regulated through p53 binding to a p53 response element (p53RE) in the *CYP1A1* promoter region, thereby enhancing its transcription and thus explaining the role of p53 function in BaP metabolism *in vitro* as described above (Wohak et al. 2014). Others have shown that p53 induces the activity of CYP3A4 in human cells via its binding to p53REs and the subsequent transcriptional enhancement of *CYP3A4* (Goldstein et al. 2013). However, the induction of

Cyps like Cyp1a1 via p53 binding to a p53RE in the *Cyp1a1* promoter region fails to explain the impact of p53 on BaP metabolism *in vivo* (present study), as Cyp1a protein levels and Cyp1a enzyme activity were actually the higher in *Trp53(-/-)* mice which lack p53 function suggesting that the mechanism is different *in vitro* and *in vivo*, at least in the rodent model.

It remains to be seen whether this observation is specific to BaP or a more general phenomenon. However, bioactivation and DNA adduct formation of 3-NBA *in vivo* was not influenced by *Trp53* status (present study) which is in concordance with previous findings that 3-NBA induces similar levels of DNA adducts in human *TP53(+/+)* and *TP53(-/-)* cell lines (Hockley et al. 2008; Simoes et al. 2008). This observation indicates that the cellular impact of p53 on carcinogen metabolism depends on the agent studied and/or that only certain XMEs depend on p53 function. The most efficient enzyme to activate 3-NBA to DNA adducts is NQO1 (Arlt et al. 2005; Stiborova et al. 2010) and thus, NQO1 seems to be an enzyme not affected by p53 expression. This is in line with the fact that overall Nqo1 protein levels and Nqo1 enzyme activity were not significantly different in the *Trp53(+/+)*, *Trp53(+/-)* and *Trp53(-/-)* mouse lines, both after BaP and 3-NBA treatment. Future studies will be required to address this question thereby testing other environmental and dietary carcinogens both *in vitro* and *in vivo*.

In summary, we found that murine Cyp-mediated bioactivation of BaP *in vivo* is influenced by p53 function thereby providing new fundamental insights into PAH-induced carcinogenesis. These results indicate that gene-environmental interactions need to be taken into account with regards to xenobiotic metabolism. Our results are in line with studies demonstrating an emerging role for p53 in carcinogen metabolism in human cells *in vitro*. Whereas in human cells BaP-induced CYP1A1 expression is regulated through p53 binding to a p53RE in the *CYP1A1* promoter region, thereby enhancing its transcription, the mechanism involved in the altered expression and activity of the Cyp1a1 enzyme by p53 *in vivo* in mice has yet to be identified. Future investigations will need to assess whether the metabolic activation of other environmental carcinogens depends on p53 *in vivo* and where the differences lie between murine and human p53.

Acknowledgement

Work at King's College London is supported by Cancer Research UK (grant C313/A14329) and the Wellcome Trust (grants 101126/Z/13/Z and 101126/B/13/Z). Annette Krais was supported by a fellowship of the German Research Foundation. Work at Charles University was supported by a UNCE 204025/2012 Center grant and the Grant Agency of the Czech Republic (GACR; grant 14-18344S in panel P301). David Phillips and Volker Arlt are members of the Wellcome Trust funded COMSIG (Causes Of Mutational SIGnatures) consortium.

References

Ariyoshi N, Imaoka S, Nakayama K, Takahashi Y, Fujita K, Funae Y, Kamataki T (2001) Comparison of the levels of enzymes involved in drug metabolism between transgenic or gene-knockout and the parental mice. Toxicol Pathol 29 Suppl:161-172

Arlt VM (2005) 3-Nitrobenzanthrone, a potential human cancer hazard in diesel exhaust and urban air pollution: a review of the evidence. Mutagenesis 20:399-410

Arlt VM, Bieler CA, Mier W, Wiessler M, Schmeiser HH (2001) DNA adduct formation by the ubiquitous environmental contaminant 3-nitrobenzanthrone in rats determined by (32)P-postlabeling. Int J Cancer 93:450-454

Arlt VM, Glatt H, Muckel E, Pabel U, Sorg BL, Schmeiser HH, Phillips DH (2002) Metabolic activation of the environmental contaminant 3-nitrobenzanthrone by human acetyltransferases and sulfotransferase. Carcinogenesis 23:1937-1945

Arlt VM, Poirier MC, Sykes SE, John K, Moserova M, Stiborova M, Wolf CR, Henderson CJ, Phillips DH (2012) Exposure to benzo[a]pyrene of Hepatic Cytochrome P450 Reductase Null (HRN) and P450 Reductase Conditional Null (RCN) mice: Detection of benzo[a]pyrene diol epoxide-DNA adducts by immunohistochemistry and 32P-postlabelling. Toxicol Lett 213:160-166

Arlt VM, Schmeiser HH, Osborne MR, Kawanishi M, Kanno T, Yagi T, Phillips DH, Takamura-Enya T (2006) Identification of three major DNA adducts formed by the carcinogenic air pollutant 3-nitrobenzanthrone in rat lung at the C8 and N2 position of guanine and at the N6 position of adenine. Int J Cancer 118:2139-2146

Arlt VM, Stiborova M, Henderson CJ, Osborne MR, Bieler CA, Frei E, Martinek V, Sopko B, Wolf CR, Schmeiser HH, Phillips DH (2005) Environmental pollutant and potent mutagen 3-nitrobenzanthrone forms DNA adducts after reduction by NAD(P)H:quinone oxidoreductase and conjugation by acetyltransferases and sulfotransferases in human hepatic cytosols. Cancer Res 65:2644-2652

Arlt VM, Stiborova M, Henderson CJ, Thiemann M, Frei E, Aimova D, Singh R, Gamboa da Costa G, Schmitz OJ, Farmer PB, Wolf CR, Phillips DH (2008) Metabolic activation of benzo[a]pyrene in vitro by hepatic cytochrome P450 contrasts with detoxification in vivo: experiments with hepatic cytochrome P450 reductase null mice. Carcinogenesis 29:656-665

Arlt VM, Stiborova M, Hewer A, Schmeiser HH, Phillips DH (2003) Human enzymes involved in the metabolic activation of the environmental contaminant 3-nitrobenzanthrone: evidence for reductive activation by human NADPH:cytochrome p450 reductase. Cancer Res 63:2752-2761

Bauer E, Guo Z, Ueng YF, Bell LC, Zeldin D, Guengerich FP (1995) Oxidation of benzo[a]pyrene by recombinant human cytochrome P450 enzymes. Chem Res Toxicol 8:136-142

Berger AH, Knudson AG, Pandolfi PP (2011) A continuum model for tumour suppression. Nature 476:163-169

Berger AH, Pandolfi PP (2011) Haplo-insufficiency: a driving force in cancer. J Pathol 223(2):137-146

Carmichael PL, Mills JJ, Campbell M, Basu M, Caldwell J (2001) Mechanisms of hormonal carcinogenesis in the p53+/- hemizygous knockout mouse: studies with diethylstilbestrol. Toxicol Pathol 29 Suppl:155-160

Donehower LA (2014) Insights into wild-type and mutant p53 functions provided by genetically engineered mice. Human Mutat 35:715-727

Ford JM (2005) Regulation of DNA damage recognition and nucleotide excision repair: another role for p53. Mutat Res 577:195-202

Goldstein I, Rivlin N, Shoshana OY, Ezra O, Madar S, Goldfinger N, Rotter V (2013) Chemotherapeutic agents induce the expression and activity of their clearing enzyme CYP3A4 by activating p53. Carcinogenesis 34:190-198

Güngör N, Haegens A, Knaapen AM, Godschalk RW, Chiu RK, Wouters EF, van Schooten FJ (2010) Lung inflammation is associated with reduced pulmonary nucleotide excision repair in vivo. Mutagenesis 25:77-82

Hakura A, Tsutsui Y, Sonoda J, Kai J, Imade T, Shimada M, Sugihara Y, Mikami T (1998) Comparison between in vivo mutagenicity and carcinogenicity in multiple organs by benzo[a]pyrene in the lacZ transgenic mouse (Muta Mouse). Mutat Res 398:123-130

Hockley SL, Arlt VM, Brewer D, Giddings I, Phillips DH (2006) Time- and concentration-dependent changes in gene expression induced by benzo(a)pyrene in two human cell lines, MCF-7 and HepG2. BMC Genomics 7:260

Hockley SL, Arlt VM, Jahnke G, Hartwig A, Giddings I, Phillips DH (2008) Identification through microarray gene expression analysis of cellular responses to benzo(a)pyrene and its diol-epoxide that are dependent or independent of p53. Carcinogenesis 29:202-210

Jacks T, Remington L, Williams BO, Schmitt EM, Halachmi S, Bronson RT, Weinberg RA. (1994) Tumor spectrum analysis in p53-mutant mice. Curr Biol 4:1-7

Kenzelmann Broz D, Attardi LD (2010) In vivo analysis of p53 tumor suppressor function using genetically engineered mouse models. Carcinogenesis 31:1311-1318

Kim JH, Stansbury KH, Walker NJ, Trush MA, Strickland PT, Sutter TR (1998) Metabolism of benzo[a]pyrene and benzo[a]pyrene-7,8-diol by human cytochrome P450 1B1. Carcinogenesis 19:1847-1853

Kondraganti SR, Fernandez-Salguero P, Gonzalez FJ, Ramos KS, Jiang W, Moorthy B (2003) Polycyclic aromatic hydrocarbon-inducible DNA adducts: evidence by 32P-postlabeling and use of knockout mice for Ah receptor-independent mechanisms of metabolic activation in vivo. Int J Cancer 103:5-11

Kucab JE, Phillips DH, Arlt VM (2010) Linking environmental carcinogen exposure to TP53 mutations in human tumours using the human TP53 knock-in (Hupki) mouse model. Febs J 277:2567-2583

Langie SA, Knaapen AM, Brauers KJ, van Berlo D, van Schooten FJ, Godschalk RW (2006) Development and validation of a modified comet assay to phenotypically assess nucleotide excision repair. Mutagenesis 21:153-158

Lozano G (2010) Mouse models of p53 functions. Cold Spring Harb Perspect Biol 2:a001115

Luch A, Baird WM (2005) Metabolic activation and detoxification of polycyclic aromatic hydrocarbons. Imperial College Press, London

Maddocks OD, Vousden KH (2011) Metabolic regulation by p53. J Mol Med 89:237-245

Mizerovska J, Dracinska H, Frei E, Schmeiser HH, Arlt VM, Stiborova M (2011) Induction of biotransformation enzymes by the carcinogenic air-pollutant 3-nitrobenzanthrone in liver, kidney and lung, after intra-tracheal instillation in rats. Mutat Res 720:34-41

Mori Y, Koide A, Fuwa K, Wanibuchi H, Fukushima S (2001) Lack of change in the levels of liver and kidney cytochrome P-450 isozymes in p53+/- knockout mice treated with N-butyl-N-(4-hydroxybutyl)nitrosamine. Mutagenesis 16:377-383

Nebert DW (2006) Comparison of gene expression in cell culture to that in the intact animal: relevance to drugs and environmental toxicants. Focus on "development of a transactivator in hepatoma cells that allows expression of phase I, phase II, and chemical defense genes". Am J Physiol Cell Physiol 290:C37-41

Nebert DW, Dalton TP (2006) The role of cytochrome P450 enzymes in endogenous signalling pathways and environmental carcinogenesis. Nature Rev 6:947-960

Nebert DW, Shi Z, Galvez-Peralta M, Uno S, Dragin N (2013) Oral benzo[a]pyrene: understanding pharmacokinetics, detoxication, and consequences--Cyp1 knockout mouse lines as a paradigm. Mol Pharmacol 84:304-313

Olivier M, Hollstein M, Hainaut P (2010) TP53 mutations in human cancers: origins, consequences, and clinical use. Cold Spring Harb Perspect Biol 2:a001008

Phillips DH, Arlt VM (2007) The 32P-postlabeling assay for DNA adducts. Nat Protocol 2:2772-2781

Phillips DH, Arlt VM (2014) (3)(2)P-postlabeling analysis of DNA adducts. Meth Mol Biol 1105:127-138

Ress NB, Donnelly KC, George SE (2002) The effect of pentachlorophenol on DNA adduct formation in p53 wild-type and knockout mice exposed to benzo[a]pyrene. Cancer Lett 178:11-17

Sagredo C, Mollerup S, Cole KJ, Phillips DH, Uppstad H, Ovrebo S (2009) Biotransformation of benzo[a]pyrene in Ahr knockout mice is dependent on time and route of exposure. Chem Res Toxicol 22:584-591

Sagredo C, Ovrebo S, Haugen A, Fujii-Kuriyama Y, Baera R, Botnen IV, Mollerup S. (2006) Quantitative analysis of benzo[a]pyrene biotransformation and adduct formation in Ahr knockout mice. Toxicol Lett 167:173-182

Sanders JM, Burka LT, Chanas B, Matthews HB (2001) Comparative xenobiotic metabolism between Tg.AC and p53+/- genetically altered mice and their respective wild types. Toxicol Sci 61:54-61

Sengupta S, Harris CC (2005) p53: traffic cop at the crossroads of DNA repair and recombination. Nat Rev Mol Cell Biol 6:44-55

Shimizu Y, Nakatsuru Y, Ichinose M, Takahashi Y, Kume H, Mimura J, Fujii-Kuriyama Y, Ishikawa T (2000) Benzo[a]pyrene carcinogenicity is lost in mice lacking the aryl hydrocarbon receptor. Proc Natl Acad Sci USA 97:779-782

Simoes ML, Hockley SL, Schwerdtle T, da Costa GG, Schmeiser HH, Phillips DH, Arlt VM (2008) Gene expression profiles modulated by the human carcinogen aristolochic acid I in human cancer cells and their dependence on TP53. Toxicol Appl Pharmacol 232:86-98

Stiborova M, Dracinska H, Hajkova J, Kaderabkova P, Frei E, Schmeiser HH, Soucek P, Phillips DH, Arlt VM. (2006) The environmental pollutant and carcinogen 3-nitrobenzanthrone and its human metabolite 3-aminobenzanthrone are potent inducers of rat hepatic cytochromes P450 1A1 and -1A2 and NAD(P)H:quinone oxidoreductase. Drug Metab Dispos 34:1398-1405

Stiborova M, Dracinska H, Mizerovska J, Frei E, Schmeiser HH, Hudecek J, Hodek P, Phillips DH, Arlt VM. (2008) The environmental pollutant and carcinogen 3-nitrobenzanthrone induces cytochrome P450 1A1 and NAD(P)H:quinone oxidoreductase in rat lung and kidney, thereby enhancing its own genotoxicity. Toxicology 247:11-22

Stiborova M, Martinek V, Svobodova M, Sístkova J, Dvorak Z, Ulrichova J, Simanek V, Frei E, Schmeiser HH, Phillips DH, Arlt VM. (2010) Mechanisms of the different DNA adduct forming potentials of the urban air pollutants 2-nitrobenzanthrone and carcinogenic 3-nitrobenzanthrone. Chem Res Toxicol 23:1192-1201

Stiborova M, Moserova M, Cerna V, Indra R, Dracinsky M, Sulc M, Henderson CJ, Wolf CR, Schmeiser HH, Phillips DH, Frei E, Arlt VM. (2014) Cytochrome b5 and epoxide hydrolase contribute to benzo[a]pyrene-DNA adduct formation catalyzed by cytochrome P450 1A1 under low NADPH:P450 oxidoreductase conditions. Toxicology 318:1-12

Taneja P, Zhu S, Maglic D, Fry EA, Kendig RD, Inoue K (2011) Transgenic and knockout mice models to reveal the functions of tumor suppressor genes. Clin Med Insights Oncol 5:235-257

Wang T, Gavin HM, Arlt VM, Lawrence BP, Fenton SE, Medina D, Vorderstrasse BA. (2011) Aryl hydrocarbon receptor activation during pregnancy, and in adult nulliparous mice, delays the subsequent development of DMBA-induced mammary tumors. Int J Cancer 128:1509-1523

Whibley C, Pharoah PD, Hollstein M (2009) p53 polymorphisms: cancer implications. Nature Rev 9:95-107

Wiechelman KJ, Braun RD, Fitzpatrick JD (1988) Investigation of the bicinchoninic acid protein assay: identification of the groups responsible for color formation. Anal Biochem 175:231-237

Wohak LE, Krais AM, Kucab JE, Stertmann J, Ovrebo S, Seidel A, Phillips DH, Arlt VM (2014) Carcinogenic polycyclic aromatic hydrocarbons induce CYP1A1 in human cells via a p53 dependent mechanism. Arch Toxicol, Nov 15. [Epub ahead of print]

Legends to Figures

Figure 1:

DNA adduct levels measured by ^{32}P-postlabelling in various organs of *Trp53(+/+)*, *Trp53(+/-)* and *Trp53(-/-)* mice after exposure to BaP (A) or BPDE (B). Values are the mean ± SD (n = 4). Statistical analysis was performed by one-way ANOVA followed by Tukey post-hoc test (*p<0.05; different from *Trp53(+/+)* mice).

Figure 2:

DNA adduct levels measured by ^{32}P-postlabelling in various organs of *Trp53(+/+)*, *Trp53(+/-)* and *Trp53(-/-)* mice after exposure to 3-NBA. Values are the mean ± SD (n = 4). Statistical analysis was performed by one-way ANOVA followed by Tukey post-hoc test; no significant differences were observed.

Figure 3:

BaP-DNA adducts, measured by ^{32}P-postlabelling, formed *ex vivo* by hepatic microsomes isolated from control (untreated) (A) and BaP-pretreated (B) *Trp53(+/+)*, *Trp53(+/-)* and *Trp53(-/-)* mice. Values are the mean ± range (n = 4); duplicate incubations and each sample was determined by two independent post-labelled analyses. Statistical analysis was performed by one-way ANOVA followed by Tukey post-hoc test (**p<0.01; different from hepatic microsomes isolated from *Trp53(+/+)* mice). Inserts: Autoradiographic profiles of DNA adducts formed in hepatic microsomes isolated from *Trp53(+/+)* mice; the origins, at the bottom left-hand corners, were cut off before exposure.

Figure 4:

Formation of BaP metabolites by hepatic microsomes isolated from control (untreated) (A, C and E) and BaP-treated (B, D and F) *Trp53(+/+)*, *Trp53(+/-)* and *Trp53(-/-)* mice. Relative peak areas of BaP metabolites were measured by HPLC analysis at 254 nm. Values are the mean ± SD (n = 3). Statistical analysis was performed by one-way ANOVA followed by Tukey post-hoc test (*p<0.05, **p<0.01, ***p<0.005; different from BaP-treated *Trp53(+/+)* mice). Structures of the BaP metabolites detected by HPLC are shown in Supplementary Figure 6C. Mx, an unknown BaP metabolite.

Figure 5:

Western blot analysis of Cyp1a1 (A and B) and Nqo1 protein expression (C and D) in hepatic and pulmonary cytosols isolated from *Trp53(+/+)*, *Trp53(+/-)* and *Trp53(-/-)* mice exposed to BaP (A and C) or 3-NBA (B and D). Representative images of the Western blotting are shown and at least duplicate analysis was performed from independent experiments.

Figure 6:

EROD activity (A-D) in hepatic (A and C) and pulmonary microsomes (B and D) isolated from *Trp53(+/+)*, *Trp53(+/-)* and *Trp53(-/-)* mice. Nqo1 enzyme activity (E-H) was determined in hepatic (E and G) and pulmonary cytosols (F and H). Values are the mean ± SD ($n = 4$). Statistical analysis was performed by one-way ANOVA followed by Tukey post-hoc test (*$p<0.05$; different from *Trp53(+/+)* mice).

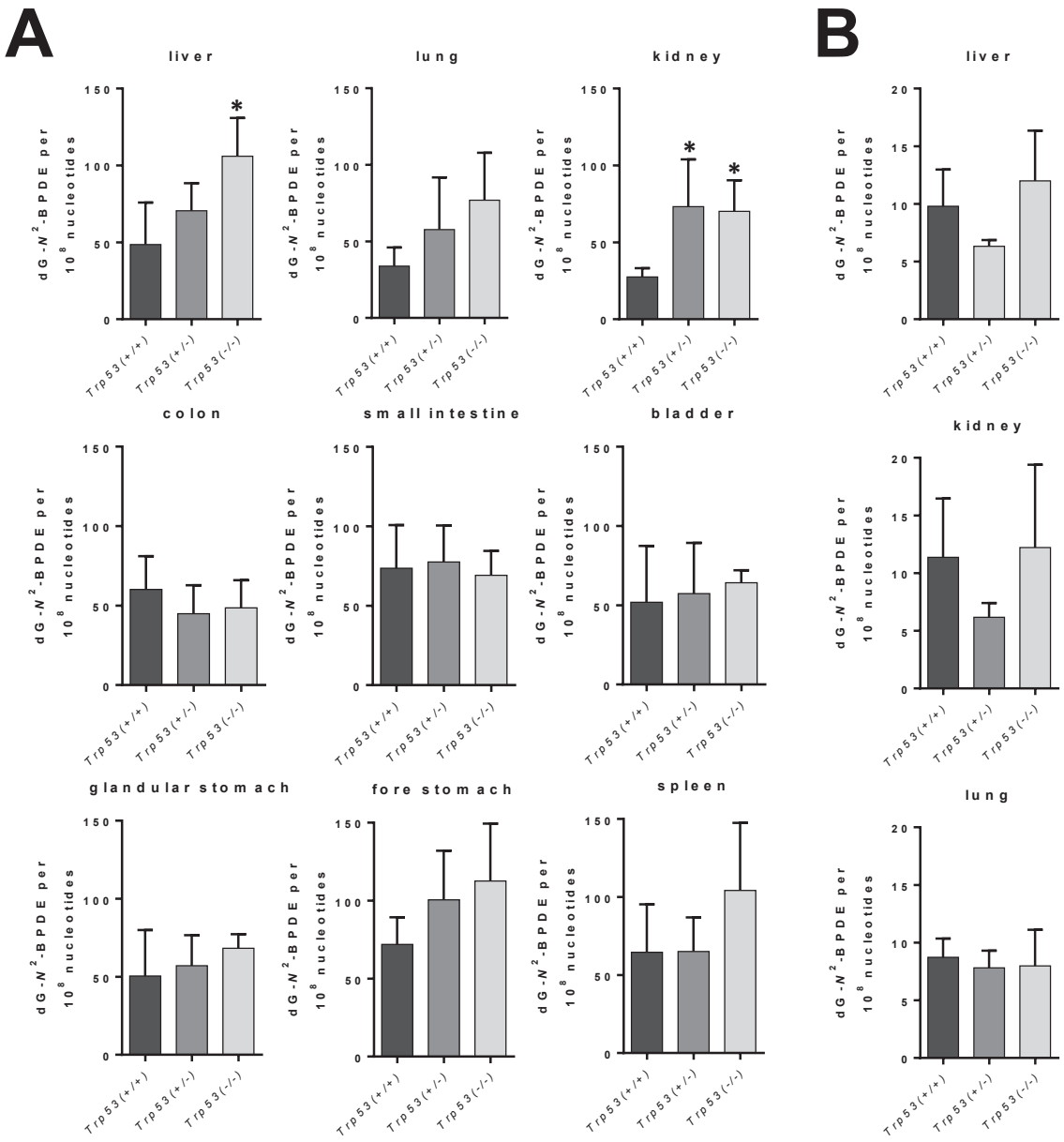
A
liver
lung
kidney
colon
small intestine
bladder
glandular stomach
fore stomach
spleen
B
liver
kidney
lung
dG-N2-BPDE per 10^8 nucleotides
Trp53(+/+)
Trp53(+/-)
Trp53(-/-)

Figure 1

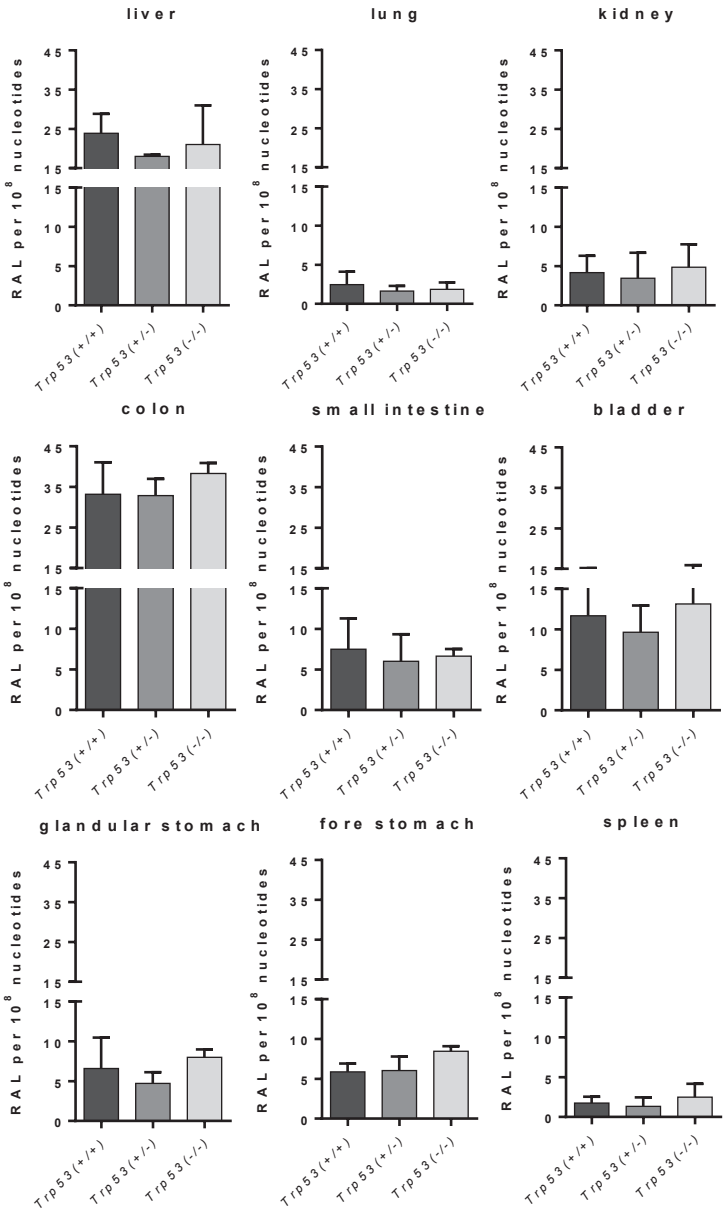
liver
lung
kidney
colon
small intestine
bladder
glandular stomach
fore stomach
spleen
RAL per 10^8 nucleotides
Trp53(+/+)
Trp53(+/-)
Trp53(-/-)

Figure 2

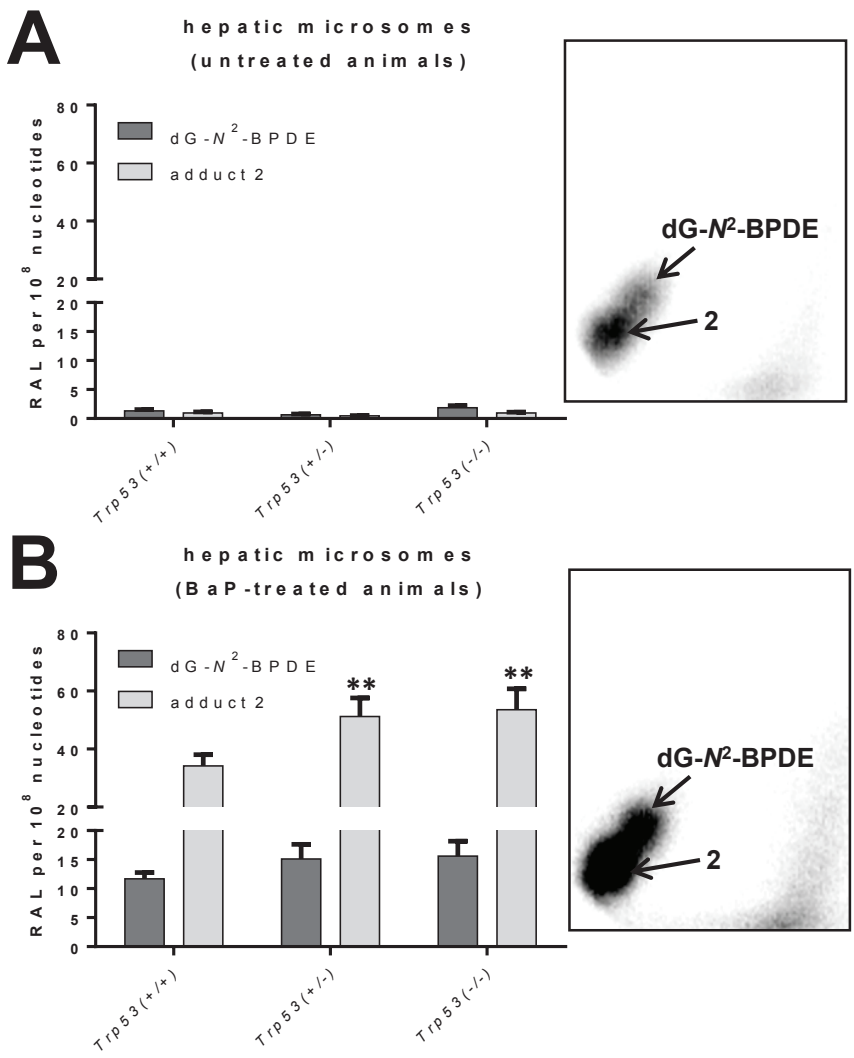
A
hepatic microsomes
(untreated animals)
RAL per 10^8 nucleotides
dG-N^2-BPDE
adduct 2
dG-N2-BPDE
2
Trp53(+/+)
Trp53(+/-)
Trp53(-/-)
B
hepatic microsomes
(BaP-treated animals)
RAL per 10^8 nucleotides
dG-N^2-BPDE
adduct 2
**
**
dG-N2-BPDE
2
Trp53(+/+)
Trp53(+/-)
Trp53(-/-)

Figure 3

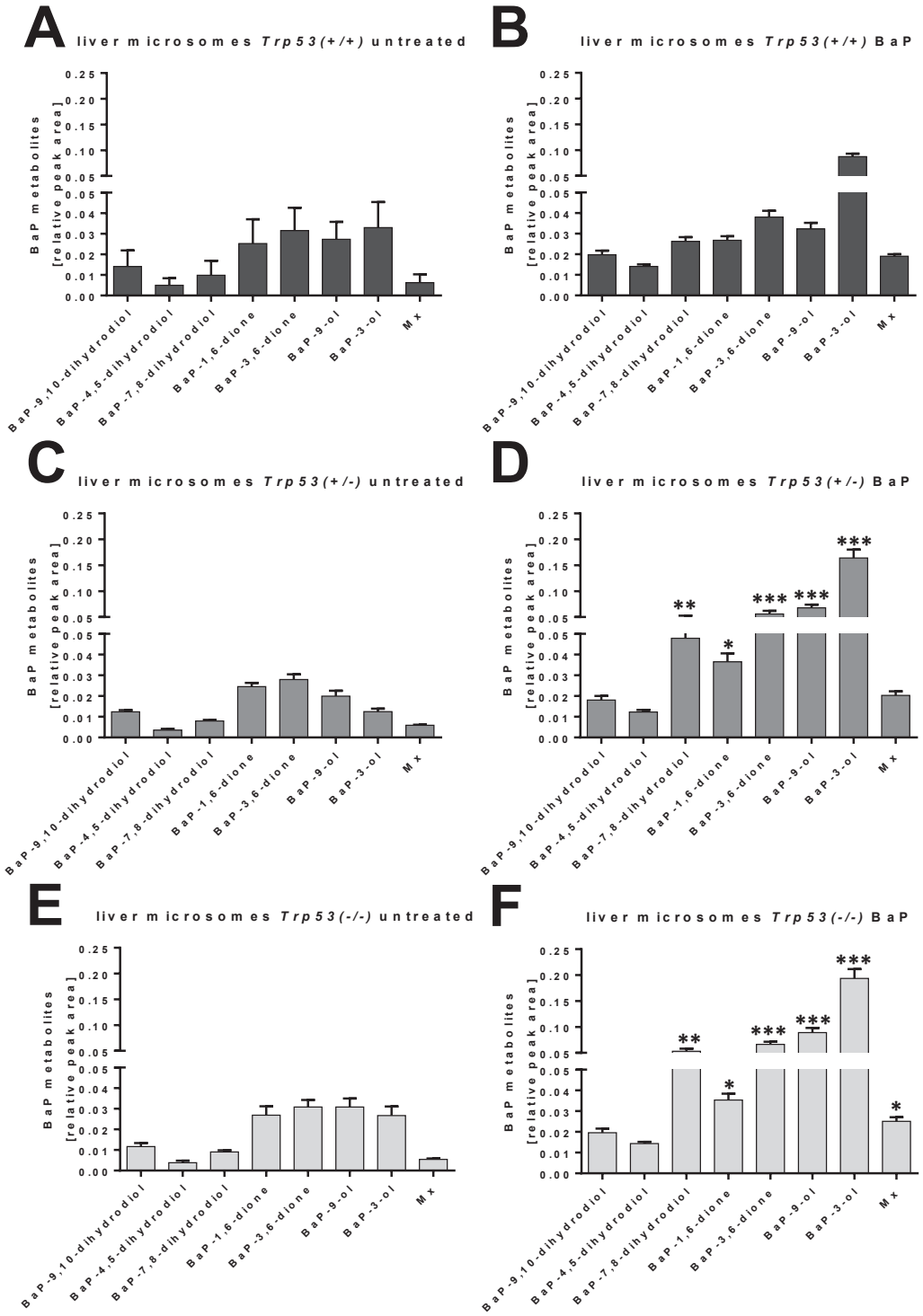
A
liver microsomes Trp53(+/+) untreated
B
liver microsomes Trp53(+/+) BaP
C
liver microsomes Trp53(+/-) untreated
D
liver microsomes Trp53(+/-) BaP
E
liver microsomes Trp53(-/-) untreated
F
liver microsomes Trp53(-/-) BaP
BaP metabolites [relative peak area]
BaP-9,10-dihydrodiol
BaP-4,5-dihydrodiol
BaP-7,8-dihydrodiol
BaP-1,6-dione
BaP-3,6-dione
BaP-9-ol
BaP-3-ol
Mx

Figure 4

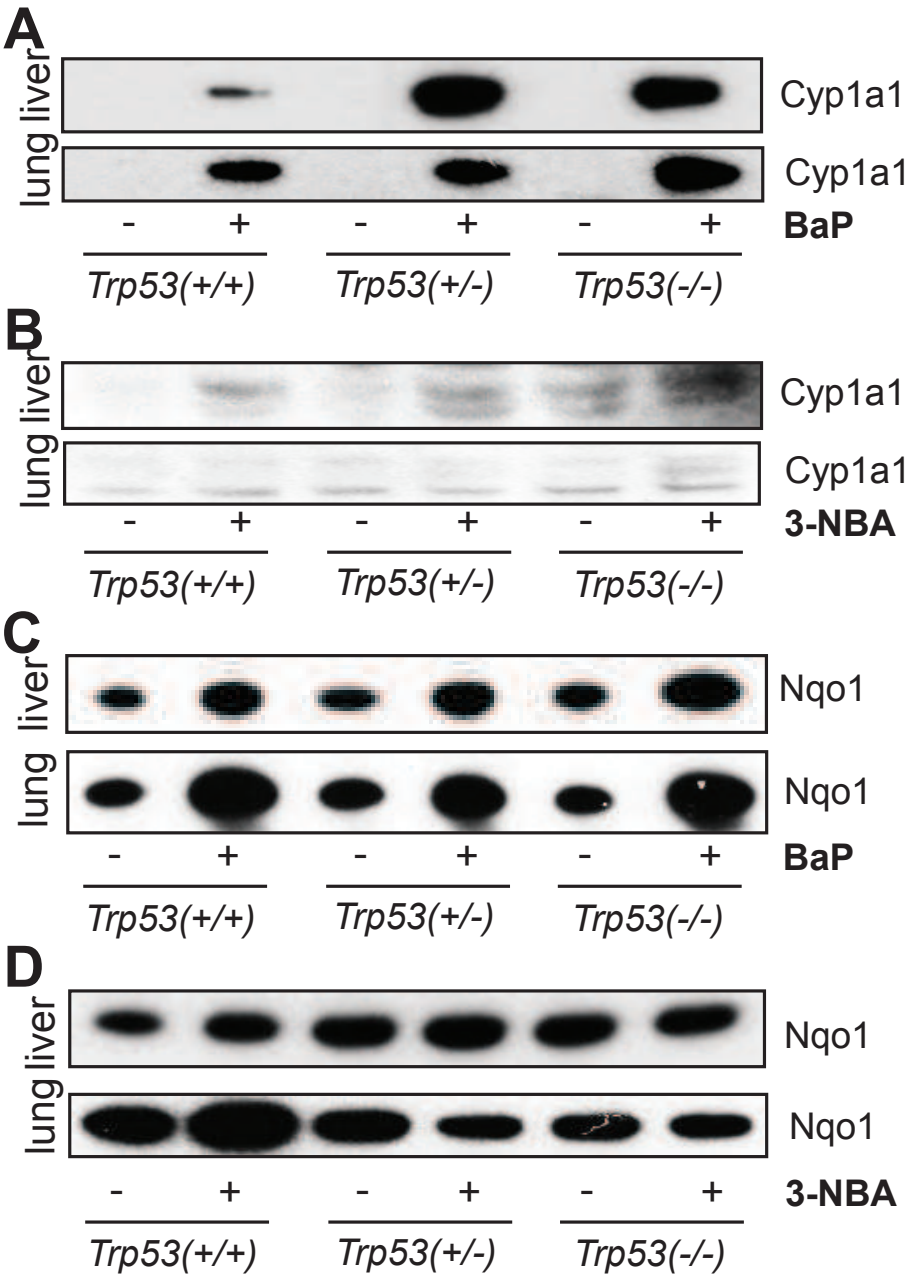
A
lung liver
Cyp1a1
Cyp1a1
- + - + - +
BaP
Trp53(+/+) Trp53(+/-) Trp53(-/-)
B
lung liver
Cyp1a1
Cyp1a1
- + - + - +
3-NBA
Trp53(+/+) Trp53(+/-) Trp53(-/-)
C
lung liver
Nqo1
Nqo1
- + - + - +
BaP
Trp53(+/+) Trp53(+/-) Trp53(-/-)
D
lung liver
Nqo1
Nqo1
- + - + - +
3-NBA
Trp53(+/+) Trp53(+/-) Trp53(-/-)

Figure 5

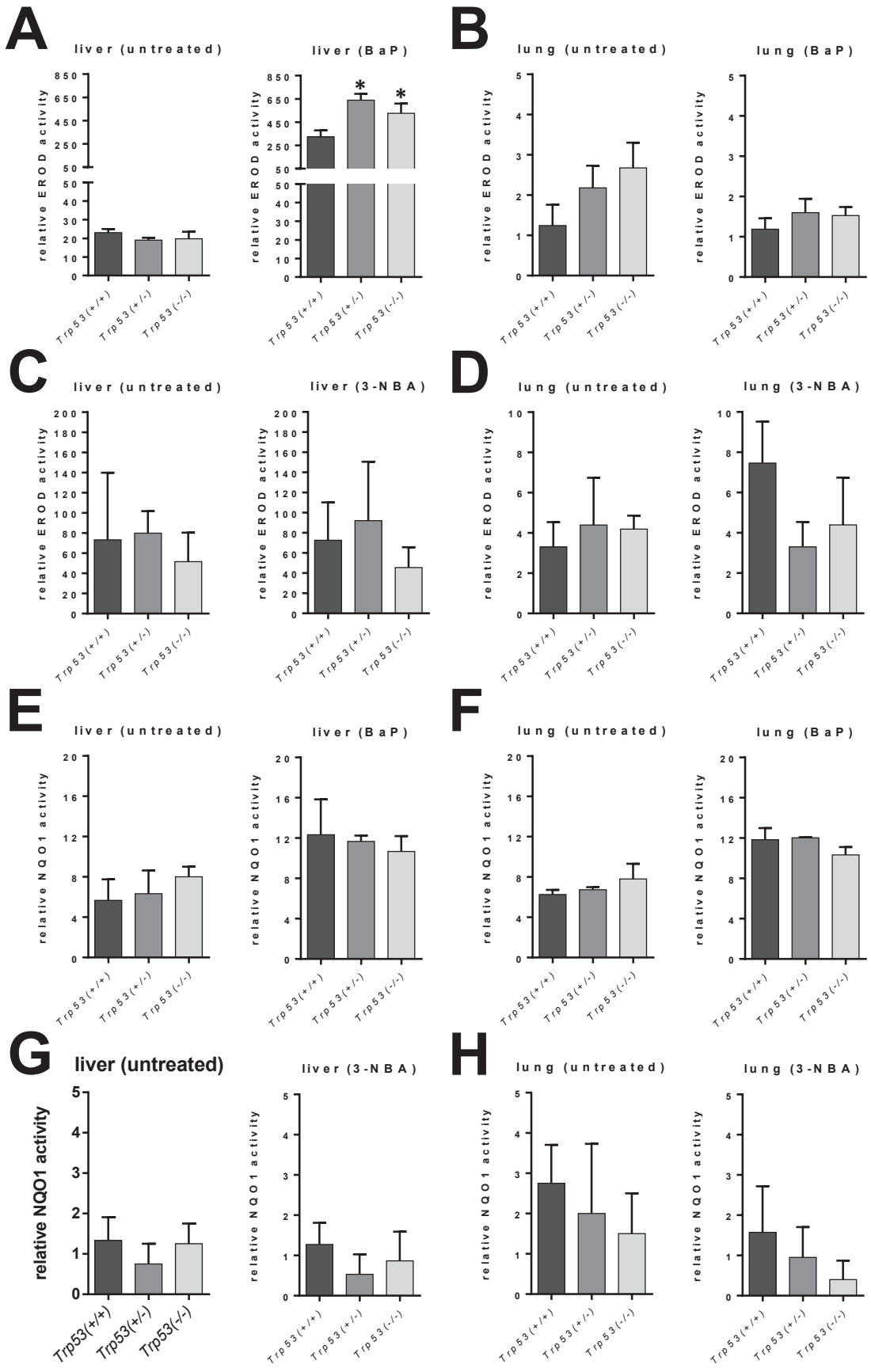
A
liver (untreated)
liver (BaP)
B
lung (untreated)
lung (BaP)
C
liver (untreated)
liver (3-NBA)
D
lung (untreated)
lung (3-NBA)
E
liver (untreated)
liver (BaP)
F
lung (untreated)
lung (BaP)
G
liver (untreated)
liver (3-NBA)
H
lung (untreated)
lung (3-NBA)
relative EROD activity
relative NQO1 activity
Trp53(+/+)
Trp53(+/-)
Trp53(-/-)

Figure 6

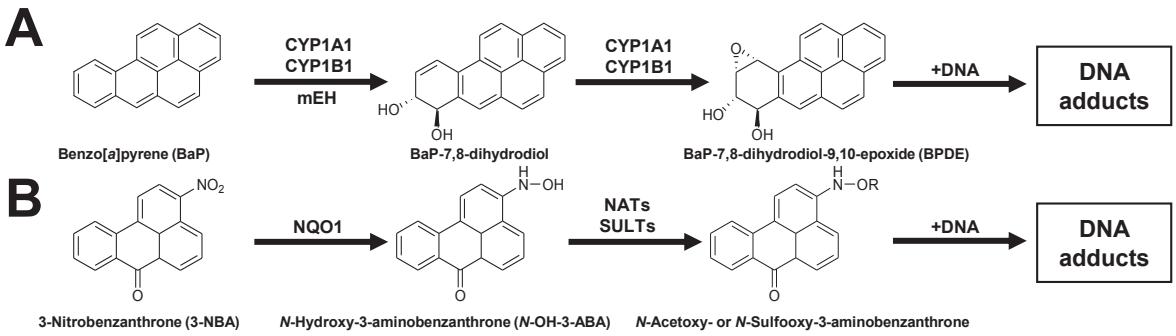

Supporting Figure 1

Main metabolic pathways in the bioactivation and DNA adduct formation *in vivo* of BaP (A) and 3-NBA (B). R = – $C(O)CH_3$; R = – SO_3H. See text for details. CYP, cytochrome P450; mEH, microsomal epoxide hydrolase; NQO1, NAD(P)H:quinone oxidoreductase; NAT, *N*-Acetyltransferase; SULT, sulfotransferase.

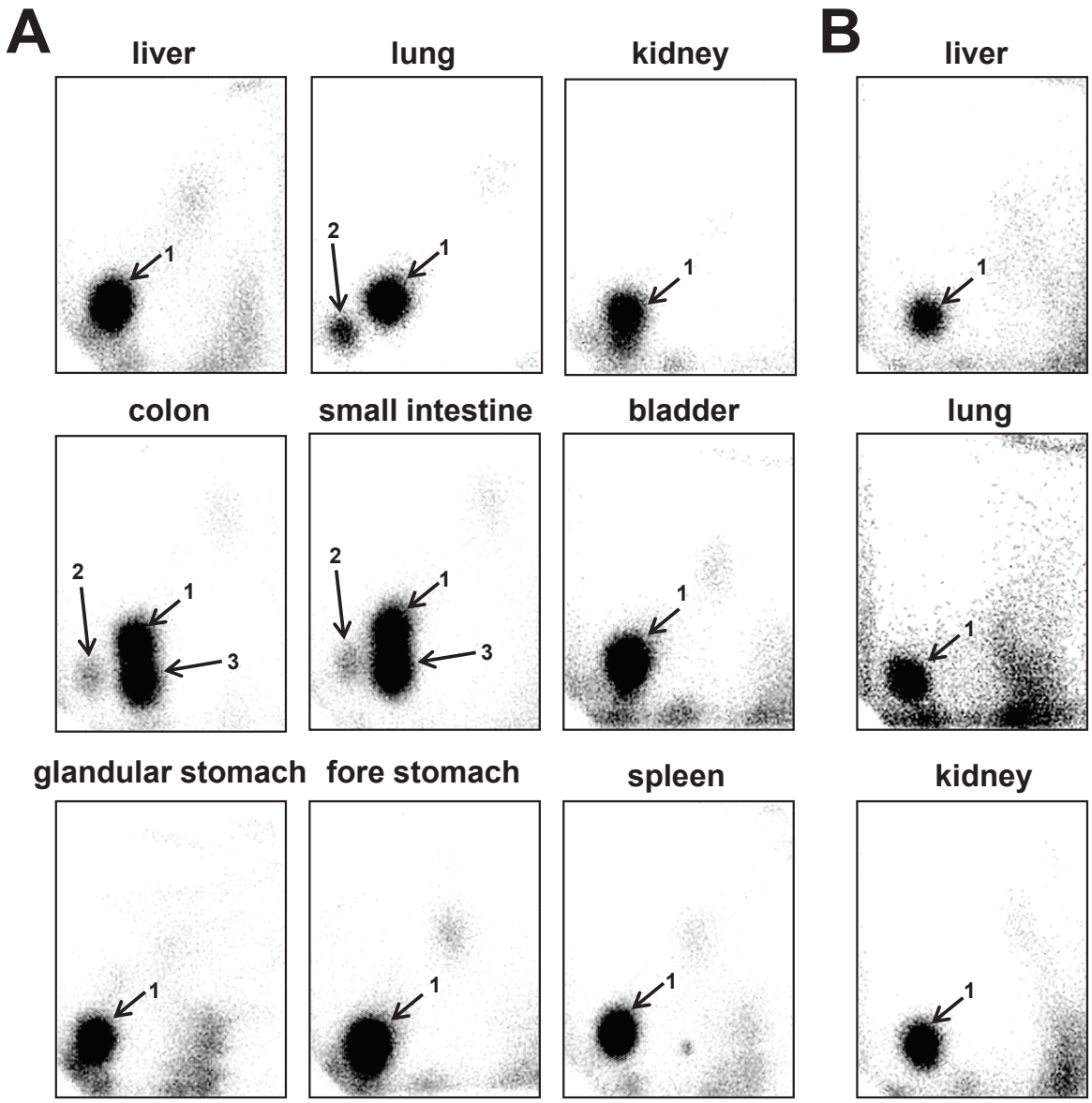

Supporting Figure 2

Autoradiographic profiles of DNA adducts, measured by ^{32}P-postlabelling, in various tissues of *Trp53(+/+)* mice exposed to BaP (A) or BPDE (B). The adduct profiles shown are representative for the same organs in *Trp53(+/-)* and *Trp53(-/-)* mice. Solvent conditions for the separation of BaP-derived DNA adducts were as follows: D1, 1.0 M sodium phosphate, pH 6.0; D3, 3.5 M lithium-formate, 8.5 M urea, pH 3.5; D4, 0.8 M lithium chloride, 0.5 M Tris, 8.5 M urea, pH 8.0. The origins, at the bottom left-hand corners, were cut off before exposure. Spot 1, 10-(deoxyguanosin-N^2-yl)-7,8,9-trihydroxy-7,8,9,10-tetrahydro-BaP (dG-N^2-BPDE); Spot 2, probable guanine adduct derived from reaction with 9-hydroxy-BaP-4,5-epoxide; Spot 3, uncharacterised BaP-derived DNA adducts. For the pathways of BaP-DNA adduct formation see Supporting Figure 4.

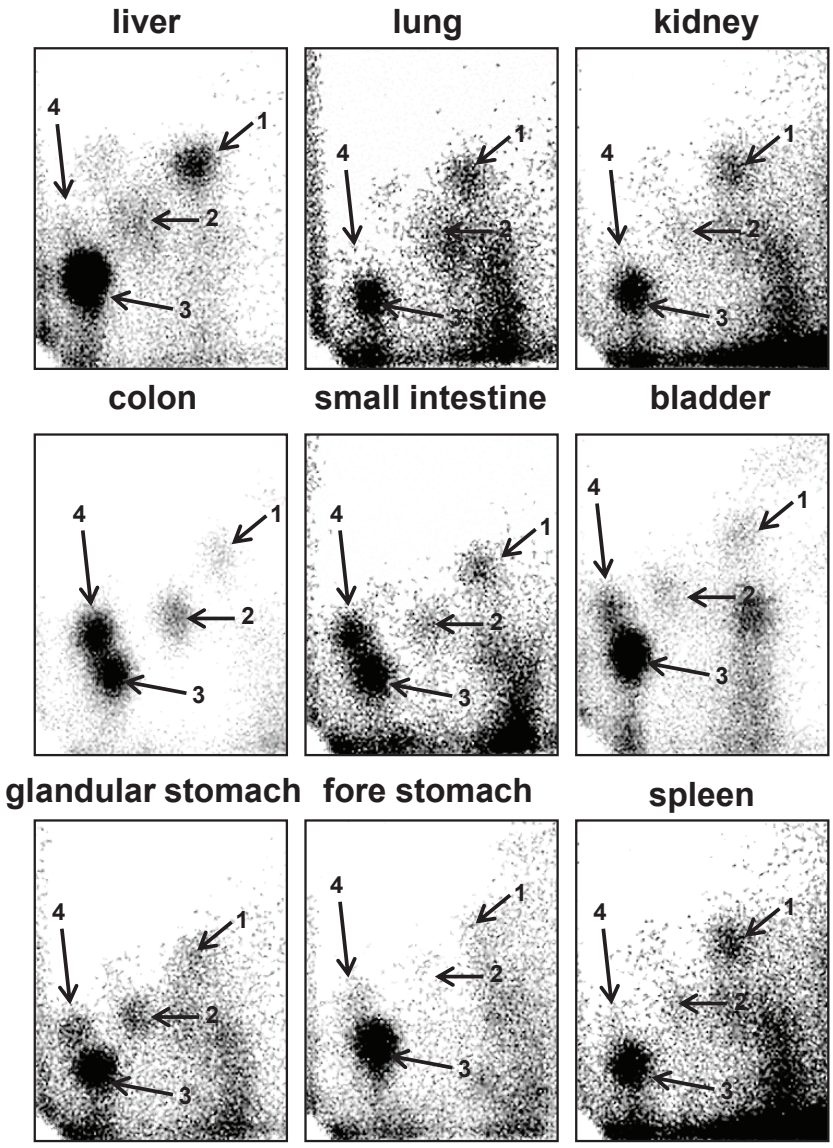

Supporting Figure 3

Autoradiographic profiles of DNA adducts, measured by ^{32}P-postlabelling, in various tissues of *Trp53(+/+)* mice exposed to 3-NBA. The adduct profiles shown are representative for the same organs in *Trp53(+/-)* and *Trp53(-/-)* mice. 3-NBA-derived DNA adducts were separated using the following solvent conditions: D1, 1.0 M sodium phosphate, pH 6.0; D3, 4.0 M lithium-formate, 7.0 M urea, pH 3.5; D4, 0.8 M lithium chloride, 0.5 M Tris, 8.5 M urea, pH 8.0. The origins, at the bottom left-hand corners, were cut off before exposure. Spot 1, 2-(2'-deoxyadenosine-N^6-yl)-3-aminobenzanthrone (dA-N^6-3-ABA); Spot 2, as-yet unidentified adenine adduct derived from nitroreduction; Spot 3, *N*-(2'-deoxyguanosine-N^2-yl)-3-aminobenzanthrone (dG-N^2-3-ABA); Spot 4, *N*-(2'-deoxyguanosin-8-yl)-3-aminobenzanthrone (dG-C8-*N*-3-ABA).

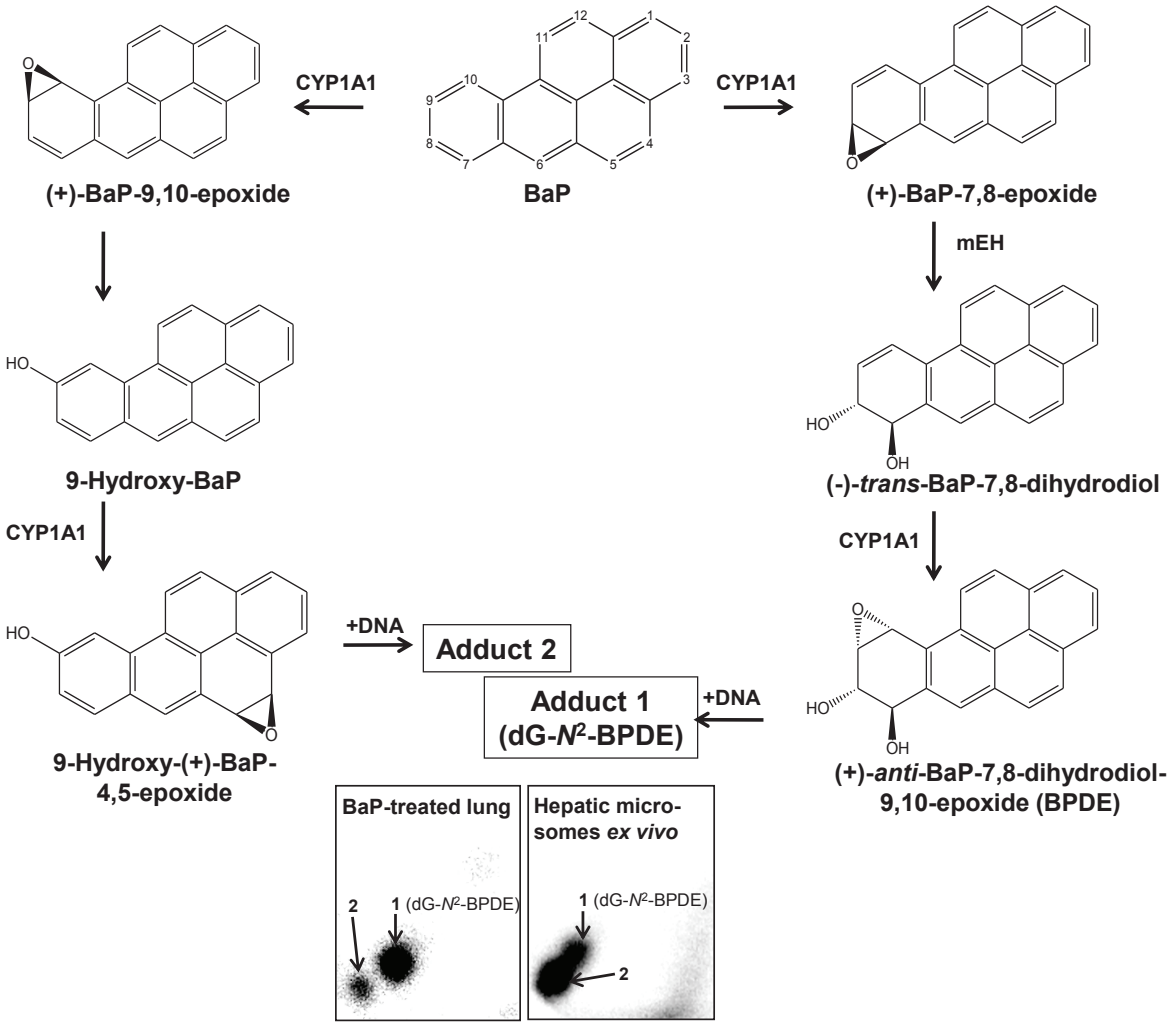

Supporting Figure 4

Pathways of biotransformation and DNA adduct formation of BaP catalysed by CYP1A1 and microsomal epoxide hydrolase (mEH) [adapted from (Stiborova et al. 2014)]. The typical three-step activation process with oxidation by CYP1A1 followed by hydrolysis by mEH leads to the ultimately reactive species BPDE which leads to the generation of the dG-N^2-BPDE adduct. The two-step activation process by CYP1A1 is leading to the formation of the ultimately reactive species, 9-hydroxy-BaP-4,5-epoxide, that can react with deoxyguanosine in DNA (adduct 2; structure unknown). Insert: Autoradiographic profiles of BaP-DNA adducts, measured by ^{32}P-postlabelling, formed in the lungs of BaP-treated *Trp53(+/+)* mice (see also Supporting Figure 2A) or *ex vivo* in hepatic microsomes isolated from BaP-pretreated *Trp53(+/+)* mice (see also Figure 3); the origin, at the bottom left-hand corners, was cut off before exposure.

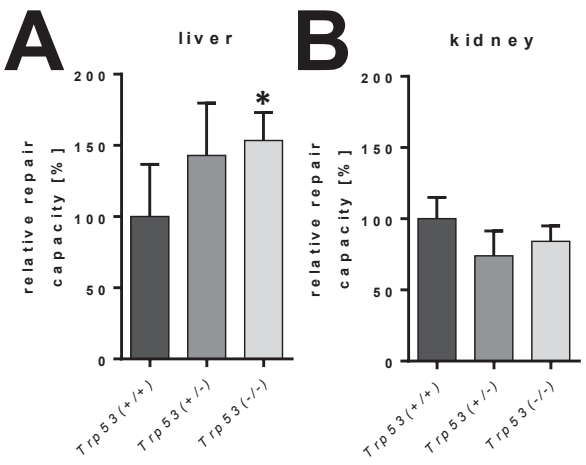

Supporting Figure 5

NER capacity in liver (A) and kidney (B) of *Trp53(+/+)*, *Trp53(+/-)* and *Trp53(-/-)* mice as assessed by Comet Assay. Values are the mean ± SD (n = 4). Statistical analysis was performed by one-way ANOVA followed by Tukey post-hoc test (*p<0.05; different from *Trp53(+/+)* mice).

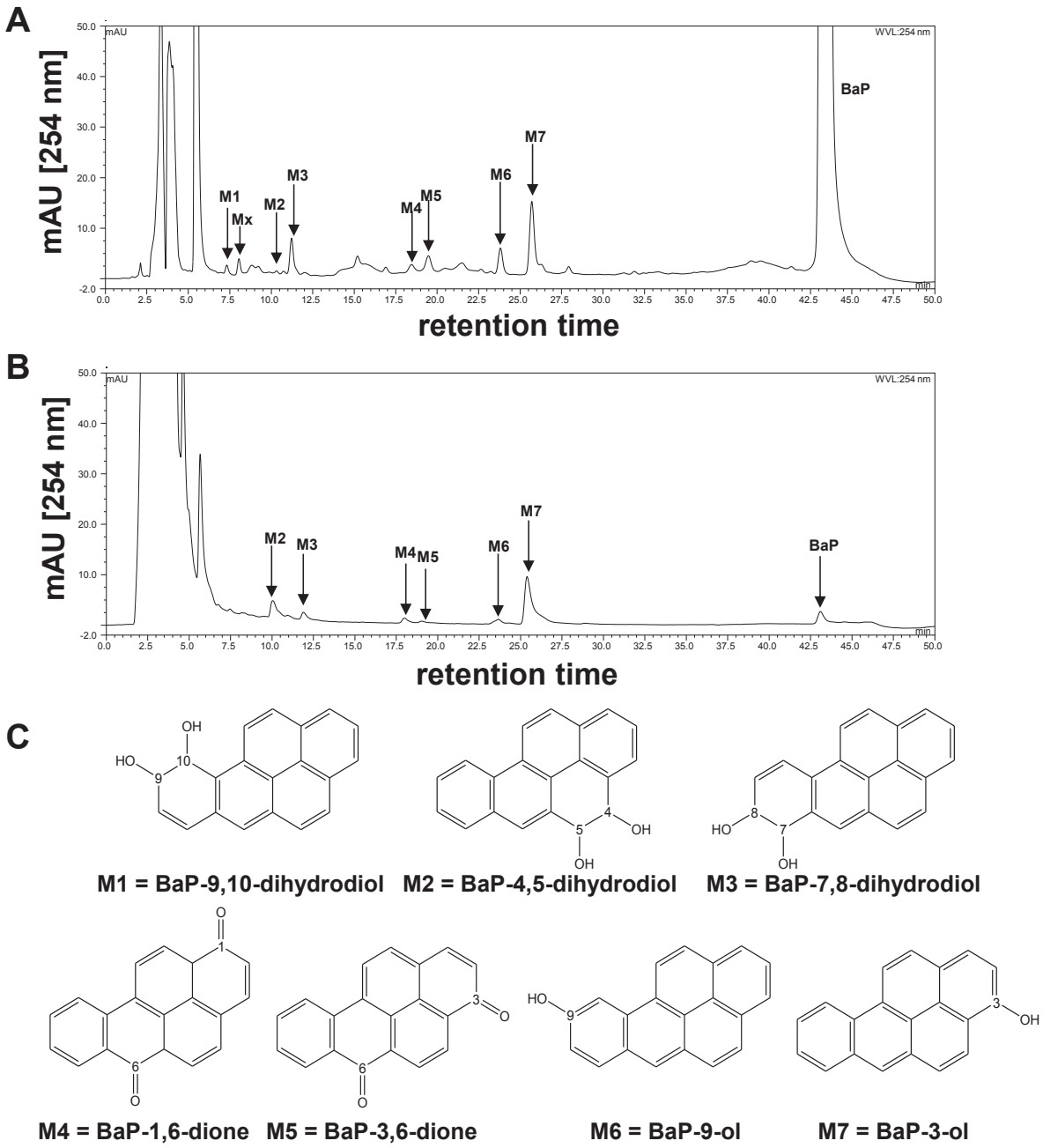

Supporting Figure 6

(A) Representative HPLC chromatogram of the BaP metabolites generated by hepatic microsomes of BaP-pretreated *Trp53(+/+)*. (B) Representative HPLC chromatogram of the BaP metabolites found in urine of *Trp53(+/+)* mice exposed to BaP. M1-M7, BaP metabolites [BaP-9,10-dihydrodiol (M1), BaP-4,5-dihydrodiol (M2), BaP-7,8-dihydrodiol (M3), BaP-1,6-dione (M4), BaP-3,6-dione (M5), BaP-9-ol (M6), BaP-3-ol (M7) and an unknown BaP metabolite (Mx)]. (C) Structures of the BaP metabolites.

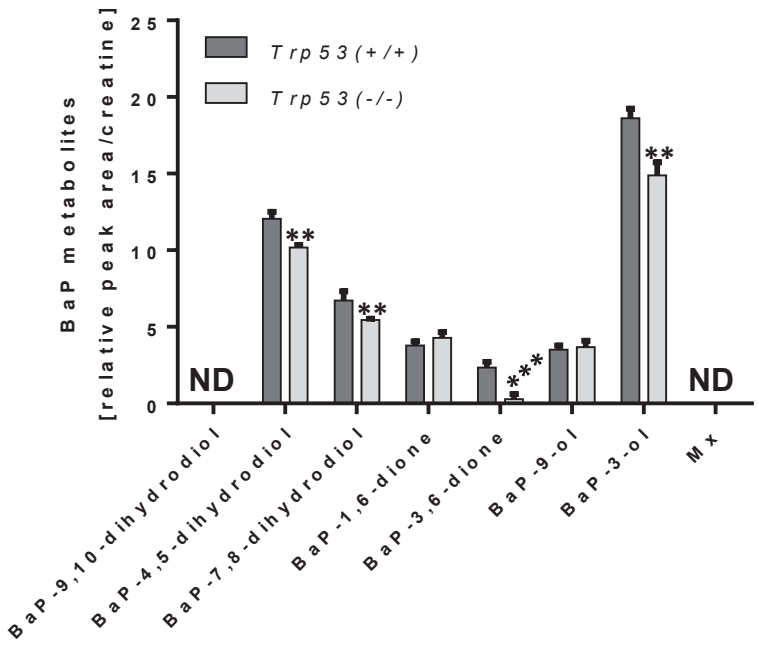

Supporting Figure 7

BaP metabolites in urine of BaP-treated *Trp53(+/+)* and *Trp53(-/-)* mice. Relative peak areas of BaP metabolites were measured by HPLC analysis at 254 nm. Values are the mean ± SD (n = 3). Statistical analysis was performed by t-test analysis (**p<0.01, ***p<0.005; different from *Trp53(+/+)* mice). Mx, an unknown BaP metabolite. ND, not detected.

ORIGINAL ARTICLE

Modulation of human cytochrome P450 1A1-mediated oxidation of benzo[*a*]pyrene by NADPH:cytochrome P450 oxidoreductase and cytochrome b_5

Radek Indra [1], Michaela Moserova [1], Natalie Kroftova [1], Miroslav Sulc [1], Marketa Martinkova [1], Vojtech Adam [2,3], Tomas Eckschlager [4], Rene Kizek [2,3], Volker M. Arlt [5], Marie Stiborova [1]

1 Department of Biochemistry, Faculty of Science, Charles University, Prague 2, Czech Republic
2 Department of Chemistry and Biochemistry, Faculty of Agronomy, Mendel University in Brno, Brno, Czech Republic
3 Central European Institute of Technology, Brno University of Technology, Brno, Czech Republic
4 Department of Pediatric Hematology and Oncology, 2nd Medical School, Charles University and University Hospital Motol, Prague 5, Czech Republic
5 Analytical and Environmental Sciences Division, MRC-PHE Centre for Environmental & Health, King's College London, London, United Kingdom

Correspondence to: Prof. RNDr. Marie Stiborova, DSc.
Department of Biochemistry, Faculty of Science, Charles University in Prague, Albertov 2030, 128 40 Prague 2, Czech Republic.
TEL: +420 221951285; FAX: +420 221951283; E-MAIL: stiborov@natur.cuni.cz

Submitted: 2014-09-23 Accepted: 2014-11-08 Published online: 2014-11-30

Key words: **benzo[*a*]pyrene; human carcinogen; metabolism; human and rat cytochrome P450 1A1; NADPH:cytochrome P450 oxidoreductase; cytochrome b_5**

Neuroendocrinol Lett 2014; **35**(Suppl. 2):105–113 **PMID:** 25638374 NEL351014A12

Abstract

OBJECTIVES: Cytochrome P450 (CYP) 1A1 located in the membrane of endoplasmic reticulum is the most important enzyme in both activation and detoxification of carcinogenic benzo[*a*]pyrene (BaP), in combination with microsomal epoxide hydrolase (mEH). However, it is still not clearly explained how the electron transfer is mediated by NADPH:CYP oxidoreductase (POR), another component of the microsomal enzymatic system, on CYP1A1 during BaP oxidation, and whether microsomal cytochrome b_5 might influence this electron transfer. **METHODS:** High performance liquid chromatography (HPLC) was employed for separation of BaP metabolites formed by enzymatic systems containing human CYP1A1. **RESULTS:** Human CYP1A1 expressed with POR in eukaryotic and prokaryotic expression cellular systems, in microsomes of insect cells (Supersomes™) and in a membrane fraction of *Escherichia coli*, respectively, and these enzyme systems reconstituted with purified cytochrome b_5 were utilized to study BaP oxidation. Human CYP1A1 expressed in Supersomes™ oxidized BaP to seven metabolites [7,8- and 9,10-dihydrodiols, 1,6-dione, 3,6-dione, 3- and 9-phenols, and a metabolite with unknown structure (Mx)], whereas this enzyme expressed in membranes of *E. coli* formed only the metabolites 1,6- and 3,6-diones, 3- and 9-phenols, and Mx. Addition of cytochrome b_5 to CYP1A1 expressed in the eukaryotic system led to a more than 2-fold increase in BaP metabolism, but had essentially no effect on BaP oxidation by CYP1A1 expressed in *E. coli*. **CONCLUSION:** The effect of cytochrome b_5 on CYP1A1 conformation and the electron transfer to this enzyme may contribute to the cytochrome b_5-mediated stimulation of BaP oxidation.

Abbreviations:

BaP	- benzo[a]pyrene
BPDE	- BaP-7,8-dihydrodiol-9,10-epoxide
CYP	- cytochrome P450
dG-N^2-BPDE	- 10-(deoxyguanosin-N^2-yl)-7,8,9-trihydroxy-7,8,9,10-tetrahydrobenzo-[a]pyrene
DLPC	- 1,2-dilauroylphosphatidylcholine
DMSO	- dimethyl sulfoxide
HPLC	- high performance liquid chromatography
HRN	- Hepatic P450 Reductase Null
mEH	- microsomal epoxide hydrolase
NADPH	- nicotinamidadeninedinucleotide phosphate (reduced)
NMR	- nuclear magnetic resonance
PAH	- polycyclic aromatic hydrocarbon
POR	- NADPH:cytochrome P450 oxidoreductase
RCN	- Reductase Conditional Null
r. t.	- retention time
UV	- ultraviolet
WT	- wild-type

INTRODUCTION

Benzo[*a*]pyrene (BaP) is a polycyclic aromatic hydrocarbon (PAH) that has been classified as human carcinogen (Group 1) by the International Agency for Research on Cancer (IARC, 2010). BaP requires metabolic activation catalyzed by cytochrome P450 (CYP) enzymes prior to reaction with DNA (Baird *et al.* 2005). Of the CYP enzymes, CYP1A1 is one of the most important CYP enzymes in metabolic activation of BaP to species forming DNA adducts (Baird *et al.* 2005; Hamouchene *et al.* 2011), in combination with microsomal epoxide hydrolase (mEH). First, CYP1A1 oxidizes BaP to an epoxide that is then converted to a dihydrodiol by mEH (*i.e.* BaP-7,8-dihydrodiol); then further bioactivation by CYP1A1 leads to the ultimately reactive species, BaP-7,8-dihydrodiol-9,10-epoxide (BPDE) that can react with DNA, forming adducts preferentially at guanine residues. The 10-(deoxyguanosin-N^2-yl)-7,8,9-trihydroxy-7,8,9,10-tetrahydrobenzo[*a*]pyrene (dG-N^2-BPDE) adduct is the major product of the reaction of BPDE with DNA *in vitro* and *in vivo* (Bauer *et al.* 1995; Arlt *et al.* 2008; 2012).

BaP is, however, oxidized also to other metabolites such as other dihydrodiols, BaP-diones and hydroxylated metabolites (Bauer *et al.* 1995; Chun *et al.* 1996; Kim *et al.* 1998; Baird *et al.* 2005; Jiang *et al.* 2007; Zhu *et al.* 2008). Even though most of these metabolites are detoxification products, BaP-9-ol is a precursor of 9-hydroxy-BaP-4,5-epoxide that can form another adduct with deoxyguanosine in DNA (Schoket *et al.* 1989; Nesnow *et al.* 1993; Fang *et al.* 2001; Stiborova *et al.* 2014). Therefore, regulation of CYP1A1-mediated oxidation of BaP leading to either metabolites forming BPDE, 9-hydroxy-BaP-4,5-epoxide or the BaP metabolites that are the detoxification products is of major importance.

Beside CYP1A1, CYP1B1 also oxidizes BaP, forming both the detoxification and activation metabolites. Its efficiency is however about half of that of CYP1A1. Among other CYP enzymes, CYP1A2, 2C8/9/19, 2E1, and 3A4 also oxidize BaP, but their efficiencies are more one order of magnitude lower than those of CYP1A1 (Bauer *et al.* 1995; Kim *et al.* 1998; Baird *et al.* 2005;).

CYP enzymes, including CYP1A1, are a component of a mixed function oxidase system located in the membrane of endoplasmic reticulum that contains beside the CYPs also another enzyme, NADPH:cytochrome P450 oxidoreductase (POR), and cytochrome b_5 accompanied with its NADH:cytochrome b_5 reductase. *Via* the activation of molecular oxygen, this multienzyme system catalyzes the monooxygenation of a variety of xenobiotics, including BaP (Coon, 1978). The oxygen is activated in the active center of CYPs by two electrons transferred from NADPH and/or NADH by means of POR and/or cytochrome b_5, respectively. Whereas POR is an essential constituent of the electron transport chain towards CYP, the role of cytochrome b_5 is still quite enigmatic (Porter, 2002; Schenkman and Jansson, 2003; Finn *et al.* 2008; McLaughin *et al.* 2010; Kotrbova *et al.* 2011; Stiborova *et al.* 2012; Sulc *et al.* 2012; Hendersson *et al.* 2013; Indra *et al.* 2013). In fact, for CYP1A1 the influence of the POR-mediated electron transfer from NADPH to this CYP by cytochrome b_5 is essentially not known. Moreover, a role of POR in the oxidative metabolism of BaP is not clearly established. Recently we found that in two mouse models [i.e. Hepatic P450 Reductase Null (HRN) and Reductase Conditional Null (RCN)], in which the expression of POR has been permanently or conditionally deleted in liver leading to a lack of almost all POR activity, the levels of the CYP- and mEH-mediated dG-N^2-BPDE adducts in livers of HRN and RCN mice treated with BaP were higher than in BaP-treated wild-type (WT) mice (Arlt *et al.* 2008; 2012; Stiborova *et al.* 2014). Therefore, in the present study we investigated the effect of POR and cytochrome b_5 on a potency of CYP1A1 to oxidize BaP.

Several model systems containing human CYPs, such as human hepatic microsomes, cells in culture including human hepatocytes, purified CYP enzymes reconstituted with POR in liposomes and/or human CYP enzymes overexpressed in baculovirus/insect cell, yeast, *Salmonella*, and other cellular systems, have already been utilized to study metabolism of several xenobiotics including BaP *in vitro* (Guengerich and Parikh, 1997; Anzenbacher and Anzenbacherova, 2001; Schwarz *et al.* 2001; Shimada *et al.* 2001; 2004; Zuber *et al.* 2002; Kramer and Tracy, 2008; Guguen-Guillouzo and Guillouzo, 2010; Davydov, 2011). However, which CYPs are most suitable for such metabolic studies remain to be further examined. In this work, human recombinant CYP1A1 expressed with its reductase (POR) in microsomes isolated from insect cells transfected with baculovirus constructs containing cDNA of human CYP1A1 and POR (Supersomes™) and in a membrane fraction of *Escherichia coli* cells transfected with *cDNA* of human CYP1A1 and/or these systems reconstituted with purified POR and/or cytochrome b_5 were used as model

systems. In addition, human hepatic microsomes containing a natural spectrum of human CYPs and other enzymes located in a membrane of endoplasmic reticulum were used as a positive control.

MATERIAL AND METHODS

Microsomal and enzymatic incubations

Male human hepatic microsomes (pooled sample; cat. no. 452172) and Supersomes™, microsomes isolated from insect cells transfected with a baculovirus construct containing cDNA of human CYP1A1 and expressing POR (CYP1A1 expressed in a eukaryotic system), were purchased from Gentest Corp. (Woburn, MI, USA) and used to study of BaP (Sigma Chemical Co, St Louis, MO, USA) oxidation. Bactosomes, a membrane fraction isolated from cells of *E. coli* transfected with construct of cDNA of human CYP1A1 and expressing either low (i.e. CYP1A1LR) or high levels of POR (i.e. CYP1A1R) were obtained from Cypex (BioDundee, Dundee, UK). Incubation mixtures used for studying BaP metabolism in human hepatic microsomes or in Supersomes™ and Bactosomes contained 100 mM potassium phosphate buffer (pH 7.4), NADPH-generating system [1 mM $NADP^+$, 10 mM D-glucose-6-phosphate, 1 U/ml D-glucose-6-phosphate dehydrogenase (all from Sigma Chemical)], 0.5 mg of microsomal protein or 100 nM CYP1A1 in Supersomes™ or Bactosomes, 50 μM BaP (dissolved in 5 μl dimethyl sulfoxide) in a final volume of 500 μl. In several experiments, these CYP1A1 systems were reconstituted with POR (CYP1A1LR), with cytochrome b_5 (all CYP1A1 systems) and/or mEH (CYP-1A1LR). The enzyme reconstitution utilizing the above systems (Supersomes™ and Bactosomes) and pure POR, cytochrome b_5 and/or mEH or POR in liposomes prepared from phospholipids such as 1,2-dilauroylphosphatidylcholine (DLPC) (Sigma) was performed as described (Stiborova *et al.* 2002; 2005; 2006; 2012; 2014; Dracinska *et al.* 2006; Kotrbova *et al.* 2011), using different molar ratios of CYP1A1 to POR and cytochrome b_5 (see Results for details). The reaction was initiated by adding 50 μl of the NADPH-generating system. Control incubations were carried out either without enzymatic system (microsomes or the CYP1A1 systems), or without NADPH-generating system, or without BaP. After incubation (37 °C, 20 min), 5 μl of 1 mM phenacetin (Sigma) in methanol was added as an internal standard. BaP metabolites were extracted twice with ethyl acetate (2 × 1 ml), solvent evaporated to dryness, residues dissolved in 25 μl methanol and BaP metabolites separated by high performance liquid chromatography (HPLC).

Isolation of POR, cytochrome b_5 and mEH

Rabbit liver POR was purified as described (Stiborova *et al.* 2002). Cytochrome b_5 was isolated from rabbit liver microsomes by the procedure described by Roos (1996). mEH was purified from liver microsomes of rabbits pretreated with phenobarbital as described by Ariyoshi *et al.* (1994). These enzymes were used for the reconstitution experiments.

HPLC analysis of BaP metabolites

HPLC analysis of BaP metabolites was performed on a Nucleosil® C18 reverse phase column, (250 × 4 mm, 5 μm; Macherey Nagel, Düren, Germany) using a Dionex system consisting of a pump P580, a UV/VIS Detector UVD 170S/340S, an ASI-100 Automated Sample Injector, a termobox COLUMN OVEN LCO 101 and an In-Line Mobile Phase Degasser Degasys DG-1210 Dionex controlled with Chromeleon™ 6.11 build 490 software. The conditions used for the chromatographic separation of BaP metabolites were as follows: 50% acetonitrile in water (*v/v*) with a linear gradient to 85% acetonitrile in 35 min, then an isocratic elution with 85% acetonitrile for 5 min, a linear gradient from 85% acetonitrile to 50% acetonitrile in 5 min, followed by an isocratic elution of 50% acetonitrile for 5 min (Moserova *et al.* 2009). Detection was by UV at 254 nm. Recoveries of BaP metabolites were around 95%. BaP metabolite peaks (Figure 1) were collected and analyzed by NMR and/or mass spectrometry as described recently (Indra *et al.* 2013; Stiborova *et al.* 2014). The peak areas at 254 nm were calculated relative to the peak area of the internal standard phenacetin, and expressed as relative peak areas.

Statistical analyses

For statistical data analysis we used Student's *t*-test. All *p*-values are two-tailed and considered significant at the 0.05 level.

RESULTS

Oxidation of BaP by human hepatic microsomes

Human hepatic microsomes are a natural system containing all components of a monooxygenase system located in a membrane of endoplasmic reticulum, CYPs, POR, cytochrome b_5 and its reductase, NADH: cytochrome b_5, reductase, in addition to mEH. Human hepatic microsomes oxidized BaP to six metabolites that were separated by HPLC (Figure 1A). The metabolites formed from BaP by human hepatic microsomes were identified by NMR and/or mass spectrometry (Indra *et al.* 2013; Stiborova *et al.* 2014) to be BaP-9,10-dihydrodiol (M1), BaP-4,5-dihydrodiol (M2), BaP-7,8-dihydrodiol (M3), BaP-1,6-dione (M4), BaP-3,6-dione (M5), and BaP-3-ol (M7), all corresponding to the metabolites that were formed by CYP1A1 in combination with mEH in other studies (Bauer *et al.* 1995; Kim *et al.* 1998; Baird *et al.* 2005; Moserova *et al.* 2009; Stiborova *et al.* 2014) (see Figures 1A and 2). Essentially no BaP metabolites were found when NADPH, a cofactor of the POR-dependent CYP monooxygenase system, was not present in the incubation mixtures (data not shown).

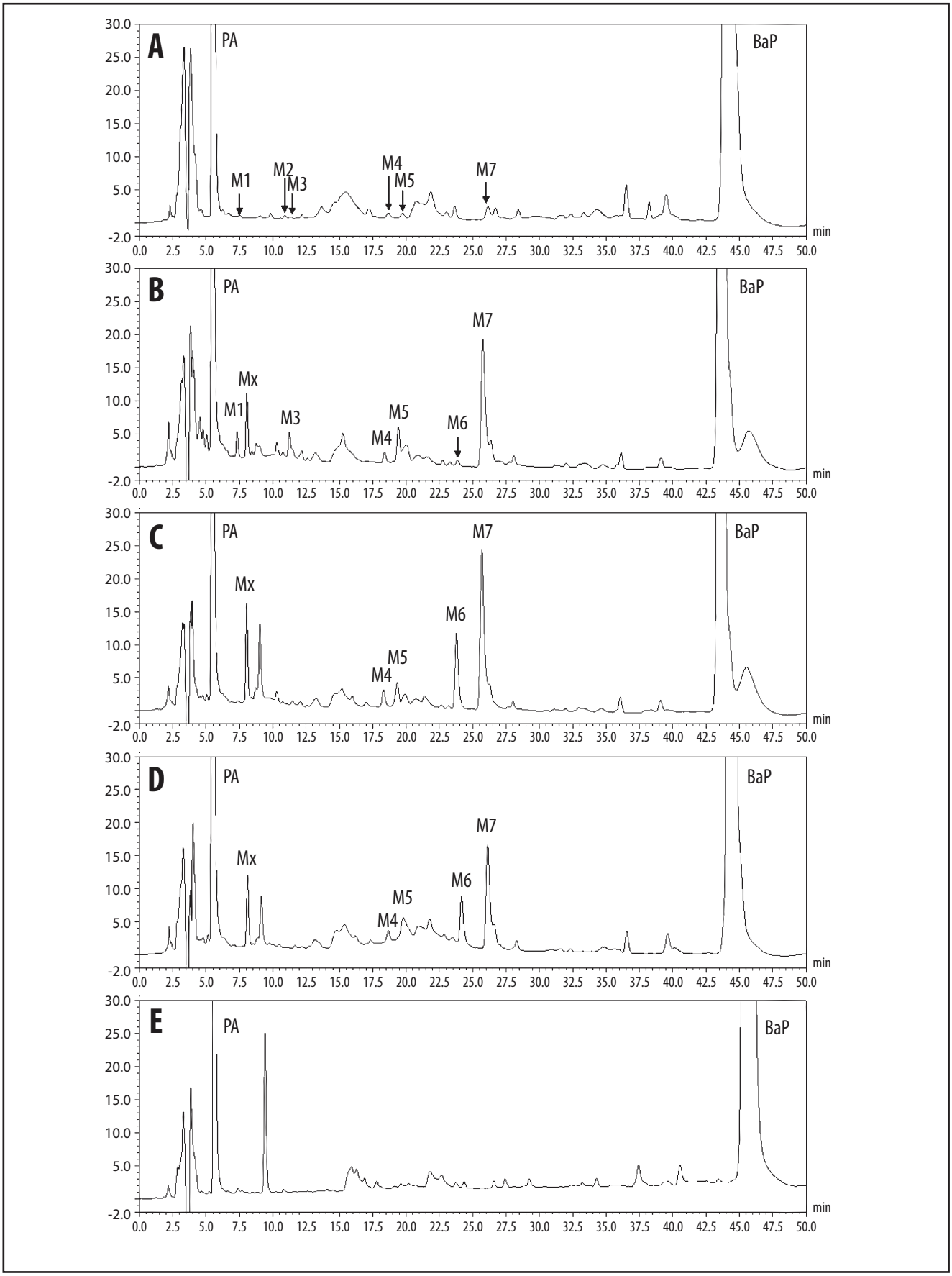

Fig. 1. HPLC of BaP metabolites formed by human hepatic microsomes (**A**), human recombinant CYP1A1 expressed in Supersomes™ (**B**), human recombinant CYP1A1 expressed in a membrane of *E. coli* - CYP1A1R (**C**) and CYP1A1LR (**D**). (**E**) HPLC of control incubation mixture containing BaP and CYP1A1LR, but without the NADPH-generating system. For BaP metabolites M1-M7 and Mx, see Fig. 2. PA, phenacetin.

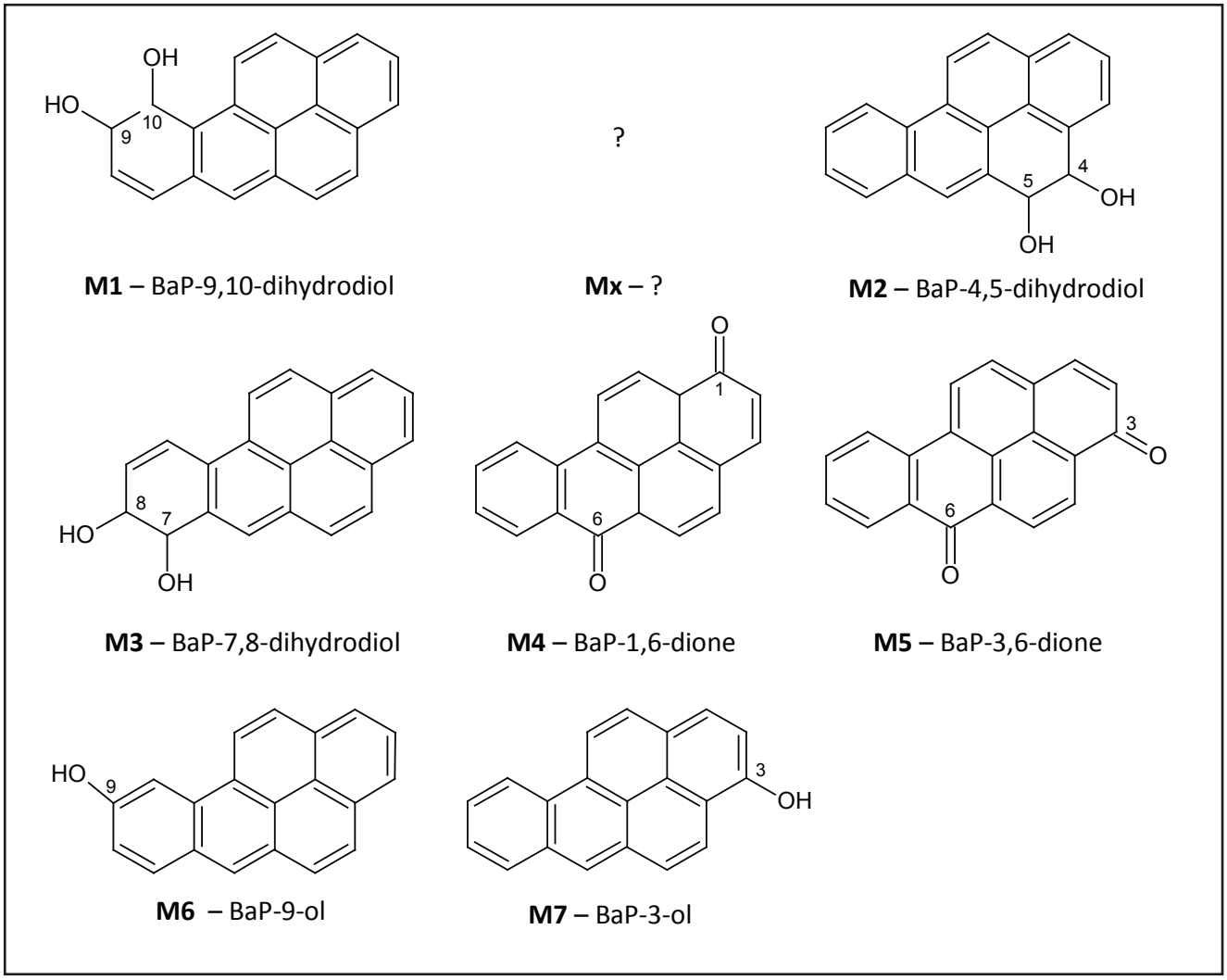

Fig. 2. BaP metabolites formed by human hepatic microsomes and human recombinant CYP1A1

Oxidation of BaP by human CYP1A1 expressed in a eukaryotic cellular system (Supersomes™)

Human CYP1A1 expressed with POR in a microsomal system of Supersomes™ oxidized BaP to seven metabolites, namely BaP-9,10-dihydrodiol, a metabolite assigned as Mx, whose structure has not been identified as yet, BaP-7,8-dihydrodiol, BaP-1,6-dione, BaP-3,6-dione, BaP-9-ol and BaP-3-ol (Figures 1B and 3). One of the dihydrodiols formed by human hepatic microsomes, BaP-4,5-dihydrodiol (M2), has not been detected in this CYP1A1 system. The highest amount of BaP-3-ol was generated by CYP1A1 in Supersomes™ (Figure 1B). The results found using this human CYP1A1 system indicated that BaP is metabolized not only by CYP1A1 present in this enzyme system, but also by mEH, which is important for the hydration of BaP epoxides to produce dihydrodiols. Therefore, this enzyme was expressed in microsomes of the Supersomal system. Essentially no BaP metabolites were found when the NADPH-generating system was deleted from the incubation mixtures (data not shown).

Addition of cytochrome b_5, to CYP1A1 in Supersomes™ led to up to a more than 2-fold increase in BaP oxidation to its metabolites. The highest stimulation effect of cytochrome b_5 has been found on formation of BaP-3-ol and BaP-7,8-dihydrodiol, followed by the effect on generation of BaP-9,10-dihydrodiol, BaP-1,6-dione, BaP-9-ol, a metabolite Mx, and BaP-3,6-dione (Figure 3).

Oxidation of BaP by human CYP1A1 expressed in a prokaryotic cellular system of E. coli (Bactosomes)

Two types of human CYP1A1 enzymatic systems expressed in prokaryotic cells were used to analyze oxidation of BaP. Namely, Bactosomes, a membrane fraction isolated from cells of *E. coli*, containing human CYP1A1 and expressing low or high levels of POR, CYP1A1LR (using a CYP1A1:POR ratio of 1:0.4) or CYP1A1R (using a CYP1A1:POR ratio of 1:0.8), respectively, were employed. Human CYP1A1 expressed in both two *E. coli* systems oxidized BaP to five metabolites; BaP-1,6-dione, BaP-3,6-dione, BaP-9-ol, BaP-3-ol

and a metabolite Mx, whereas no BaP-dihydrodiols were detected (Figure 1C and 1D). Essentially no BaP metabolites were found when the NADPH-generating system was deleted from the incubation mixture containing BaP and the CYP1A1LR (Figure 1E) or CYP1A1R (data not shown) systems.

Of the BaP metabolites formed, BaP-3-ol, BaP-9-ol and a metabolite Mx were the major BaP metabolites, whereas BaP-1,6-dione and BaP-3,6-dione were generated in much lower amounts (Figures 1 and 3). BaP-9-ol metabolite was formed in more than the 3.5-fold higher amounts in this CYP1A1 system than by CYP1A1 in Supersomes™ (Figures 1 and 3). The results found in experiments using a membrane fraction of *E. coli* containing CYP1A1 and POR indicated that mEH, which is the enzyme important for the hydration of BaP epoxides to dihydrodiols, seems to be present in very low concentrations that are not sufficient for catalysis of these reactions.

As shown in Figure 3, only an up to 1.6-fold higher efficiency of the CYP1A1R *E. coli* system containing higher expression levels of POR to oxidize BaP than CYP1A1LR was found. This finding indicates that even the low amounts of POR are capable of an efficient transfer of electrons from the POR cofactor, NADPH, to CYP1A1 during BaP oxidation in this enzymatic system. In order to investigate the effect of various amounts of POR on the electron transport from NADPH to CYP1A1 in BaP oxidation in more detail, CYP1A1LR was reconstituted with increasing concentrations of POR and used as an additional enzymatic system for testing BaP oxidation.

No significant changes in amounts of most BaP metabolites and their profiles were produced by the addition of POR to the CYP1A1LR system until its concentration was equimolar to CYP1A1. Only BaP-3-ol was increased significantly under these conditions. However, under CYP1A1 to POR ratios of 1:2 or 1:3, a significant increase in BaP oxidation was caused by CYP1A1, mainly to the detoxification metabolite BaP-3-ol (Figure 4). Moreover, the low but detectable amounts of BaP-4,5-dihydrodiol and BaP-7,8-dihydrodiol were also produced under these CYP1A1 to POR ratios, indicating that low levels of mEH are expressed in the membrane of *E. coli* (and under the conditions suitable for effective oxidation of BaP to its metabolites) are capable of catalyzing the hydration of BaP-4,5-epoxide and BaP-7,8-epoxide. Similar changes in BaP metabolite profiles were also found in experiments in which POR was added in its liposomal form [POR introduced into liposomes simulating the membrane of endoplasmic reticulum (microsomes)], prepared from membrane phospholipids such as DLPC (Stiborova *et al.* 2002; 2006; 2012, Kotrbova *et al.* 2011) (data not shown). All these findings suggested that the membrane of *E. coli* provides a suitable environment for the appropriate conformation of POR and CYP1A1 proteins to form a reconstituted system catalyzing BaP oxidation.

In contrast to the stimulation effect of cytochrome b_5 on BaP oxidation by human CYP1A1 in Supersomes™, essentially no such effect was detected in the system of CYP1A1 expressed in *E. coli*. Only production of BaP-3-ol by the system with low expression of POR (CYP1A1LR) was significantly increased by addition of

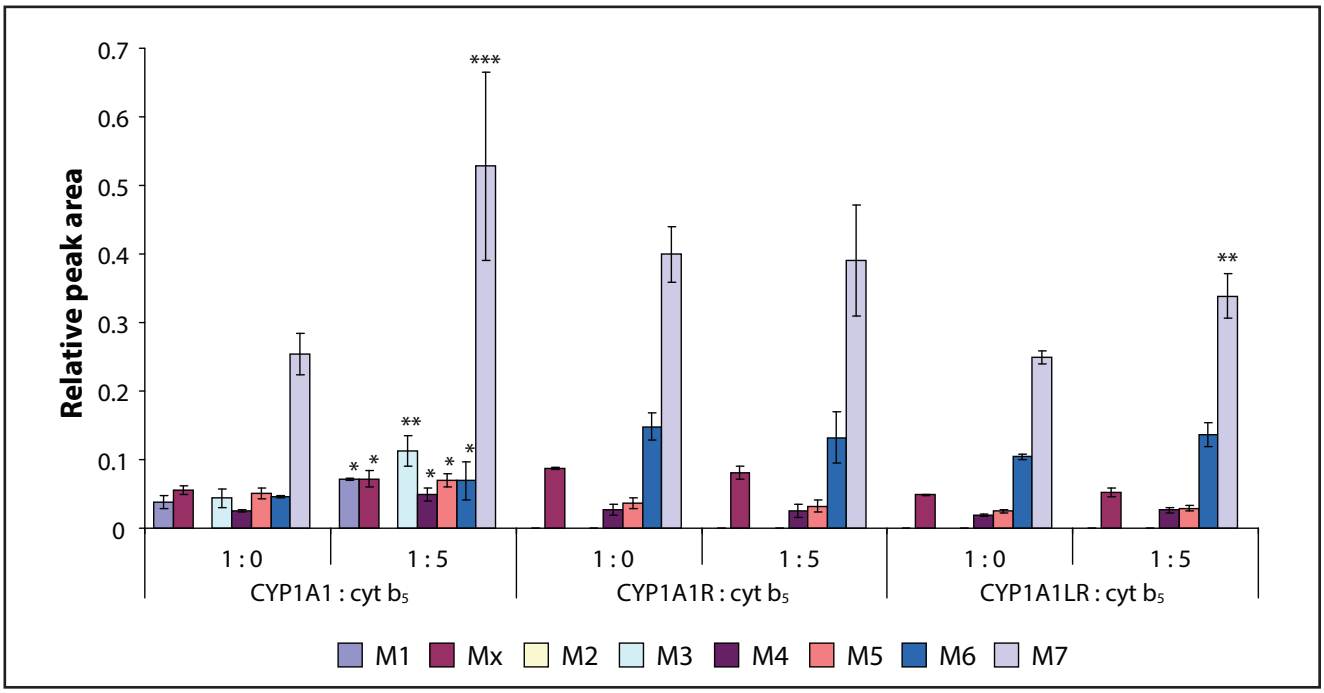

Fig. 3. Oxidation of BaP by human recombinant CYP1A1 expressed in Supersomes™ (CYP1A1) and in a membrane of *E. coli* (CYP1A1R and CYP1A1LR) and the effect of cytochrome b_5 on this oxidation. Comparison was performed by *t*-test analysis; *p<0.05, **p<0.01, ***p<0.001, different from CYP1A1-mediated oxidation of BaP without cytochrome b_5. For BaP metabolites M1-M7 and Mx, see Fig. 2.

cytochrome b_5 (Figure 3). The reason for the opposite effects of cytochrome b_5 on CYP1A1 expressed either in eukaryotic or prokaryotic systems is not yet known. Nevertheless, one can speculate that cytochrome b_5 in the membrane of *E. coli* is not in a conformation appropriate for its function in the CYP1A1 system.

DISCUSSION

The results of this work showed that oxidation of BaP by human CYP1A1 is dependent on a variety of factors. Our experiments utilizing different enzymatic systems of human CYP1A1 showed that one of the most important factors determining efficiency of BaP metabolism is, beside expression of individual enzymes of the microsomal system (CYP1A1, POR, cytochrome b_5 and mEH), mainly the ratios among these enzymes. Other factors determining the efficiency of BaP metabolism are the properties of the subcellular (microsomes, a membrane of *E.coli*) or artificial system (liposomes), i.e. how they simulate the membrane of endoplasmic reticulum. Our results demonstrated that the system of human CYP1A1 expressed in microsomes of eukaryotic cells (Supersomes™) is the better suited enzymatic system for the investigation of BaP metabolism than CYP1A1 expressed in prokaryotic cells of *E. coli*. The low (if any) mEH expression levels, which are essential for the formation of BaP-dihydrodiols, makes this system insufficient for formation of the whole spectrum of BaP metabolites generated during the first (derivative) phase of BaP biotransformation. Nevertheless, the bacterial expression system of *E. coli* was appropriate to evaluate the effect of different concentrations of POR in the CYP1A1 enzymatic system on BaP oxidation. Interestingly, even under low concentrations of POR (using a ratio of CYP1A1 to POR of 1:0.4), CYP1A1 was capable of oxidizing BaP, and increased POR levels in the CYP1A1 reconstituted system resulted in an increase of the BaP detoxification metabolite BaP-3-ol. These results might, to some extent, explain our findings in experiments utilizing the HRN and RCN mouse models indicating that hepatic CYP enzymes in these mouse models seem to be more important for detoxification of BaP *in vivo* despite being important for its bioactivation to form BaP-DNA adducts *in vitro* (Arlt *et al.* 2008; 2012).

The results of this study also showed that the addition of cytochrome b_5 to human CYP1A1 in Supersomes™ resulted in an increased formation of BaP metabolites. Our *in vitro* experiments in the present study, together with previous findings showing that BaP acts as an inducer of cytochrome b_5 (Arlt *et al.* 2012) indicate the potential importance of this protein to greatly influence BaP oxidation *in vivo*. Interestingly, in the case of human CYP1A1 expressed in the membrane of prokaryotic cells of *E. coli*, addition of cytochrome b_5 led to almost no stimulation of BaP oxidation; only oxidation of BaP to BaP-3-ol by the system with low expression of POR was enhanced by cytochrome b_5.

A stimulation of CYP1A1-mediated catalysis by cytochrome b_5 has already been found in the oxidation of its marker substrate Sudan I (Stiborova *et al.* 1988; 2005; 2006) and an anticancer drug ellipticine (Kotr-

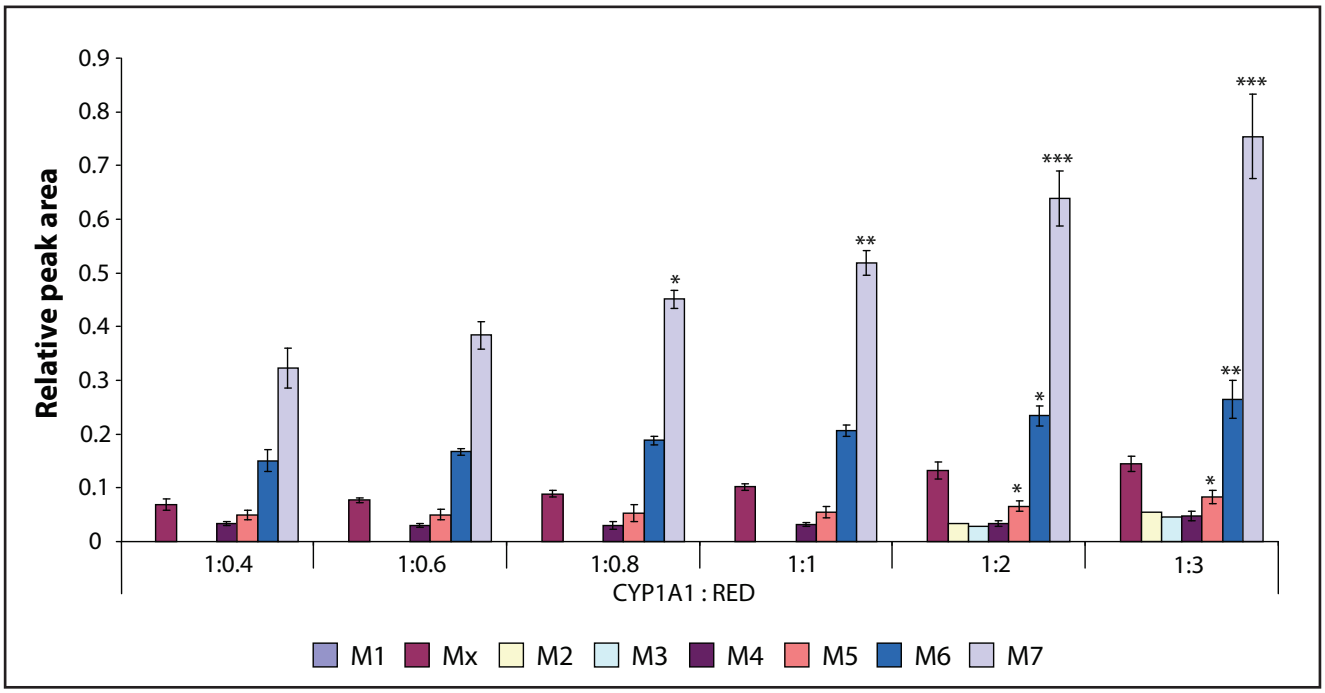

Fig. 4. The effect of a ratio of CYP1A1 to POR on oxidation of BaP by human CYP1A1 expressed in a membrane of *E. coli*. Comparison was performed by *t*-test analysis; *p<0.05, **p<0.01, ***p<0.001, different from oxidation of BaP by CYP1A1LR without addition of POR. For BaP metabolites M1-M7 and Mx, see Fig. 2.

bova *et al.* 2011), but not in that of 7-ethoxyresorufin (Stiborova *et al.* 2005). Two mechanisms of cytochrome b_5-mediated modulation of CYP catalysis have been suggested previously: it can affect the CYP catalytic activities by donating the second electron to CYP in a CYP catalytic cycle and/or act as an allosteric modifier of the oxygenase (Yamazaki *et al.* 1997; 2001; Loughran *et al.* 2001; Porter, 2002; Zhang *et al.* 2005; Schenkman and Jansson, 2003; Guengerich, 2005; Kotrbova *et al.* 2009; 2011; Stiborova *et al.* 2012). The mechanism(s) underlying such allosteric effects, based on reports that apo-cytochrome b_5 can stimulate CYP catalysis, remains uncertain. However, it does seem clear that cytochrome b_5 binding can cause conformational changes to the substrate access channel and binding pocket in the CYP enzyme (Yamazaki *et al.* 1997; 2003; Loughran *et al.* 2001; Porter, 2002; Zhang *et al.* 2005; Schenkman and Jansson, 2003; Guengerich, 2005; Kotrbova *et al.* 2009; 2011; Stiborova *et al.* 2012; Estrada *et al.* 2014). Addition of cytochrome b_5 changed the levels of individual BaP metabolites formed by CYP1A1, and, partially their profiles. Thus interaction of CYP1A1 with cytochrome b_5 can result both in conformational change of the CYP1A1 protein molecule as well as impact on the electron transfer from cytochrome b_5 to CYP1A1, thereby providing mechanisms explaining the observed increase in BaP oxidation. Nevertheless, the real mechanism responsible for the effects of cytochrome b_5 on CYP1A1-mediated oxidation of BaP and a variety of other substrates (e.g. ellipticine) (Kotrbova *et al.* 2011) needs to be explored in further investigations.

CONCLUSION

The results found in this study indicated that the POR-mediated electron transfer from NADPH to human CYP1A1, which is one of the key steps in oxidation of carcinogenic BaP, is mediated by even low concentrations of POR using a ratio of CYP1A1 to POR equaling to 1:0.4. Moreover, BaP oxidation by human CYP1A1 expressed in microsomes of eukaryotic (insect) cells was stimulated by the heme protein cytochrome b_5 that finally leads to more effective oxidative metabolism of this carcinogen. Because of this effect, our study suggests that cytochrome b_5 is an important biological factor influencing BaP-mediated carcinogenesis.

ACKNOWLEDGEMENTS

This work was supported by the Grant Agency of the Czech Republic (grant 14-18344S in panel P301), Charles University in Prague (grants 640712 and UNCE 204025/2012). Work at King's College London is supported by Cancer Research UK.

REFERENCES

1 Anzenbacher P, Anzenbacherova E (2001). Cytochromes P450 and metabolism of xenobiotics. Cell Mol Life Sci. **58**: 737–747.
2 Ariyoshi N, Tanak, M, Ishii Y and Oguri K (1994). Purification and characterization of dog liver microsomal epoxide hydrolase. J Biochem. **115**: 985–990.
3 Arlt VM, Stiborova M, Henderson CJ, Thiemann M, Frei E, Aimova D, Singhs R, da Costa GG, Schmitz OJ, Farmer PB, Wolf CR and Philips DH (2008). Metabolic activation of benzo[a]pyrene in vitro by hepatic cytochrome P450 contrasts with detoxification in vivo: experiments with hepatic cytochrome P450 reductase null mice. Carcinogenesis. **29**: 656–665.
4 Arlt VM, Poirier MC, Sykes SE, Kaarthik J, Moserova M, Stiborova M, Wolf R, Henderson CJ and Phillips DH (2012). Exposure to benzo[a]pyrene of hepatic cytochrome P450 reductase null (HRN) and P450 reductase conditional null (RCN) mice: detection of benzo[a]pyrene diol epoxide-DNA adducts by immunohistochemistry and ^{32}P-postlabelling. Toxicol Lett. **213**: 160–166.
5 Baird WM, Hooven LA and Mahadevan B (2005). Carcinogenic polycyclic aromatic hydrocarbon-DNA adducts and mechanism of action. Environ Mol Mutagen. **45**: 106–114.
6 Bauer E, Guo Z, Ueng YF, Bell LC, Zeldin D and Guengerich FP (1995). Oxidation of benzo[a]pyrene by recombinant human cytochrome P450 enzymes. Chem Res Toxicol. **8**: 136–142.
7 Chun YJ Shimada T and Guengerich FP (1996). Construction of a human cytochrome P450 1A1: rat NADPH-cytochrome P450 reductase fusion protein cDNA and expression in Escherichia coli, purification, and catalytic properties of the enzyme in bacterial cells and after purification. Arch Biochem Biophys. **330**: 48–58.
8 Coon MJ (1978). Oxygen activation in the metabolism of lipids, drugs and carcinogens. Nutr Rev. **36**: 319–328.
9 Davydov DR (2011). Microsomal monooxygenase as a multienzyme system: the role of P450-P450 interactions. Expert Opin Drug Metab Toxicol. **7**: 543–558.
10 Dracinska H, Miksanová M, Svobodová M, Smrcek S, Frei E, Schmeiser HH, Stiborová M (2006). Oxidative detoxication of carcinogenic 2-nitroanisole by human, rat and rabbit cytochrome P450. Neuroendocrinol Lett. **27**(Suppl 2): 9–13.
11 Estrada DF, Skinner AL, Laurence JS and Scott EE (2014). Human cytochrome P450 17A1 conformational celection. J Biol Chem. **289**: 14310–14320.
12 Fang AH, Smith WA, Vouros P and Gupta RC (2001). Identification and characterization of a novel benzo[a]pyrene-derived DNA adduct. Biochem Biophys Res Commun. **281**: 383–389.
13 Finn RD, McLaughlin LA, Ronseaux S, Rosewell I, Houston JB, Henderson CJ and Wolf CR (2008). Defining the in vivo role for cytochrome b_5 in cytochrome P450 function through the conditional hepatic deletion of microsomal cytochrome b_5. J Biol Chem. **283**: 31385–31393.
14 Guengerich FP (2005). Reduction of cytochrome b_5 by NADPH-cytochrome P450 reductase. Arch Biochem Biophys. **440**: 204–211.
15 Guengerich FP and Parikh A (1997). Expression of drug-metabolizing enzymes. Curr Opin Biotechnol. **8**: 623–628.
16 Guguen-Guillouzo C and Guillouzo A (2010). General review on in vitro hepatocyte models and their applications. Methods Mol Biol. **640**: 1–40.
17 Hamouchene H, Arlt VM, Giddings I and Phillips DH (2011). Influence of cell cycle on responses of MCF-7 cells to benzo[a]pyrene. BMC Genomics. **12**: 333.
18 Henderson CJ, McLaughlin LA and Wolf CR (2013). Evidence that cytochrome b_5 and cytochrome b_5 reductase can act as sole electron donors to the hepatic cytochrome P450 system. Mol Pharmacol. **83**: 1209–1217.
19 International Agency for Research on Cancer (IARC) (2010). Some non-heterocyclic polycyclic aromatic hydrocarbons and some related exposures. In: IARC Monogr. Eval. Carcinog. Risks Hum. **92**: 1–853.

20 Indra R., Moserova M., Sulc M, Frei E and Stiborova M (2013). Oxidation of carcinogenic benzo[a]pyrene by human and rat cytochrome P450 1A1 and its influencing by cytochrome b_5 – a comparative study. Neuroendocrinol Lett. **34**(Suppl 2): 55–63.

21 Jiang H, Gelhaus SL, Mangal,D, Harvey RG, Blair IA and Penning TM (2007). Metabolism of benzo[a]pyrene in human bronchoalveolar H358 cells using liquid chromatography-mass spectrometry. Chem Res Toxicol. **20**: 1331–1341.

22 Kim JH, Stansbury KH, Walker NJ, Trush MA, Strickland PT and Sutter TR (1998). Metabolism of benzo[a]pyrene and benzo[a] pyrene-7,8-diol by human cytochrome P450 1B1. Carcinogenesis. **19**: 1847–1853.

23 Kotrbova V, Aimova D, Ingr M, Borek-Dohalska L, Martinek V and Stiborova M (2009). Preparation of a biologically active apocytochrome b_5 via heterologous expression in Escherichia coli. Protein Expr Purif. **66**: 203–209.

24 Kotrbova V, Mrazova B, Moserova M, Martinek V, Hodek P, Hudecek J, Frei E, Stiborova M (2011). Cytochrome b_5 shifts oxidation of the anticancer drug ellipticine by cytochromes P450 1A1 and 1A2 from its detoxication to activation, thereby modulating its pharmacological efficacy. Biochem Pharmacol. **82**: 669–680.

25 Kramer MA and Tracy TS (2008). Studying cytochrome P450 kinetics in drug metabolism. Expert Opin Drug Metab Toxicol. **4**: 591–603.

26 Loughran PA, Roman LJ, Miller RT and Masters BS (2001). The kinetic and spectral characterization of the E. coli-expressed mammalian CYP4A7: cytochrome b_5 effects vary with substrate. Arch Biochem Biophys. **385**: 311–321.

27 McLaughin LA, Ronseaux S, Finn RD, Henderson CI and, Wolf CR (2010). Deletion of microsomal cytochrome b_5 profoundly affects hepatic and extrahepatic drug metabolism. Mol Pharmacol. **75**: 269–278.

28 Moserova M, Kotrbova V, Aimova D, Sulc M, Frei E and Stiborova M (2009). Analysis of benzo[a]pyrene metabolites formed by rat hepatic microsomes using high pressure liquid chromatography: optimization of the method. Interdiscip Toxicol. **2**: 239–244.

29 Nesnow S, Ross J, Nelson G, Holden K, Erexson G, Kligerman A, Gupta RC (1993). Quantitative and temporal relationships between DNA adduct formation in target and surrogate tissues: implications for biomonitoring. Environ Health Perspect. **101** Suppl 3: 37–42.

30 Porter TD (2002). The roles of cytochrome b_5 in cytochrome P450 reactions. J Biochem Mol Toxicol. **16**: 311–316.

31 Rendic S and Di Carlo FJ (1997). Human cytochrome P450 enzymes: a status report summarizing their reactions, substrates, inducers, and inhibitors. Drug Metab Rev. **29**: 413–580.

32 Roos PH (1996). Chromatographic separation and behavior of microsomal cytochrome P450 and cytochrome b_5. J Chromatogr B Biomed Appl. **684**: 107–131.

33 Schenkman JB and Jansson I (2003). The many roles of cytochrome b_5. Pharmacol Ther. **97**: 139–152.

34 Schoket B, Lévay K, Philips DH and Vincze I (1989). ^{32}P-postlabelling analysis of DNA adducts of benzo[a]pyrene formed in complex metabolic activation systems in vitro. Cancer Lett. **48**: 67–75.

35 Schwarz D, Kisselev P, Honeck H, Cascorbi I, Schunck WH and Roots I (2001). Co-expression of human cytochrome P4501A1 (CYP1A1) variants and human NADPH-cytochrome P450 reductase in the baculovirus/insect cell system. Xenobiotica. **31**: 345–356.

36 Shimada T, Oda Y, Gillam EM, Guengerich FP and Inouye K (2001). Metabolic activation of polycyclic aromatic hydrocarbons and other procarcinogens by cytochromes P450 1A1 and P450 1B1 allelic variants and other human cytochromes P450 in Salmonella typhimurium NM2009. Drug Metab Dispos. **29**: 1176–1182.

37 Shimada T and Fujii-Kuriyama Y (2004). Metabolic activation of polycyclic aromatic hydrocarbons to carcinogens by cytochrome P450 1A1 and 1B1. Cancer Sci. **95**: 1–6.

38 Stiborova M, Asfaw B, Anzenbacher P and Hodek P (1988) A new way to carcinogenicity of azo dyes: the benzenediazonium ion formed from a non-aminoazo dye, 1-phenylazo-2-hydroxynaphthalene(Sudan I) by microsomal enzymes binds to deoxyguanosine residues of DNA. Cancer Lett. **40**: 327–333.

39 Stiborova M, Indra R, Moserova M, Cerna V, Rupertova M, Martinek V, Eckschlager T, Kizek R, Frei E (2012). Cytochrome b_5 increases cytochrome P450 3A4-mediated activation of anticancer drug ellipticine to 13-hydroxyellipticine whose covalent binding to DNA is elevated by sulfotransferases and N,O-acetyltransferases. Chem Res Toxicol. **25**: 1075–1085.

40 Stiborova M, Martinek V, Rydlova H, Hodek P and Frei E (2002). Sudan I is a potential carcinogen for humans: Evidence for its metabolic activation and detoxication by human recombinant cytochrome P450 1A1 and liver microsomes. Cancer Res. **62**: 5678–5684.

41 Stiborova M, Martinek V, Rydlova H, Koblas T and Hodek P (2005). Expression of cytochrome P450 1A1 and its contribution to oxidation of a potential human carcinogen 1-phenylazo-2-naphthol (Sudan I) in human livers. Cancer Lett. **220**: 145–154.

42 Stiborova M, Martinek V, Schmeiser HH and Frei E (2006). Modulation of CYP1A1-mediated oxidation of carcinogenic azo dye Sudan I and its binding to DNA by cytochrome b_5. Neuroendocrinol Lett. **27**(Suppl 2): 35–39.

43 Stiborova M, Moserova M, Cerna V, Indra R, Dracinsky M, Šulc M, Henderson CJ, Wolf CR, Schmeiser HH, Phillips DH, Frei E and Arlt VM (2014). Cytochrome b_5 and epoxide hydrolase contribute to benzo[a]pyrene-DNA adduct formation catalyzed by cytochrome P450 1A1 under low NADPH:P450 oxidoreductase conditions. Toxicology. **318**: 1–12.

44 Sulc M, Jecmen T, Snajdrova R, Novak P, Martinek V, Hodek P, Stiborova M, and Hudecek J (2012). Mapping of interaction between cytochrome P450 2B4 and cytochrome b_5; the first evidence of two mutual interactions. Neuroendocrinol Lett. **33**(Suppl 3): 41–47.

45 Yamazaki H, Gillam EM, Dong MS, Johnson WW, Guengerich FP and Shimada T (1997). Reconstitution of recombinant cytochrome P450 2C10(2C9) and comparison with cytochrome P450 3A4 and other forms: effects of cytochrome P450-P450 and cytochrome P450-b_5 interactions. Arch Biochem Biophys. **342**: 329–337.

46 Yamazaki H, Shimada T, Martin MV and Guengerich FP (2001). Stimulation of cytochrome P450 reactions by apo-cytochrome b_5: evidence against transfer of heme from cytochrome P450 3A4 to apo-cytochrome b_5 or heme oxygenase. J Biol Chem. **276**: 30885–30891.

47 Zhang H, Myshkin E and Waskell L (2005). Role of cytochrome b_5 in catalysis by cytochrome P450 2B4. Biochem Biophys Res Commun. **338**: 499–506.

48 Zhu S, Li L, Thornton C, Carvalho P, Avery BA and Willett KL (2008). Simultaneous determination of benzo[a]pyrene and eight of its metabolites in *Fundulus heteroclitus* bile using ultra-performance liquid chromatography with mass spectrometry. J Chromatogr B Analyt Technol Biomed Life Sci. **863**: 141–149.

49 Zuber R, Anzenbacherova E and Anzenbacher P (2002). Cytochromes P450 and experimental models of drug metabolism. J Cell Mol Med. **6**: 189–198.

Toxicology 318 (2014) 1–12

Contents lists available at ScienceDirect

Toxicology

journal homepage: www.elsevier.com/locate/toxicol

Cytochrome b_5 and epoxide hydrolase contribute to benzo[*a*]pyrene-DNA adduct formation catalyzed by cytochrome P450 1A1 under low NADPH:P450 oxidoreductase conditions

Marie Stiborová[a,*], Michaela Moserová[a], Věra Černá[a], Radek Indra[a], Martin Dračínský[b], Miroslav Šulc[a], Colin J. Henderson[c], C. Roland Wolf[c], Heinz H. Schmeiser[d], David H. Phillips[e], Eva Frei[f], Volker M. Arlt[e]

[a] *Department of Biochemistry, Faculty of Science, Charles University, Albertov 2030, 128 40 Prague 2, Czech Republic*
[b] *Institute of Organic Chemistry and Biochemistry, v.v.i. Academy of Sciences, Flemingovo n. 2, 166 10 Prague 6, Czech Republic*
[c] *Division of Cancer Research, Medical Research Institute, Jacqui Wood Cancer Centre, University of Dundee, Dundee DD1 9SY, United Kingdom*
[d] *Research Group Genetic Alterations in Carcinogenesis, German Cancer Research Center (DKFZ), Im Neuenheimer Feld 280, 69120 Heidelberg, Germany*
[e] *Analytical and Environmental Sciences Division, MRC-PHE Centre for Environment and Health, King's College London, 150 Stamford Street, London SE1 9NH, United Kingdom*
[f] *Division of Preventive Oncology, National Center for Tumour Diseases, German Cancer Research Center (DKFZ), Im Neuenheimer Feld 280, 69120 Heidelberg, Germany*

ARTICLE INFO

Article history:
Received 5 December 2013
Received in revised form 31 January 2014
Accepted 4 February 2014
Available online 14 February 2014

Keywords:
Benzo[*a*]pyrene
Cytochrome P450 1A1
NADPH:cytochrome P450 oxidoreductase
Epoxide hydrolase
Cytochrome b_5

ABSTRACT

In previous studies we had administered benzo[*a*]pyrene (BaP) to genetically engineered mice (HRN) which do not express NADPH:cytochrome P450 oxidoreductase (POR) in hepatocytes and observed higher DNA adduct levels in livers of these mice than in wild-type mice. To elucidate the reason for this unexpected finding we have used two different settings for *in vitro* incubations; hepatic microsomes from control and BaP-pretreated HRN mice and reconstituted systems with cytochrome P450 1A1 (CYP1A1), POR, cytochrome b_5, and epoxide hydrolase (mEH) in different ratios. In microsomes from BaP-pretreated mice, in which Cyp1a1 was induced, higher levels of BaP metabolites were formed, mainly of BaP-7,8-dihydrodiol. At a low POR:CYP1A1 ratio of 0.05:1 in the reconstituted system, the amounts of BaP diones and BaP-9-ol formed were essentially the same as at an equimolar ratio, but formation of BaP-3-ol was ~1.6-fold higher. Only after addition of mEH were BaP dihydrodiols found. Two BaP-DNA adducts were formed in the presence of mEH, but only one when CYP1A1 and POR were present alone. At a ratio of POR:CYP1A1 of 0.05:1, addition of cytochrome b_5 increased CYP1A1-mediated BaP oxidation to most of its metabolites indicating that cytochrome b_5 participates in the electron transfer from NADPH to CYP1A1 required for enzyme activity of this CYP. BaP-9-ol was formed even by CYP1A1 reconstituted with cytochrome b_5 without POR. Our results suggest that in livers of HRN mice Cyp1a1, cytochrome b_5 and mEH can effectively activate BaP to DNA binding species, even in the presence of very low amounts of POR.

1. Introduction

Benzo[*a*]pyrene (BaP) is a polycyclic aromatic hydrocarbon (PAH) that has been classified as human carcinogen (Group 1) by the International Agency for Research on Cancer (IARC, 2010). BaP and other PAHs are produced mainly by incomplete combustion of organic matter and are ubiquitous in the environment, leading to measurable levels of exposure in the general population (IARC, 2010). Beside the inhalation of polluted air, the main sources of exposure are tobacco smoke and the diet (Kim et al., 2011; Labib et al., 2012; Phillips and Venitt, 2012; Siddens et al., 2012). Chronic

Abbreviations: AHR, aryl hydrocarbon receptor; BaP, benzo[*a*]pyrene; BPDE, BaP-7,8-dihydrodiol-9,10-epoxide; CYP, cytochrome P450; dG-N^2-BPDE, 10-(deoxyguanosin-N^2-yl)-7,8,9-trihydroxy-7,8,9,10-tetrahydrobenzo[*a*]pyrene; EROD, 7-ethoxyresorufin *O*-deethylation; HPLC, high pressure liquid chromatography; HRN, hepatic P450 reductase null; mEH, microsomal epoxide hydrolase; NMR, nuclear magnetic resonance; PA, phenacetin; PAH, polycyclic aromatic hydrocarbon; POR, NADPH:cytochrome P450 oxidoreductase; RAL, relative adduct labeling; RCN, reductase conditional null; TLC, thin-layer chromatography; WT, wild-type.

* Corresponding author. Tel.: +420 221951285; fax: +420 221951283.
E-mail address: stiborov@natur.cuni.cz (M. Stiborová).

http://dx.doi.org/10.1016/j.tox.2014.02.002
0300-483X/

exposure of laboratory animals to BaP has been associated with the development of cancer, primarily skin, stomach and lung (IARC, 2010).

BaP requires metabolic activation prior to reaction with DNA (Baird et al., 2005). Cytochrome P450 (CYP) enzymes, mainly CYP1A1 and 1B1, are the most important enzymes in this process (Baird et al., 2005; Hamouchene et al., 2011), in combination with microsomal epoxide hydrolase (mEH). First, CYP1A1 or 1B1 enzymes oxidize BaP to an epoxide that is then converted to a dihydrodiol by mEH (*i.e.* BaP-7,8-dihydrodiol); then further bioactivation by CYP1A1 or 1B1 leads to the ultimately reactive species BaP-7,8-dihydrodiol-9,10-epoxide (BPDE) that can react with DNA, forming adducts preferentially at guanine residues. The 10-(deoxyguanosin-N^2-yl)-7,8,9-trihydroxy-7,8,9,10-tetrahydrobenzo[*a*]pyrene (dG-N^2-BPDE) adduct is the major product of BPDE with DNA *in vitro* and *in vivo* (Phillips, 2005). BaP is, however, oxidized also to other metabolites such as the other dihydrodiols, BaP-diones and hydroxylated metabolites (Bauer et al., 1995; Chun et al., 1996; Kim et al., 1998; Jiang et al., 2007; Zhu et al., 2008). Among them, 3-hydroxy-BaP (BaP-3-ol), formed by CYP1A1, is considered the major detoxification product of BaP oxidation, because it is known to inhibit mutagenesis and tumorigenesis (Huang et al., 1986). In mouse hepatoma Hepa1c1c7 cells, which express inducible CYP1A1, this metabolite was the major metabolite formed after exposure to BaP (Holme et al., 2007). Even though this CYP1A1-mediated BaP oxidation product as well as most of the other BaP metabolites are detoxification products, 9-hydroxy-BaP (BaP-9-ol) is a precursor of 9-hydroxy-BaP-4,5-epoxide (Fig. 1) which can form another adduct with guanine (Schoket et al., 1989; Nesnow et al., 1993; Fang et al., 2001). Thus, the levels and activities of CYP1A1 seem to be crucial both for the initiation of BaP-mediated carcinogenesis and BaP detoxification. The expression of CYP1A1 is known to be up-regulated by the aryl hydrocarbon receptor (AHR) and BaP can bind to and activate AHR thereby enhancing its own metabolic activation (Hockley et al., 2007).

The level of BaP-DNA adducts in cells is most probably the result of a balance between their formation and their loss through either DNA repair processes, or cell turnover. Collectively, BaP genotoxicity depends on various factors: (i) metabolism of BaP by phase I enzymes (activation) to reactive DNA-binding species; (ii) detoxification of reactive BaP metabolites by both phase I and phase II enzymes (conjugation); (iii) rate of repair of BaP-DNA adducts; and (iv) BaP-induced expression of genes such as those encoding enzymes involved in activation/detoxification or in DNA damage response (Uno et al., 2004).

Recently, controversial results have been found showing a more important role of CYP1A1 in BaP detoxification *in vivo* than in its activation (Uno et al., 2004, 2006; Arlt et al., 2008, 2012). *Cyp1a1*(−/−) mice treated with repeated oral doses of BaP (125 mg/kg body weight [bw]/day), die within ∼28 days due to immune suppression, whereas wild-type (WT) mice remain healthy for at least 1 year on this regimen (Uno et al., 2004). Using the hepatic P450 reductase null (HRN) and the reductase conditional null (RCN) mouse models we also showed that hepatic CYP enzymes appear to be more important for detoxification of BaP *in vivo* (Arlt et al., 2008, 2012). In these mice NADPH:P450 oxidoreductase (POR), the essential electron donor to CYPs is deleted specifically in hepatocytes, resulting in a decrease in hepatic CYP function (Henderson et al., 2003; Finn et al., 2007). We found however that the levels of dG-N^2-BPDE adducts in livers of these mice treated with BaP were higher than in WT mice (Arlt et al., 2008, 2012).

We postulate that the reason for these unexpected findings could be found *in vitro* by analyzing the roles of the different contributing enzymes at different ratios to each other. This can be achieved in reconstituted systems where single enzymes can be added at definite amounts without interference from other constituents as in microsomal systems. These data were compared with the metabolism of BaP and its activation to BaP-DNA adducts *in vivo*. We evaluated CYP1A1-mediated BaP metabolism and its bioactivation in mouse hepatic microsomes and by recombinant CYP1A1 reconstituted with POR. Because microsomal cytochrome b_5 has been found to participate in transfer of electrons to CYP enzymes during the CYP catalysis or cause allosteric changes in CYP protein structures that can augment the CYP mediated reactions (Porter, 2002; Schenkman and Jansson, 2003; Guengerich, 2005; Stiborová et al., 2006, 2012; Kotrbová et al., 2011; Riddick et al., 2013), we also analyzed its effects on BaP oxidation in the reconstituted system of CYP1A1 with POR. Moreover, since mEH is essential for the formation of the dG-N^2-BPDE adduct (Kim et al., 1998; Baird et al., 2005), its influence upon BaP-DNA adduct levels formed in a CYP1A1 reconstituted system was also elucidated. The levels of CYP1A1, POR, cytochrome b_5 and EH in mouse hepatic microsomes were determined in previous studies (Arlt et al., 2008, 2012). In the present work, we used a wide range of various ratios of these enzymes in the reconstituted systems to analyze their individual contribution to oxidation/activation of BaP. Among them, at least the reconstitution systems containing low concentrations of POR likely mimic the situation in the tested hepatic microsomes or *in vivo*. The formation of BaP metabolites was measured by high pressure liquid chromatography (HPLC) with UV-detection. DNA adduct formation was investigated by the thin-layer chromatography (TLC)-^{32}P-postlabeling method.

2. Material and methods

2.1. Chemicals

BaP (>96%) was purchased from Sigma-Aldrich (St. Louis, MO). All other chemicals were of analytical purity or better.

2.2. Animal experiments

All animal experiments were carried out under license in accordance with the law, and with local ethical approval. HRN ($Por^{lox/lox}/Cre^{ALB}$) mice on a C57BL/6 background were derived as described previously (Henderson et al., 2003). BaP was dissolved in corn oil at a concentration of 12.5 mg/ml. Groups of female HRN mice (3 months old, 25–30 g, $n = 3$) were treated intraperitoneally with 125 mg/kg bw of BaP for five days. This BaP dosage induces mutagenicity in multiple organs (Hakura et al., 1999) and is carcinogenic (Hakura et al., 1998). It is also noteworthy that the deletion of the *Por* gene in mouse hepatocytes resulted in higher expression of several Cyp proteins in female than in male mice (Henderson et al., 2003) and thus female mice were used in our previous study (Arlt et al., 2008). Control mice received corn oil only (Arlt et al., 2008). Animals were killed 24 h after the last dose. Livers were removed, snap frozen and stored at −80 °C until analysis.

2.3. Preparation of microsomes

Hepatic microsomes were isolated as described previously (Arlt et al., 2008) and pooled for further experiments. Protein concentration in the microsomal fraction was measured using bicinchoninic acid protein assay (Wiechelman et al., 1988) with bovine serum albumin as a standard.

2.4. Isolation of CYP1A1, POR, cytochrome b_5 and mEH

Recombinant rat CYP1A1 protein was purified to homogeneity from membranes of *Escherichia coli* transfected with a modified

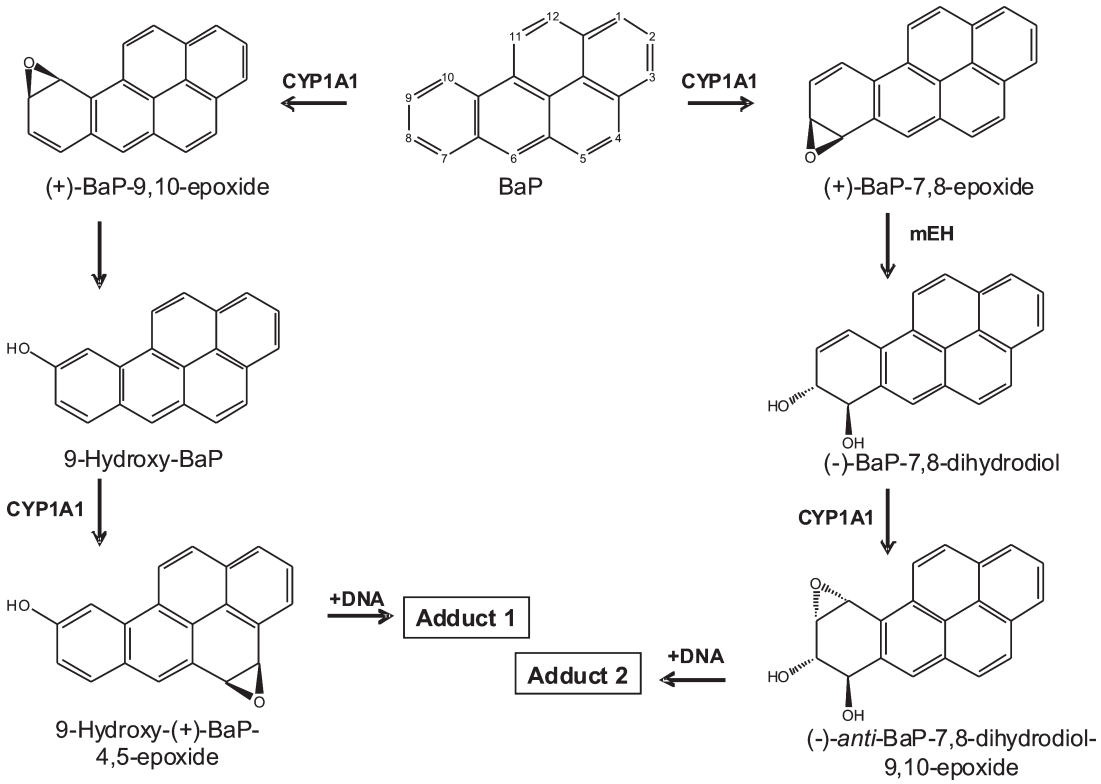

Fig. 1. Pathways of biotransformation and DNA adduct formation of BaP catalyzed by CYP1A1 and mEH. The two-step activation process by CYP1A1 leading to the formation of the ultimately reactive species, 9-hydroxy-BaP-4,5-epoxide, that can react with deoxyguanosine in DNA (adduct 1) is shown on the left. The typical three-step activation process with oxidation by CYP1A1 followed by hydrolysis by mEH leads to the ultimately reactive species, BPDE, forming the dG-N^2-BPDE adduct (adduct 2) is shown on the right.

CYP1A1 cDNA (Stiborová et al., 2002), in the laboratory of H. W. Strobel (University of Texas, Medical School of Houston, Texas, USA) by P. Hodek (Charles University, Prague, Czech Republic). Rabbit liver POR was purified as described (Stiborová et al., 2002). Cytochrome b_5 was isolated from rabbit liver microsomes by the procedure described by Roos (1996). mEH was purified from liver microsomes of rabbits pretreated with phenobarbital as described by Ariyoshi et al. (1994). These enzymes were used for the CYP1A1 reconstitution experiments. As shown in our previous studies (Stiborová et al., 2002, 2004, 2006, 2012; Kotrbová et al., 2009, 2011), the enzymatic activity of rat or human CYP1A1 reconstituted with rabbit POR and cytochrome b_5 was essentially the same as that of the enzyme reconstituted with the rat orthologs of these enzymes.

2.5. Microsomal and enzymatic incubations

Incubation mixtures used to study BaP metabolism in mouse hepatic microsomes or by purified CYP1A1 (100 pmol) reconstituted with POR (5–150 pmol), with or without cytochrome b_5 (100–500 pmol), with or without mEH (20–250 pmol) contained 100 mM potassium phosphate buffer (pH 7.4), NADPH-generating system (1 mM $NADP^+$, 10 mM D-glucose-6-phosphate, 1 U/ml D-glucose-6-phosphate dehydrogenase), 0.5 mg of microsomal protein or 100 pmol CYP1A1 in the reconstituted system, 50 μM BaP (dissolved in 5 μl dimethyl sulfoxide) in a final volume of 500 μl. The enzyme reconstitution was performed as described [(Stiborová et al., 2002, 2006; Kotrbová et al., 2011), using different molar ratios of CYP1A1 to POR and cytochrome b_5 and/or mEH (see Section 4 for details). Briefly, purified CYP1A1 was reconstituted with pure POR as follows (2 μM CYP, 0.1–3 μM POR, 0.5 μg/μl CHAPS, 0.1 μg/μl liposomes [dilauroyl phosphatidylcholine, dioleyl phosphatidylcholine, and dilauroylphosphatidylserine (1:1:1)], 3 mM reduced glutathione, and 50 mM HEPES/KOH, pH 7.4). The reaction was initiated by adding 50 μl of the NADPH-generating system. Control incubations were carried out either without enzymatic system (microsomes or the CYP1A1-reconstituted system), or without NADPH-generating system, or without BaP. After incubation (37 °C, 20 min), 5 μl of 1 mM phenacetin (PA) in methanol was added as an internal standard. BaP metabolites were extracted twice with ethyl acetate (2 × 1 ml), solvent evaporated to dryness, residues dissolved in 25 μl methanol and BaP metabolites separated by HPLC.

Incubation mixtures used to analyze BaP-induced DNA adduct formation were as described above but contained 1 mM NADPH instead of the NADPH-generating system plus 1 mg calf thymus DNA. The reaction was initiated by adding BaP. Incubations were carried out at 37 °C for 90 min; BaP-DNA adduct formation was linear up to 120 min (Arlt et al., 2008). Control incubations were carried out either without CYP, without NADPH, without DNA, or without BaP. After the incubation, DNA was isolated from the residual water phase by the phenol/chloroform extraction method as described (Stiborová et al., 2002).

2.6. CYP1A1 enzyme activity assays

The samples containing CYP1A1 reconstituted with POR (see the procedure described above) were characterized for enzyme activity using Sudan I oxidation for CYP1A1 (Stiborová et al., 2002) and 7-ethoxyresorufin *O*-deethylation (EROD) for CYP1A (Guengerich and Shimada, 1991).

2.7. HPLC analysis of BaP metabolites

HPLC analysis of BaP metabolites was performed on a Nucleosil® C18 reverse phase column, (250 × 4 mm, 5 μm; Macherey Nagel,

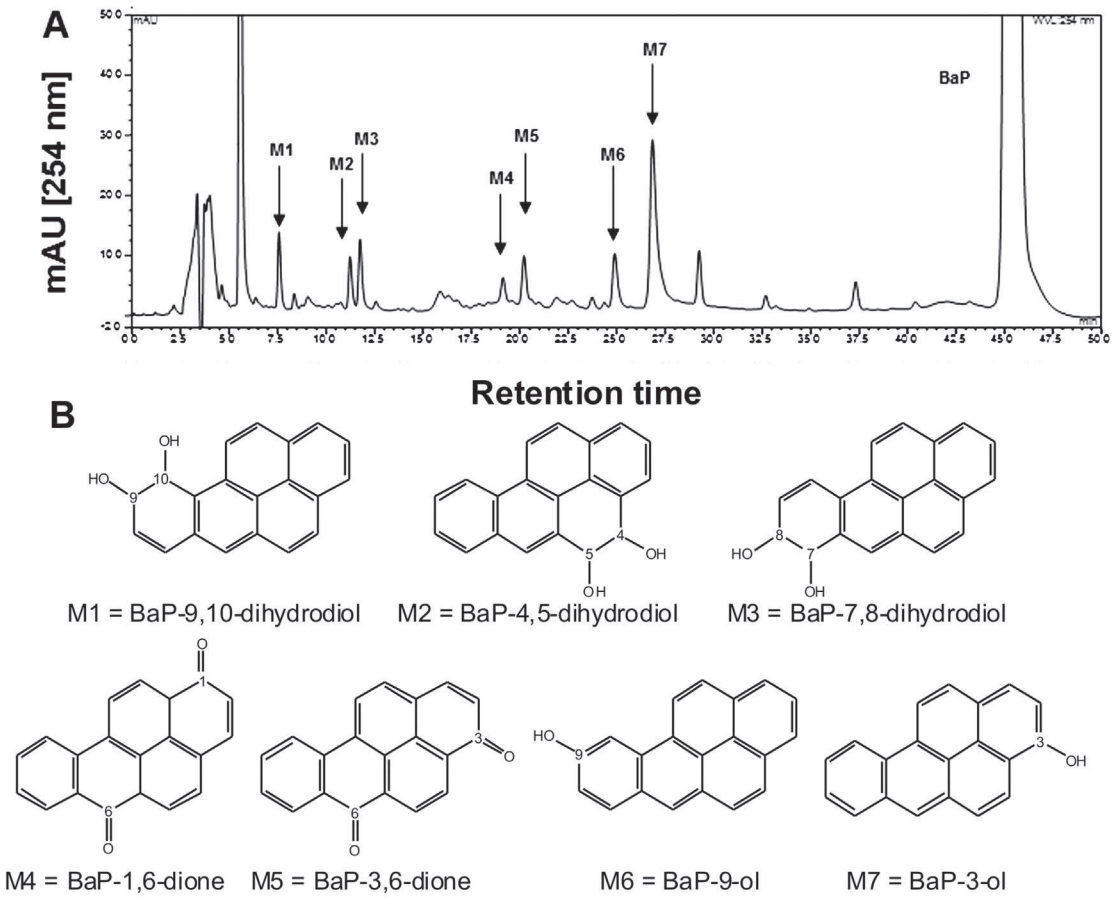

Fig. 2. (A) HPLC separation of the BaP metabolites generated by hepatic microsomes of HRN mice treated with BaP using Nucleosil® C18 reverse phase column. PA, phenacetin, M1–M7, BaP metabolites [BaP-9,10-dihydrodiol (M1), BaP-4,5-dihydrodiol (M2), BaP-7,8-dihydrodiol (M3), BaP-1,6-dione (M4), BaP-3,6-dione (M5), BaP-9-ol (M6) and BaP-3-ol (M7)]. (B) Structures of the BaP metabolites.

Düren, Germany) using a Dionex system consisting of a pump P580, a UV/VIS Detector UVD 170S/340S, an ASI-100 Automated Sample Injector, a termobox COLUMN OVEN LCO 101 and an In-Line Mobile Phase Degasser Degasys DG-1210 Dionex controlled with Chromeleon™ 6.11 build 490 software. The conditions used for the chromatographic separation of BaP metabolites were as follows: 50% acetonitrile in water; (*v*/*v*), with a linear gradient to 85% acetonitrile in 35 min, then an isocratic elution with 85% acetonitrile for 5 min, a linear gradient from 85% acetonitrile to 50% acetonitrile in 5 min, followed by an isocratic elution of 50% acetonitrile for 5 min. Detection was by UV absorption at 254 nm. BaP metabolite peaks (Fig. 2A) were collected and analyzed by NMR and/or mass spectrometry. The areas under the curve at 254 nm were calculated relative to the peak area of the internal standard phenacetin and expressed as relative peak areas.

2.8. NMR spectrometry

NMR spectra (δ, ppm; J, Hz) of BaP and its metabolites M1, M4, M5 and M7 were measured on a Bruker Avance II-600 and/or Bruker Avance II-500 instruments equipped with a cryoprobe (600.1 or 500.0 MHz for ^{1}H and 150.9 or 125.7 MHz for ^{13}C) in hexadeuterated acetone and $CDCl_3$ and referenced to the solvent signals (δ 2.05 and 7.27, respectively). Due to the low amounts of metabolites it was not possible to acquire ^{13}C NMR spectra or perform heteronuclear correlation experiments.

2.8.1. BaP

^{1}H NMR spectrum of BaP contains five isolated spin systems: one three-spin system of hydrogens H-1, H-2 and H-3, one four-spin system of H-7, H-8, H-9 and H-10, one isolated spin of H-6 and two two-spin systems of H-4, H-5 and of H-11, H-12. The assignment of signals in the spectrum could be done with the help of homonuclear COSY spectrum, where strong cross-peaks corresponding to three-bond couplings were observed. However, the signals of the two two-spin systems (H-4, H-5 and H-11, H-12) could not be assigned with the use of COSY spectrum only and heteronuclear correlation spectra (HSQC and HMBC) had to be used. The assignment of all ^{1}H signals and coupling constants of BaP and its metabolites is shown in Table 1 (for structures see Fig. 2B).

2.8.2. M1

Two signals of the four-spin system of M1 were shifted upfield (to 4.5 and 5.7 ppm). These values are too low for the fully aromatic BaP skeleton. The structure of M1 was identified as *trans*-9,10-dihydro-BaP-9,10-diol (BaP-9,10-dihydrodiol) by comparison with previously reported NMR data of this compound (Platt and Oesch, 1983). The *trans* arrangement of the two hydroxy groups was supported by the inspection of the vicinal coupling constant between hydrogen atoms H-9 and H-10. The torsion angle between these two hydrogen atoms calculated using the generalized Karplus type equation (Haasnoot et al., 1980) was predicted to be 48°. This value is very close to the torsion angle observed in the molecular model of the *trans*-derivative with the two hydroxyl groups in

Table 1
^{1}H chemical shifts of BaP and its metabolites M1, M4, M5 and M7 in hexadeuterated acetone. Coupling constants are in parenthesis.

	BaP	M1	M4	M5	M7
H-1	8.33d (7.8)	8.26[a]d (7.6)	–	8.02d (9.7)	8.20d (8.5)
H-2	8.04t (7.6)	8.04t (7.6)	6.74d (9.8)	6.69d (9.7)	7.68d (8.4)
H-3	8.18d (7.4)	8.27[a]d (7.6)	8.03d (9.7)	–	–
H-4	8.09d (9.2)	8.12[b]d (8.9)	8.19d (7.4)	8.83[a]d (7.7)	8.30d (9.3)
H-5	8.01d (9.1)	8.15[b]d (8.9)	8.68d (7.4)	8.71[a]d (7.7)	8.00d (9.5)
H-6	8.65s	8.09s	–	–	8.52s
H-7	8.37dm (8.1)	7.02d (9.5)	8.41dm (7.7)	8.41dm (7.9)	8.32s (8.1)
H-8	7.83ddd (8.0, 6.7, 1.2)	6.38dd (9.6, 5.3)	7.73m	7.70m	7.79m
H-9	7.88ddd (8.4, 6.7, 1.4)	4.50dd (5.2, 1.7)	7.92m	7.90m	7.81m
H-10	9.18dm (8.5)	5.69m	8.66dm (8.0)	8.61dm (8.1)	9.12d (8.3)
H-11	9.20d (9.2)	8.58d (9.2)	8.60[a]d (7.9)	8.76d (7.7)	8.97d (9.1)
H-12	8.43d (9.1)	8.23d (9.3)	8.92[a]d (7.9)	8.12d (7.7)	8.30d (9.3)

[a],[b] Chemical shifts with the same letter in one column may be interchanged.

pseudo-axial positions. The molecular model of the *cis*-derivative predicts the torsion angle between the two hydrogen atoms to be close to −75°. We were unable to determine the absolute configuration on the new asymmetric centers (C-9 and C-10). It is possible that both enantiomers are present in metabolite M1.

2.8.3. M4 and M5

In the spectra of both compounds we observed the four-spin system of H-7, H-8, H-9 and H-10 and three two-spin systems. Two substituents are therefore attached to the BaP skeleton: one in position 6 and the second one in position 1 or 3. Furthermore, the unusually shielded H-2 proton at 6.7 ppm was characteristic of the α-proton (next to carbonyl) in phenalones (Prinzbach et al., 1967) suggesting that the structures of M4 and M5 could be BaP-1,6-dione and -3,6-dione, respectively. Because both compounds were synthesized previously and their ^{1}H NMR spectra was reported (Leeruff et al., 1986; Xu et al., 2009), spectra in $CDCl_3$ were used for comparison and the metabolites could be identified as BaP-1,6-dione (M4) and BaP-3,6-dione (M5).

2.8.4. M7

In the spectrum of M7, the three-spin system was replaced with a two-spin system suggesting that one substituent is attached to the position 1 or 3 of the BaP. The structure of M7 was confirmed to be BaP-3-ol by comparison of the chemical shifts and coupling constants with those reported previously (Xu et al., 2009).

2.8.5. M2, M3 and M6

Because the amounts of M2, M3 and M6 samples were insufficient for NMR spectroscopy, these metabolites were analyzed only by mass spectrometry only as described below.

2.9. Mass spectrometry

Mass spectra of BaP and its metabolites M2, M3 and M6 were measured on a matrix-assisted laser desorption/ionization reflectron time-of-flight MALDITOF mass spectrometer ultraFLEX III (Bruker-Daltonics, Bremen, Germany). Positive spectra were calibrated externally using the monoisotopic $[M+H]^+$ ion of MRFA peptide 524.26 *m*/*z* and CCA matrix peaks 190.05, 379.09 *m*/*z*. A 10 mg/ml solution of α-cyano-4-hydroxy-cinnamic acid or 2,5-dihydrobenzoic acid in 50% MeCN/0.3% acetic acid was used as MALDI matrix. A 0.5 μl of sample dissolved in MeCN was premixed with 0.5 μl of the matrix solution on the target and allowed to dry at ambient temperature. The MALDI-TOF positive spectra were collected in reflectron mode. Positive $[M^+]$ of BaP corresponded to this compound (*m*/*z* 252.1). The metabolites with retention times of 11.9 (M2) and 12.9 min (M3) gave a positive molecular ion each at *m*/*z* 286.1 which is indicative of BaP-dihydrodiol metabolites. The metabolite eluted at 24.6 min (M6) gave a positive molecular ion at *m*/*z* 268.1 which is indicative of a hydroxylated BaP metabolite. These results are consistent with previous studies on the metabolism of BaP by human CYP1A1 (Bauer et al., 1995; Kim et al., 1998), in which these metabolites were identified as BaP-4,5-dihydrodiol (M2), BaP-7,8-dihydrodiol (M3), and BaP-9-ol (M6).

2.10. BaP-DNA adduct detection by ^{32}P-postlabeling analysis

DNA adducts were measured using the nuclease P1 enrichment version of the TLC-^{32}P-postlabeling method essentially as described previously (Arlt et al., 2008; Phillips and Arlt, 2007). Briefly, DNA samples (4 μg) were digested with micrococcal nuclease (120 mU; Sigma) and calf spleen phosphodiesterase (40 mU; Calbiochem), enriched and labeled as reported. Solvent conditions for the resolution of ^{32}P-labeled adducts on polyethyleneimine-cellulose (PEI) TLC were: D1, 1.0 M sodium phosphate, pH 6; D3, 4.0 M lithium-formate, 7.0 M urea, pH 3.5; D4, 0.8 M lithium chloride, 0.5 M Tris, 8.5 M urea, pH 8. After D3 or D4 developments to the top of the plates, the plates were developed an additional 30 min with the TLC tank partially opened, to prolong the resolution time of the BaP-DNA adducts. After chromatography TLC plates were scanned using a Packard Instant Imager (Dowers Grove, IL, USA). DNA adduct levels (RAL, relative adduct labeling) were calculated as described (Arlt et al., 2008). Results were expressed as DNA adducts/10^8 nucleotides. An external BPDE-DNA standard (Phillips and Castegnaro, 1999) was employed to identify adducts in experimental samples.

3. Results

3.1. Oxidation of BaP by hepatic microsomes and CYP1A1 reconstituted with POR, cytochrome b, and mEH

BaP metabolism in the CYP1A1 reconstituted system containing POR combined with cytochrome b_5 and/or mEH was compared with its metabolism by hepatic microsomes isolated from control (untreated) and BaP-pretreated HRN mice. In studies using mouse hepatic microsomes, a spectrum of hydroxylated BaP metabolites, BaP-dihydrodiols as well as BaP diones (quinones) was found (Fig. 2). Seven BaP oxidation products (designated as M1–M7) were generated both by hepatic microsomes of control HRN mice and by those with induced CYP1A1 expression mediated by pretreating HRN mice with BaP. These metabolites have been reported to be formed by CYP1A1 in combination with mEH (Bauer et al., 1995; Kim et al., 1998; Baird et al., 2005). The HPLC method using an acetonitrile/water gradient as mobile phase and UV detection at 254 nm resulted in mostly base-line separation of all BaP metabolites (Fig. 2A).

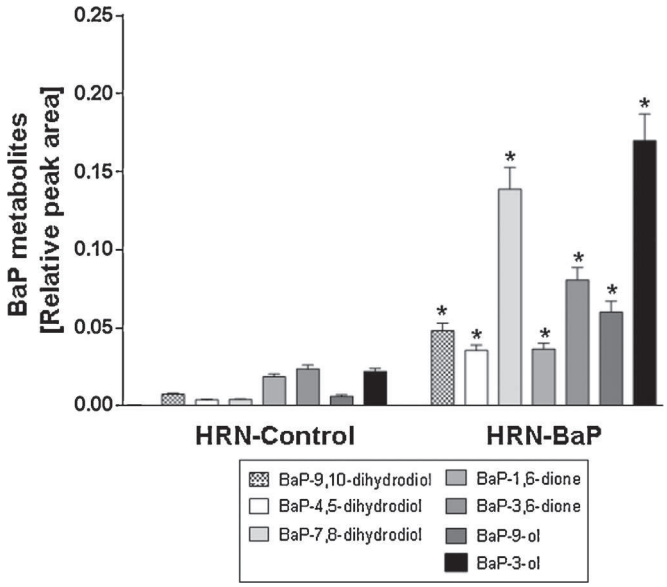

Fig. 3. Relative peak areas of BaP metabolites at 254 nm formed by hepatic microsomes isolated from control and BaP-treated HRN mice. Values are averages ± SD of three parallel experiments. Comparison was performed by *t*-test analysis; * $P < 0.001$, different from HRN control microsomes.

The BaP metabolites formed by mouse hepatic microsomes were collected and subsequently characterized by NMR or mass spectrometry. They were identified to be BaP-9,10-dihydrodiol (M1), BaP-4,5-dihydrodiol (M2), BaP-7,8-dihydrodiol (M3), BaP-1,6-dione, (M4), BaP-3,6-dione (M5), BaP-9-ol (M6), and BaP-3-ol (M7) (see Fig. 2). Very low expression levels of mouse POR in the liver of untreated HRN mice that constitutively express Cyp1a1 (Arlt et al., 2008) resulted in the formation of very low amounts of these BaP metabolites. However, Cyp1a1 induction by BaP pretreatment of HRN mice (Arlt et al., 2008) was sufficient for the effective oxidation of BaP by hepatic microsomes, even at the very low POR concentrations in these microsomes (Fig. 3). The efficiency of these microsomes to oxidize BaP to BaP-7,8-dihydrodiol, the precursor of BPDE, was more than 34-fold higher than that of microsomes of

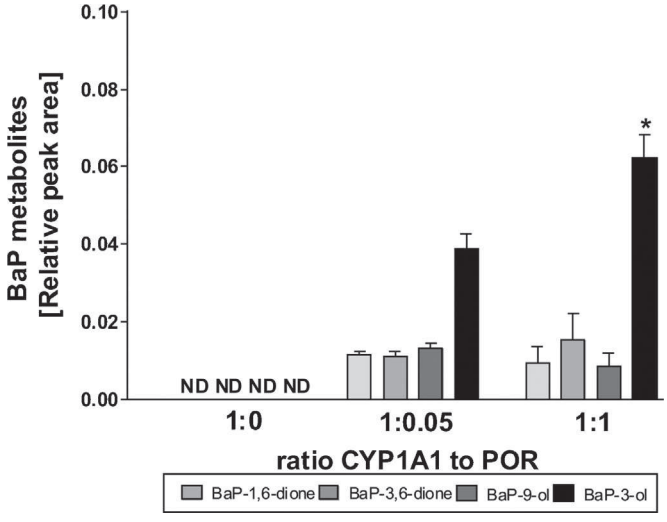

Fig. 4. Relative peak areas of BaP metabolites at 254 nm formed by rat CYP1A1 reconstituted with POR. Values are averages ± SD of three parallel experiments. ND—not detected. Comparison was performed by *t*-test analysis; * $P < 0.001$, different from BaP oxidation by CYP1A1:POR in a ratio of 1:1 than by CYP1A1:POR in a ratio of 1:0.05.

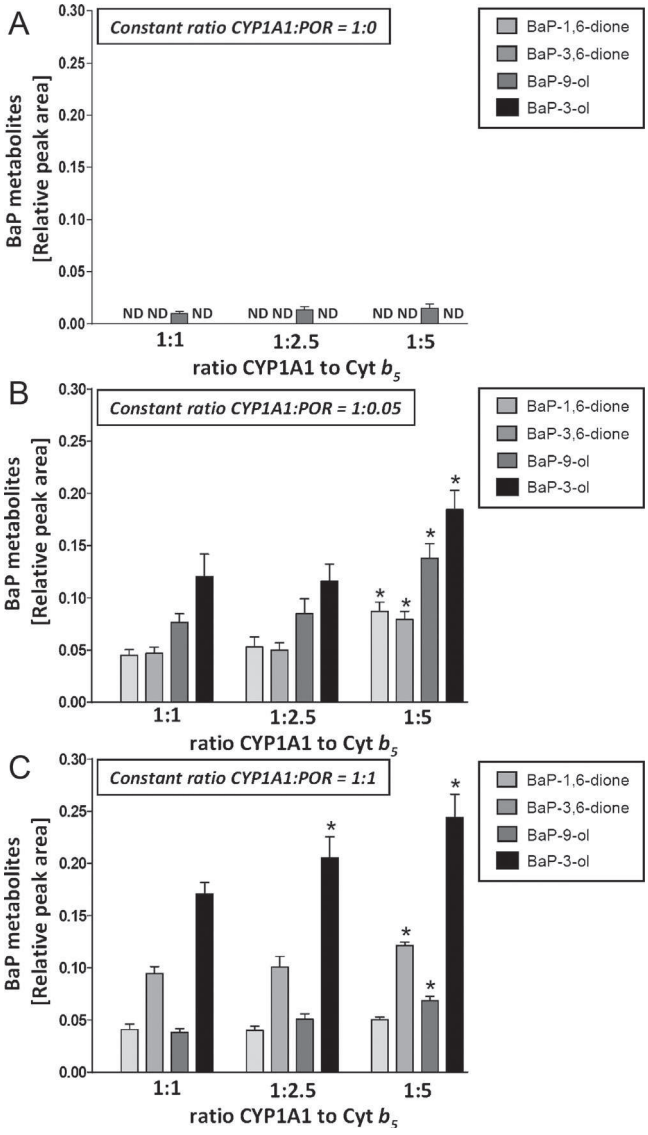

Fig. 5. The effect of increasing amounts of cytochrome b_5 on oxidation of BaP by (A) rat CYP1A1 without POR; B, CYP1A1 reconstituted with POR in a ratio of CYP1A1 to POR 1:0.05 and C, of 1:1. The values are averages ± SD of relative peak areas of three parallel experiments. Comparison was performed by *t*-test analysis; * $P < 0.001$, different from BaP oxidation with the CYP1A1/POR system containing cytochrome b_5 in a ratio of CYP1A1:cytochrome b_5 of 1:5 than by that with CYP1A1:cytochrome b_5 of 1:1 or 1:2.5.

untreated mice, while formation of other metabolites was less pronounced. Amounts of BaP-9,10-dihydrodiol, BaP-4,5-dihydrodiol, BaP-1,6-dione, BaP-3,6-dione, BaP-9-ol and BaP-3-ol were 6.6-, 9.6-, 2-, 3.4-, 10- and 7.7-times higher, respectively, in microsomes of HRN mice exposed to BaP than in those of untreated HRN mice (Fig. 3).

To investigate the role of CYP1A1 in oxidation of BaP to individual metabolites, purified CYP1A1 was reconstituted with POR and used as the oxidation system. CYP1A1 reconstituted with POR was active with its typical substrates, Sudan I (Stiborová et al., 2002) and 7-ethoxyresorufin (Guengerich and Shimada, 1991) (data not shown). Isolated CYP1A1 reconstituted with POR oxidized BaP to only four metabolites, namely BaP-1,6-dione (M4), BaP-3,6-dione (M5), BaP-9-ol (M6), and BaP-3-ol (M7) (Fig. 4). As expected, no BaP-dihydrodiols were detected in this system because of the absence of mEH which is important for the hydration of BaP epoxides. In the enzymatic systems where mEH was reconstituted

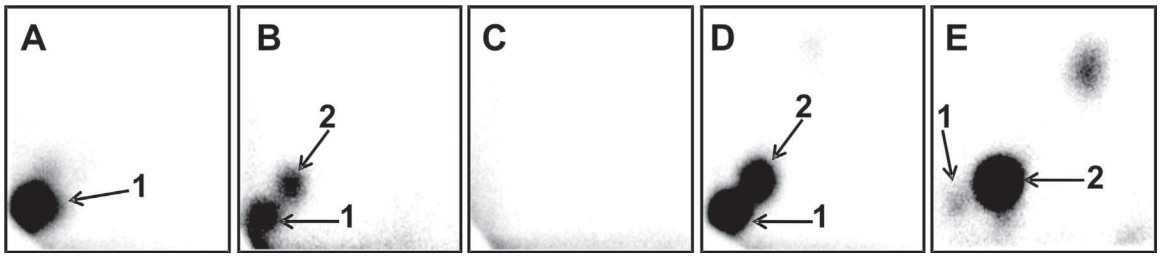

Fig. 6. Autoradiographic profile of ^{32}P-labeled DNA adducts generated in calf thymus DNA by BaP after its activation with (A) CYP1A1 reconstituted with POR (CYP1A1:POR of 1:0.2) in the presence of NADPH; (B) CYP1A1 reconstituted with POR, mEH and cytochrome b_5 at ratios of 1:0.2:1:3 in the presence of NADPH; (C) the same reconstituted system but without NADPH (control incubation); (D) hepatic microsomes from HRN mice treated with BaP. (E) adduct profile of DNA from liver of HRN mice treated with BaP. Analyses were performed by the nuclease P1 version of the ^{32}P-postlabeling assay with the TLC conditions described in Section 2. Adduct 1—derived from reaction of 9-hydroxy-BaP-4,5-epoxide with deoxyguanosine in DNA; Adduct 2—dG-N^2-BPDE.

with CYP1A1 and POR, BaP-9,10-dihydrodiol (M1) and BaP-7,8-dihydrodiol (M3) were formed as expected, however the whole metabolic profile of BaP could not be quantified because some impurities in the mEH preparation interfered with BaP metabolites eluting between 22 and 35 min during HPLC (data not shown).

Interestingly, no significant differences in levels of BaP-1,6-dione, BaP-3,6-dione and BaP-9-ol were found in the systems where CYP1A1 was reconstituted with low amounts of POR (the CYP1A1:POR ratio was 1:0.05) or equimolar concentrations of these enzymes (Fig. 4). Only BaP-3-ol formation was significantly higher (1.6-fold) in the system containing equimolar CYP1A1:POR ratios. No BaP metabolites were formed when POR was omitted from the CYP1A1 reconstitution system (Fig. 4). However, when CYP1A1 was reconstituted with cytochrome b_5 without POR (under CYP1A1:cytochrome b_5 ratios of 1:1, 1:2.5 or 1:5), BaP was oxidized (Fig. 5A) to only low amounts of BaP-9-ol. Addition of cytochrome b_5 to the CYP1A1/POR reconstituted system led to a cytochrome b_5-concentration-dependent increase in BaP oxidation (compare 4 and 5B and C); the increase was found both at 1:0.05 and 1:1 CYP1A1:POR ratios. BaP-3-ol was the major metabolite formed under both CYP1A1:POR ratios but its amount was up to 1.8-fold higher when POR was present at an equimolar ratio to CYP1A1 than at the 1:0.05 CYP1A1:POR ratio. In contrast, the amount of BaP-9-ol was always higher in the system with low POR concentrations. Like BaP-3-ol, the amount of BaP-3,6-dione formed in the system was always higher at equimolar CYP1A1/POR concentrations relative to the systems containing low POR concentrations, while overall no differences were found for BaP-1,6-dione. Collectively, all these results indicate that cytochrome b_5 may contribute quite substantially to the CYP1A1-mediated oxidation of BaP, even under conditions with very low quantities of POR.

3.2. BaP-DNA adduct formation by hepatic microsomes and CYP1A1 reconstituted with POR, cytochrome b_5 and mEH

In further experiments the formation of BaP-derived DNA adducts was investigated in analogous enzymatic systems.

Activation of BaP by CYP1A1 reconstituted with POR in the presence of DNA resulted in the formation of only one BaP-DNA adduct (adduct spot 1 shown in Fig. 6A). Therefore, this adduct is formed by CYP1A1-catalyzed oxidation of BaP, without the contribution of mEH. Comparison with previous ^{32}P-postlabeling studies (Schoket et al., 1989; Nesnow et al., 1993; Fang et al., 2001) showed that adduct spot 1 has similar chromatographic properties on PEI-cellulose TLC to a guanine adduct derived from reaction with 9-hydroxy-BaP-4,5-epoxide (see Fig. 1). In accordance with these previous results, DNA adduct 1 (Fig. 6) had more hydrophobic properties on PEI-cellulose than another BaP-derived DNA adduct (assigned adduct spot 2) formed by hepatic microsomes (compare Fig. 6D), which was identified as dG-N^2-BPDE (Schoket et al., 1989; Fang et al., 2001; Arlt et al., 2008).

As shown in Fig. 7A formation of BaP-DNA adduct 1 was dependent on the CYP1A1:POR ratio and was formed even at low POR concentrations (*i.e.* a CYP1A1:POR ratio of 1:0.2). However, when BaP was incubated with DNA using a CYP1A1:POR ratio of 1:2, lower levels of this adduct were produced (Fig. 7A). Addition of increasing amounts of mEH to the CYP1A1/POR reconstituted system led to a decrease in the formation of this adduct, while BaP-DNA adduct

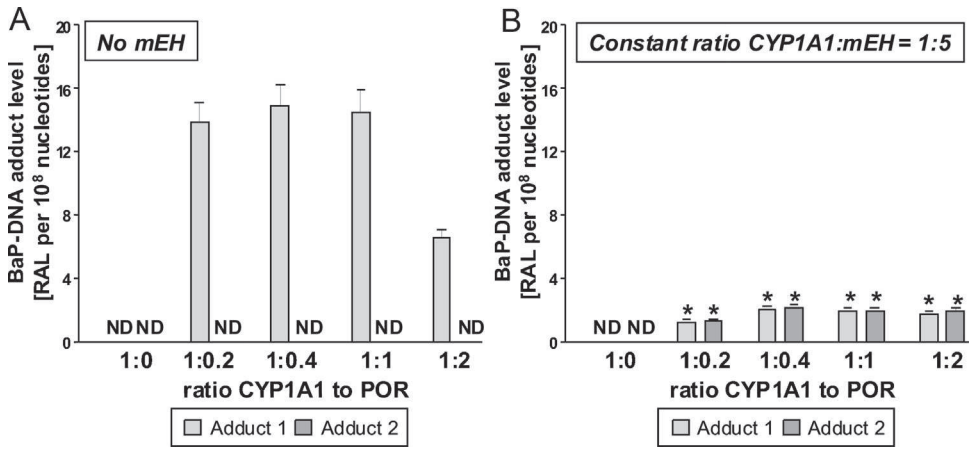

Fig. 7. BaP-DNA adducts formed by CYP1A1 reconstituted with (A) POR and (B) with POR and mEH at a ratio of CYP to mEH of 1:5. RAL—relative adduct labeling. Values are averages ± SD of three parallel experiments. Comparison was performed by *t*-test analysis; * $P < 0.001$, different from BaP-DNA adduct formation by the CYP1A1/POR system containing microsomal epoxide hydrolase (mEH) than by that without this enzyme. ND—not detected.

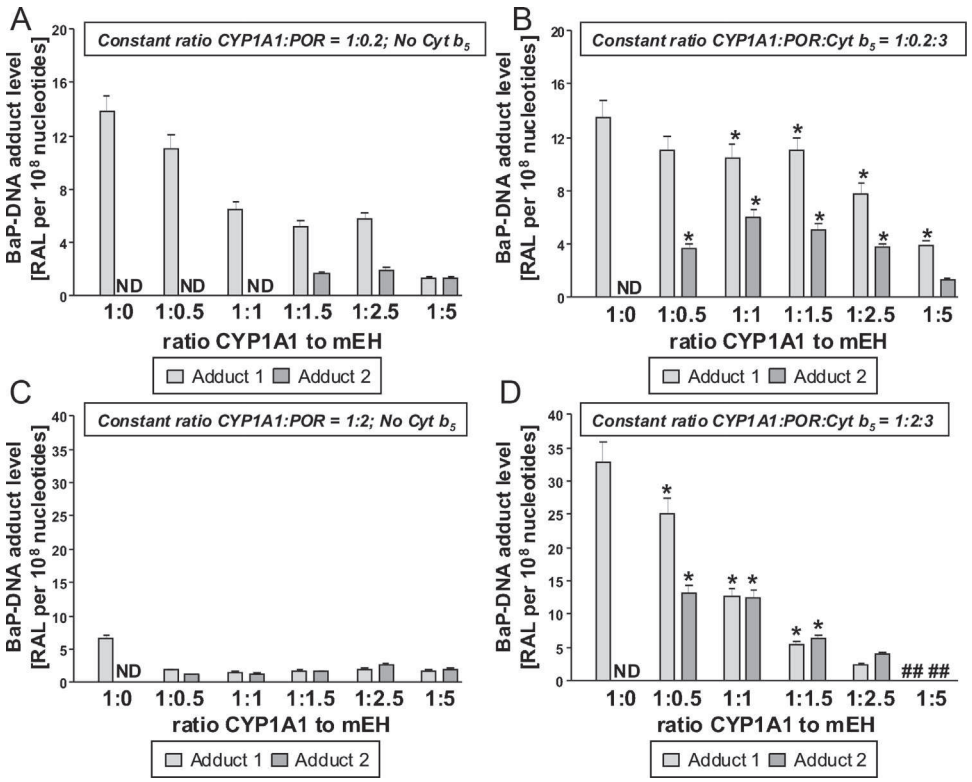

Fig. 8. The effect of cytochrome b_5 on BaP-DNA adduct formation catalyzed by CYP1A1 reconstituted with POR and mEH at different ratios of the four constituents: (A) a ratio of CYP1A1 to POR of 1:0.2 with mEH added either without cytochrome b_5; (B) with this protein at a ratio of 1:3 (CYP to cytochrome b_5); C, at a CYP1A1 to POR ratio of 1:2 with mEH either without cytochrome b_5: (D) with this protein at a ratio of 1:3 (CYP to cytochrome b_5). ##—the samples were not analyzed. ND—not detected. RAL—relative adduct labeling. Values are averages ± SD of three parallel experiments. Comparison was performed by *t*-test analysis; * $P < 0.001$, different from BaP-DNA adduct formation by the CYP1A1/POR system containing cytochrome b_5 than by that without this protein.

2 (adduct spot 2 shown in Fig. 6B and D) was generated (7B and 8A and C). No BaP-DNA adducts were detected by ^{32}P-postlabeling when NADPH, the cofactor of the NADPH-dependent CYP system, was omitted from incubations with the CYP1A1 reconstituted systems (Fig. 6C).

Addition of cytochrome b_5 to the CYP1A1 reconstituted system resulted in increased formation of both BaP-DNA adducts formed under a CYP1A1:POR ratio of 1:2, both in the absence and presence of mEH (Fig. 8). However, levels of BaP-DNA adduct 1 at a CYP1A1:POR ratio of 1:0.2 were nearly identical in the presence or absence of cytochrome b_5 when mEH was absent, whereas addition of cytochrome b_5 to this system in the presence of mEH increased formation of both BaP-DNA adducts (Fig. 8A and B). The levels of adduct 1 formed by CYP1A1, POR and cytochrome b_5 in a ratio of 1:2:3 were higher than in any other enzyme combination (Fig. 8). Among all enzyme combinations used, the highest levels of both BaP-DNA adducts were produced by the system containing CYP1A1, POR, mEH and cytochrome b_5 in a ratio of 1:2:0.5:3 (Fig. 8D) followed by the systems containing these enzymes in ratios of 1:0.2:1:3 (Fig. 8B) or 1:2:1:3 (Fig. 8D). These results showed that even under low POR concentrations, CYP1A1 in the presence of appropriate concentrations of mEH and cytochrome b_5 efficiently activates BaP to DNA binding species. These results are in line with the BaP metabolite profile in the CYP1A1 reconstituted experimental systems described above.

The DNA adduct results obtained in reconstituted enzyme systems corresponded to those found in hepatic microsomes of HRN mice. As shown in our previous study (Arlt et al., 2008), incubation of BaP with hepatic microsomes from these mice led to DNA adducts detectable by ^{32}P-postlabeling. Using this method one major asymmetric BaP-DNA adduct spot was detectable, in which the dG-N^2-BPDE adduct was identified by cochromatographic analysis, and DNA adduct levels increased substantially in incubations with microsomes from BaP pretreated HRN mice (Arlt et al., 2008). After closer inspection of this asymmetric BaP-DNA adduct spot and improved chromatographic separation, two major BaP-DNA adducts (still partially overlapping one another) were detectable. Better separation of these BaP-DNA adducts as well as those found in liver of HRN mice treated with BaP was achieved on PEI-cellulose TLC (Fig. 6D and E) by a slightly modified development in D3 and

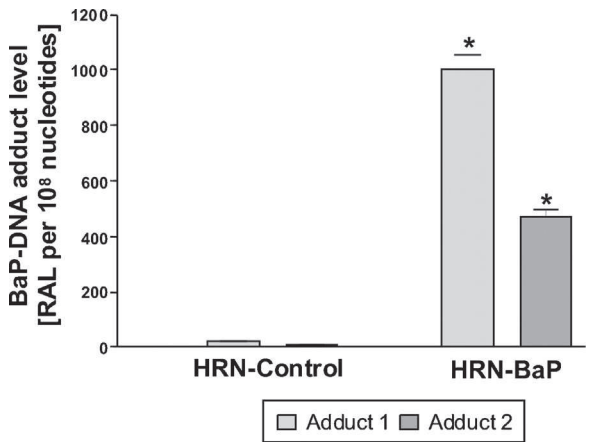

Fig. 9. BaP-DNA adducts formed by liver microsomes isolated from control and BaP treated HRN mice. RAL—relative adduct labeling. Values are averages ± SD of three parallel experiments (Adduct 1 and 2 see Fig. 6). Comparison was performed by *t*-test analysis; * $P < 0.001$, different from HRN control microsomes.

D4 directions as outlined in Section 2. The chromatographic properties of both adducts on TLC were similar to the two BaP-DNA adducts found in experiments utilizing CYP1A1-reconstituted systems (compare adduct spots 1 and 2 in Fig. 6B and D). Therefore, in the present study we re-analyzed the BaP-DNA adduct levels found in hepatic microsomal incubations from control (untreated) HRN mice and those pretreated with BaP. While only low levels of both BaP-DNA adducts were formed by hepatic microsomes from untreated HRN mice, formation of both adducts increased substantially (~50-fold) in hepatic microsomes isolated from BaP-pretreated HRN mice (Fig. 9). These results indicate that Cyp1a1 induction in combination with relative low POR expression still provides an efficient BaP activation system leading to DNA adduct formation. BaP-DNA adduct 1 was, however, hardly detectable in liver DNA from BaP-treated HRN mice (Fig. 6E) which is in full concordance with results obtained previously (Arlt et al., 2008) where dG-N^2-BPDE (assigned BaP-DNA adduct 2 in the present study) was the major adduct identified *in vivo*.

4. Discussion

Previously we worked with two different mouse models lacking POR expression in hepatocytes and found that the levels of BaP-DNA adducts were up to 13-fold higher in livers of HRN mice treated with BaP than in those of WT mice (Arlt et al., 2008). More recently, these results were confirmed in the RCN mouse model (Arlt et al., 2012), indicating that hepatic CYP enzymes are more important for detoxification of BaP *in vivo* despite being required for its bioactivation *in vitro*. Nevertheless, hepatic microsomes from HRN mice expressing very low POR levels, and particularly those from BaP-pretreated HRN mice were capable of activating BaP to form DNA adducts *in vitro* (compare Fig. 6 in Arlt et al., 2008 and 6D and 9 in the present work), suggesting that Cyp1a1-mediated bioactivation of BaP takes place in these microsomes. In order to confirm this finding in a flexible modular experimental system we investigated the oxidative metabolism of BaP and its bioactivation to BaP-DNA adducts in a reconstituted enzyme system that allows the addition and removal of individual enzymes. Purified CYP1A1 was reconstituted with POR and other components of the microsomal enzymatic system (cytochrome b_5 and mEH) in various combinations and ratios were employed. For comparison mouse microsomal enzymatic systems were utilized. Among the tested reconstituted systems, at least those containing low concentrations of POR likely mimic the situation in mouse hepatic microsomes or *in vivo*. However, it should be noted that the reconstituted systems may only provide mechanistic insights and cannot be fully extrapolated to microsomes and/or to the *in vivo* situation.

Interestingly, as shown in Figs. 2 and 3 the results obtained in the present study demonstrated that BaP is oxidized by hepatic microsomes of control (untreated) and BaP-pretreated HRN mice containing very low amounts of POR to hydroxylated BaP metabolites (BaP-3-ol and BaP-9-ol), BaP-dihydrodiols (BaP-4,5-dihydrodiol, BaP-7,8-dihydrodiol and BaP-9,10-dihydrodiol) as well as BaP diones (BaP-1,6-dione and BaP-3,6-dione). The same metabolites have been formed in several previous studies utilizing enzyme systems of CYP1A1 combined with POR and mEH (Kim et al., 1998; Jiang et al., 2007; Zhu et al., 2008). We also found that BaP is activated by these microsomes to form BaP-DNA adducts (Fig. 6) which have been detected in previous studies (Nesnow et al., 1993; Schoket et al., 1989; Fang et al., 2001; Siddens et al., 2012).

As expected, mEH was essential for the formation of BaP-dihydrodiols; CYP1A1 reconstituted with POR but without mEH generated only BaP-1,6-dione, BaP-3,6-dione, BaP-3-ol, and BaP-9-ol. It is known that oxidation of various substrates by CYP1A1 or other CYPs is dependent on the POR:CYP1A1 ratio; optimal ratios of these enzymes are usually 1:1 or higher (Buters et al., 1995; Chun et al., 1996; Schwarz et al., 2001; Shimada et al., 1999, 2001; Shimada and Fujii-Kuriyama, 2004; Yamazaki et al., 2001; Stiborová et al., 2002; Guengerich, 2005; Farooq and Roberts, 2010; Davydov, 2011; Kotrbová et al., 2011; Davydov et al., 2013). Interestingly, in contrast to these findings, with the exception of BaP-3-ol, formation of BaP metabolites by CYP1A1 reconstituted with POR was the same, even when the CYP1A1:POR ratio was only 1:0.05. This CYP1A1:POR ratio essentially mimics the expression level of these enzymes in the livers of HRN mice (Arlt et al., 2008), while a higher than equimolar POR:CYP1A1 ratio more reflects the situation in the livers of WT mice suggesting an effective transfer of electrons from NADPH to the CYP1A1-BaP binary complex mediated by POR. The only detoxification BaP metabolite, BaP-3-ol, was formed at higher amounts in the CYP1A1 system reconstituted with an equimolar ratio of POR. This high efficiency of BaP metabolism at ratios of CYP1A1:POR of less than 0.5 are unusual, but seems to be a specific phenomenon for oxidation of BaP by CYP1A1 rather than a general feature. For other substrates such as Sudan I (Stiborová et al., 2002) and ellipticine (Mrázová et al., 2007; Kotrbová et al., 2011) a reconstitution system of CYP1A1 with POR at a ratio of 1:1 was optimal. It seems that binding of BaP to CYP1A1 mediating formation of the high-spin state of CYP1A1 facilitates the enzyme oligomerization (aggregation) in an artificial membrane of liposomes and such CYP1A1-CYP1A1 interactions may have evolved to optimize the functioning of the reconstitution system at limiting concentrations of POR. Indeed, there are numerous observations demonstrating a crucial effect of oligomerization of microsomal CYPs on their functional properties. One of the most prominent consequences of oligomerization is given by "persistent heterogeneity" or apparent divergence of a pool of a single CYP species into non-interconverting and functionally separate fractions (Davydov, 2011). This suggestion was supported by several investigations for substrate oxidation by various CYP enzymes in the reconstituted systems (Kaminsky and Guengerich, 1985; Backes and Eyer, 1989; Iwase et al., 1991; Fernando et al., 2007, 2008; Davydov, 2011). The reasons for the results found in the present work seem to be even more complex, as BaP oxidation by the CYP1A1 reconstituted system was substantially stimulated by cytochrome b_5.

The major BaP-DNA adduct formed in HRN/RCN mice and in hepatic microsomes of HRN mice was previously identified by TLC, HPLC and LC–MS/MS to be dG-N^2-BPDE. In addition, another adduct found and assigned adduct 1 in the present study, exhibited more hydrophobic properties on ^{32}P-postlabeling TLC (see Fig. 1 in Arlt et al., 2008 and Fig. 2 in Arlt et al., 2012) and could be separated from adduct 2 (*i.e.* dG-N^2-BPDE). Since mouse hepatic Cyp enzyme activity had been largely obliterated by the permanent (HRN model) or conditional (RCN model) deletion of POR in hepatocytes, the levels of BaP-DNA adduct formation in livers in HRN or RCN mice *in vivo* and in hepatic microsomes of HRN mice *ex vivo* was difficult to rationalize (Arlt et al., 2008, 2012). Previous results indicated that the process leading to DNA adducts did not involve the generation of a reactive species different from that formed in WT mice (Arlt et al., 2008, 2012). Since the structure of the dG-N^2-BPDE adduct formed *in vivo* was identified by mass spectrometry (Arlt et al., 2008), BPDE (Fig. 1) must be the reactive species formed both in HRN/RCN and WT mice. Moreover, enzymes different from CYPs such as cyclooxygenases were not found to be involved in BaP activation in these mouse models (Arlt et al., 2008). Indeed, formation of dG-N^2-BPDE by hepatic microsomes of HRN mice *ex vivo*, which depended on NADPH, and was attenuated by inhibitors of CYP1A1 (α-naphthoflavone, ellipticine) and POR (α-lipoic acid), supported this conclusion (Arlt et al., 2008). Although the CYP specificity of chemical inhibitors can sometimes be problematic (Rendic and DiCarlo, 1997), these results indicated that hepatic Cyp1a1 in combination with even a very low POR expression level can be responsible for the formation of BaP-DNA adducts in

hepatic microsomes of HRN mice. Nevertheless, it should be noted that human CYP1B1 is also an efficient enzyme metabolizing BaP and the BaP metabolite profiles are similar to those generated by CYP1A1 (Kim et al., 1998; Shimada et al., 1999; Shimada and Fujii-Kuriyama, 2004). However, expression of Cyp1b1 has not been detected in the liver of HRN mice (Wang et al., 2005; Arlt et al., 2008). Therefore, mouse Cyp1b1 does not seem to be important for BaP metabolism and activation in the liver of HRN mice.

Induction of Cyp1a1 in HRN mice with BaP resulted in a more than 34-fold increase in the production of BaP-7,8-dihydrodiol in *ex vivo* incubations of BaP with such microsomes relative to microsomes of untreated mice. BaP-7,8-dihydrodiol is the precursor of BDPE which subsequently can generate the dG-N^2-BPDE adduct, explaining the formation of the dG-N^2-BPDE adduct in the microsomes of HRN mice pretreated with BaP (Arlt et al., 2008 and present work). In contrast, BaP-3-ol the major CYP1A1-mediated metabolite detoxicating BaP (Baird et al., 2005) only increased 7.7-fold after pretreatment of mice with BaP.

In this study two DNA adducts were generated by hepatic microsomes of HRN mice and levels of both were dependent on pretreatment of these mice with BaP, a CYP1A1 inducer. When CYP1A1 reconstituted with POR only was used for BaP activation, one BaP-DNA adduct (assigned adduct 1; Fig. 6A) was generated. After addition of mEH to the CYP1A1/POR reconstituted system, the dG-N^2-BPDE adduct (assigned adduct 2; Fig. 6) was also formed. Again, higher amounts of both BaP-DNA adducts were formed by CYP1A1 in the presence of low POR levels (*i.e.* a ratio of CYP1A1:POR of 1:0.2) than at equimolar ratios in the reconstitution system. Moreover, cytochrome b_5 substantially stimulated BaP-DNA adduct formation. Both these BaP-DNA adducts have also been found by Schoket et al. (1989) and Fang et al. (2001) to be generated by rat hepatic microsomes and separated as two adduct spots by TLC-^{32}P-postlabeling. The highly hydrophobic adduct 1 was tentatively identified by these authors as an adduct derived from 9-hydroxy-BaP-4,5-epoxide. This BaP metabolite is bound to the exocyclic amino group of a guanine residue, and the site of attachment is most likely either the 4 or the 5 position of BaP (Fang et al., 2001). Analogous to our results, the formation of adduct 1 was independent of the activity of mEH; an inhibitor of this enzyme, 1,2-epoxy-3,3,3-trichloropropane, did not influence its formation (Schoket et al., 1989). In contrast the formation of dG-N^2-BPDE (adduct 2) was strongly inhibited by this mEH inhibitor. Nevertheless, even though a precursor of 9-hydroxy-BaP-4,5-epoxide, BaP-9-ol, was formed both in mouse hepatic microsomes and by the CYP1A1 reconstitution system, further work is required to demonstrate that adduct 1 is derived from 9-hydroxy-BaP-4,5-epoxide. The synthesis of an authentic standard should help with the structural identification.

It is well known that BaP is a strong CYP1A1 inducer in many organisms including HRN mice (Arlt et al., 2008). BaP also induced expression of POR protein (by 2.9-fold) and the activity of this enzyme as well as mEH and cytochrome b_5 in HRN mice (Arlt et al., 2008, 2012), thereby enhancing its own metabolic activation. Indeed, pretreatment of HRN mice with BaP led to more than ~50-fold higher DNA adduct levels *ex vivo* using hepatic microsomes (Fig. 9). Because microsomal cytochrome b_5 influences the CYP1A1-mediated activation of BaP *in vitro*, and is induced by BaP treatment in HRN mice (Arlt et al., 2012), this protein can modulate Cyp1a1-catalyzed activation of BaP also in this mouse model *in vivo*. Several mechanisms of cytochrome b_5-mediated modulation of CYP catalysis have been suggested. One of them suggests a role of cytochrome b_5 in the direct transfer of the second electron to the CYP enzyme, which is considered to be the rate limiting step in the catalytic cycle of the CYP monooxygenase reaction. The electron transfer from reduced cytochrome b_5 to CYP is faster than the input of electrons from POR. Due to this stimulation effect CYPs are prevented from uncoupling of partially activated oxygen. Moreover, the addition of cytochrome b_5 enhances the stability of the oxy-CYP complex, therefore a higher amount of activated oxygen is available to form hydroxylated products. Another possible mechanism of the cytochrome b_5 action is the formation of a complex between cytochrome b_5 and CYP, which can receive two electrons from POR in a single step, one for reduction of CYP and another for that of cytochrome b_5. While CYP without cytochrome b_5 has to undergo two separate interactions with POR to complete one catalytic cycle, in the presence of cytochrome b_5 a single interaction of the complex of CYP and cytochrome b_5 with POR is sufficient; cytochrome b_5 provides the second electron to CYP promptly after oxygen binding. Cytochrome b_5 can also act as an allosteric modifier of the oxygenase (Porter, 2002; Schenkman and Jansson, 2003; Guengerich, 2005; Kotrbová et al., 2011; Stiborová et al., 2012; Riddick et al., 2013). Thus, in HRN mice cytochrome b_5 may not only modulate the Cyp-mediated (*i.e.* Cyp1a1) bioactivation of BaP *in vivo* if very low levels of POR are present, but it may also stimulate CYP-mediated metabolic activation of BaP because of its increased expression induced by BaP. Therefore, it would be interesting to examine the potential role of cytochrome b_5 in the metabolic activation of BaP *in vivo*. Recently, a mouse model has been developed, in which cytochrome b_5 has been deleted in all tissues [Cytochrome b_5 Complete Null (BCN)] (McLaughin et al., 2010), allowing the investigation of general functions of cytochrome b_5 in carcinogen metabolism *in vivo*. To dissect the role of hepatic cytochrome b_5 *versus* hepatic POR in Cyp-mediated bioactivations a conditional liver-specific cytochrome b_5 knockout mouse ($Cytb5^{lox/lox}/Cre^{ALB}$; HBN mouse) has been generated (Finn et al., 2008) with or without the expression of hepatic POR (Henderson et al., 2013). In the future we plan to investigate the balance between Cyp-mediated activation and detoxification of BaP *in vivo* in these potentially improved mouse models.

As shown in the present study, even low POR expression in livers of HRN mice (POR probably expressed in non-parenchymal cells of liver), in combination with the induction of Cyp1a1, cytochrome b_5 and mEH by BaP, might be sufficient for an efficient oxidative activation of BaP. This feature might follow from a specific pattern of protein levels and activities of these enzymes in hepatic microsomes of HRN mice pretreated with BaP that resulted in a more than 10- and 34-fold increase in formation of metabolic precursors essential for the generation of BaP-DNA adducts; BaP-9-ol as the precursor of 9-hydroxy-BaP-4,5-epoxide potentially forming adduct 1, and BaP-7,8-dihydrodiol as the precursor of BPDE forming the dG-N^2-BPDE adduct (adduct 2), respectively. We believe that these findings might be one of the potential reasons for the high levels of BaP-DNA adducts formed in livers of HRN mice relative to WT mice, but other factors may also contribute. Since it has been shown that BaP can increase the activity of some conjugation enzymes (*i.e.* glutathione *S*-transferase) participating in BaP detoxification (Banni et al., 2009), their expression levels increased by induction by BaP and contribution to the detoxication of BaP metabolites in the HRN model needs further investigation. In addition, the formation and rate of repair of BaP-DNA adducts and the effect of BaP on the expression of DNA repair proteins may be different in HRN and WT mice. Furthermore, the ratio of the hydrophobic DNA adduct 1 to dG-N^2-BPDE formed by hepatic microsomes and in the CYP1A1-reconstituted systems were much higher than the ratios detected in the livers of HRN (compare Fig. 6E) and RCN mice *in vivo*. This might be caused, beside other factors, by differences in the DNA repair of the two adducts *in vivo* or due to efficient conjugation of the BaP-9-ol intermediate.

Conflict of interest

The authors declare that there are no conflicts of interest.

Transparency document

The Transparency document associated with this article can be found in the online version.

Acknowledgments

This work was supported by the Grant Agency of the Czech Republic (grant P301/10/0356), Charles University (grants 640712 and UNCE 204025/2012), Cancer Research UK and ECNIS[2] (Environmental Cancer Risk, Nutrition and Individual Susceptibility) a European Union Network of Excellence.

References

Ariyoshi, N., Tanaka, M., Ishii, Y., Oguri, K., 1994. Purification and characterization of dog liver microsomal epoxide hydrolase. J. Biochem. 115, 985–990.

Arlt, V.M., Poirier, M.C., Sykes, S.E., Kaarthik, J., Moserova, M., Stiborova, M., Wolf, C.R., Anderson, C.J., Philips, D.H., 2012. Exposure to benzo[*a*]pyrene of hepatic cytochrome P450 reductase null (HRN) and P450 reductase conditional null (RCN) mice: detection of benzo[*a*]pyrene diol epoxide-DNA adducts by immunohistochemistry and ^{32}P-postlabelling. Toxicol. Lett. 213, 160–166.

Arlt, V.M., Stiborová, M., Henderson, C.J., Thiemann, M., Frei, E., Aimová, D., Singh, R., Gamboa da Costa, G., Schmitz, O.J., Farmer, P.B., Wolf, C.R., Philips, D.H., 2008. Metabolic activation of benzo[*a*]pyrene *in vitro* by hepatic cytochrome P450 contrasts with detoxification *in vivo*: experiments with hepatic cytochrome P450 reductase null mice. Carcinogenesis 29, 656–665.

Baird, W.M., Hooven, L.A., Mahadevan, B., 2005. Carcinogenic polycyclic aromatic hydrocarbon-DNA adducts and mechanism of action. Environ. Mol. Mutagen. 45, 106–114.

Backes, W.L., Eyer, C.S., 1989. Cytochrome P-450 LM2 reduction. Substrate effects on the rate of reductase-LM2 association. J. Biol. Chem. 264, 6252–6259.

Banni, M., Bouraoui, Z., Ghedira, J., Clerandeau, C., Guerbej, H., Narbonne, J.F., Boussetta, H., 2009. Acute effects of benzo[*a*]pyrene on liver phase I and II enzymes, and DNA damage on sea bream *Sparus aurata*. Fish Physiol. Biochem. 35, 293–299.

Bauer, E., Guo, Z., Ueng, Y.F., Bell, L.C., Zeldin, D., Guengerich, F.P., 1995. Oxidation of benzo[*a*]pyrene by recombinant human cytochrome P450 enzymes. Chem. Res. Toxicol. 8, 136–142.

Buters, J.T., Shou, M., Hardwick, J.P., Korzekwa, K.R., Gonzalez, F.J., 1995. cDNA-directed expression of human cytochrome P450 CYP1A1 using baculovirus. Purification, dependency on NADPH-P450 oxidoreductase, and reconstitution of catalytic properties without purification. Drug Metab. Dispos. 23, 696–701.

Chun, Y.J., Shimada, T., Guengerich, F.P., 1996. Construction of a human cytochrome P450 1A1: rat NADPH-cytochrome P450 reductase fusion protein cDNA and expression in *Escherichia coli*, purification, and catalytic properties of the enzyme in bacterial cells and after purification. Arch. Biochem. Biophys. 330, 48–58.

Davydov, D.R., 2011. Microsomal monooxygenase as a multienzyme system: the role of P450–P450 interactions. Expert Opin. Drug Metab. Toxicol. 7, 543–558.

Davydov, D.R., Davydova, N.Y., Sineva, E.V., Kufareva, I., Halpert, J.R., 2013. Pivotal role of P450–P450 interactions in CYP3A4 allostery: the case of α-naphthoflavone. Biochem. J. 453, 219–230.

Fang, A.H., Smith, W.A., Vouros, P., Gupta, R.C., 2001. Identification and characterization of a novel benzo[*a*]pyrene-derived DNA adduct. Biochem. Biophys. Res. Commun. 281, 383–389.

Farooq, Y., Roberts, G.C., 2010. Kinetics of electron transfer between NADPH-cytochrome P450 reductase and cytochrome P450 3A4. Biochem. J. 432, 485–493.

Fernando, H., Davydov, D.R., Chin, C.C., Halpert, J.R., 2007. Role of subunit interactions in P450 oligomers in the loss of homotropic cooperativity in the cytochrome P450 3A4 mutant L211F/D214E/F304W. Arch. Biochem. Biophys. 460, 129–140.

Fernando., H., Halpert, J.R., Davydov, D.R., 2008. Kinetics of electron transfer in the complex of cytochrome P450 3A4 with the flavin domain of cytochrome P450BM-3 as evidence of functional heterogeneity of the heme protein. Arch. Biochem. Biophys. 471, 20–31.

Finn, R.D., McLaren, A.W., Carrie, D., Henderson, C.J., Wolf, C.R., 2007. Conditional deletion of cytochrome P450 oxidoreductase in the liver and gastrointestinal tract: a new model for studying the functions of the P450 system. J. Pharmacol. Exp. Ther. 322, 40–47.

Finn, R.D., McLaughlin, L.A., Ronseaux, S., Rosewell, I., Houston, J.B., Henderson, C.J., Wolf, C.R., 2008. Defining the *in vivo* role for cytochrome b_5 in cytochrome P450 function through the conditional hepatic deletion of microsomal cytochrome b_5. J. Biol. Chem. 283, 31385–31393.

Guengerich, F.P., 2005. Reduction of cytochrome b_5 by NADPH-cytochrome P450 reductase. Arch. Biochem. Biophys. 440, 204–211.

Guengerich, F.P., Shimada, T., 1991. Oxidation of toxic and carcinogenic chemicals by human cytochrome P450 enzymes. Chem. Res. Toxicol. 4, 391–407.

Haasnoot, C.A.G., Deleeuw, F.A.A.M., Altona, C., 1980. The relationship between proton–proton NMR coupling-constants and substituent electronegativies. 1. An empirical generalization of the Karplus equation. Tetrahedron 36, 2783–2792.

Hakura, A., Tsutsui, Y., Sonoda, J., Kai, J., Imade, T., Shimada, M., Sugihara, Y., Mikami, T., 1998. Comparison between in vivo mutagenicity and carcinogenicity in multiple organs by benzo[*a*]pyrene in the lacZ transgenic mouse (*Muta mouse*). Mutat. Res. 398, 123–130.

Hakura, A., Tsutsui, Y., Sonoda, J., Mikami, T., Tsukidate, K., Sagami, F., Kerns, W.D., 1999. Multiple organ mutation in the lacZ transgenic mouse (*Muta mouse*) 6 months after oral treatment (5 days) with benzo[*a*]pyrene. Mutat. Res. 426, 71–77.

Hamouchene, H., Arlt, V.M., Giddings, I., Phillips, D.H., 2011. Influence of cell cycle on responses of MCF-7 cells to benzo[*a*]pyrene. BMC Genomics 12, 333.

Henderson, C.J., McLaughlin, L.A., Wolf, C.R., 2013. Evidence that cytochrome b_5 and cytochrome b_5 reductase can act as sole electron donors to the hepatic cytochrome P450 system. Mol. Pharmacol. 83, 1209–1217.

Henderson, C.J., Otto, D.M., Carrie, D., Magnuson, M.A., McLaren, A.W., Rosewell, I., Wolf, C.R., 2003. Inactivation of the hepatic cytochrome P450 system by conditional deletion of hepatic cytochrome P450 reductase. J. Biol. Chem. 278, 13480–13486.

Hockley, S.L., Arlt, V.M., Brewer, D., Te Poele, R., Workman, P., Giddings, I., Phillips, D.H., 2007. AHR- and DNA-damage-mediated gene expression responses induced by benzo(*a*)pyrene in human cell lines. Chem. Res. Toxicol. 20, 1797–1810.

Holme, J.A., Gorria, M., Arlt, V.M., Ovrebø, S., Solhaug, A., Tekpli, X., Ludvik, N.E., Huc, L., Fardel, O., Lagadic-Gossmann, D., 2007. Different mechanisms involved in apoptosis following exposure to benzo[*a*]pyrene in F258 and Hepa1c1c7 cells. Chem. Biol. Interact. 167, 41–55.

Huang, M.T., Wood, A.W., Chang, R.L., Yagi, H., Sayer, J.M., Jerina, D.M., Conner, A.H., 1986. Inhibitory effect of 3-hydroxybenzo(a)pyrene on the mutagenicity and tumorigenicity of (+/−)-7 beta, 8 alpha-dihydroxy-9 alpha, 10 alpha-epoxy-7,8,9,10-tetrahydrobenzo(a)pyrene. Cancer Res. 46, 558–566.

IARC, 2010. Some non-heterocyclic polycyclic aromatic hydrocarbons and some related exposures. IARC Monogr. Eval. Carcinog. Risks Hum. 92, 1–853.

Iwase, T., Sakaki, T., Yabusaki, Y., Ohkawa, H., Ohta, Y., Kawato, S., 1991. Rotation and interactions of genetically expressed cytochrome P-450IA1 and NADPH-cytochrome P-450 reductase in yeast microsomes. Biochemistry 30, 8347–8351.

Jiang, H., Gelhaus, S.L., Mangal, D., Harvey, R.G., Blair, I.A., Penning, T.M., 2007. Metabolism of benzo[*a*]pyrene in human bronchoalveolar H358 cells using liquid chromatography–mass spectrometry. Chem. Res. Toxicol. 20, 1331–1341.

Kaminsky, L.S., Guengerich, F.P., 1985. Cytochrome P-450 isozyme/isozyme functional interactions and NADPH-cytochrome P-450 reductase concentrations as factors in microsomal metabolism of warfarin. Eur. J. Biochem. 149, 479–489.

Kim, S.I., Arlt, V.M., Yoon, J.I., Cole, K.J., Pfeifer, G.P., Phillips, D.H., Besaratinia, A., 2011. Whole body exposure of mice to secondhand smoke induces dose-dependent and persistent promutagenic DNA adducts in the lung. Mutat. Res. 716, 92–98, Erratum in: Mutat. Res. 2013, 745–746, 55–56.

Kim, J.H., Stansbury, K.H., Walker, N.J., Trush, M.A., Strickland, P.T., Sutter, T.R., 1998. Metabolism of benzo[*a*]pyrene and benzo[*a*]pyrene-7,8-diol by human cytochrome P450 1B1. Carcinogenesis 19, 1847–1853.

Kotrbová, V., Aimová, D., Ingr, M., Bořek-Dohalská, L., Martínek, V., Stiborová, M., 2009. Preparation of a biologically active apo-cytochrome b_5 *via* heterologous expression in *Escherichia coli*. Protein Expression Purif. 66, 203–209.

Kotrbová, V., Mrázová, B., Moserová, M., Martínek, V., Hodek, P., Hudeček, J., Frei, E., Stiborová, M., 2011. Cytochrome *b5* shifts oxidation of anticancer drug ellipticine by cytochromes P450 1A1 and 1A2 from its detoxication to activation metabolites, thereby modulating its pharmacological efficacy. Biochem. Pharmacol. 82, 669–680.

Labib, S., Nauk, C., Williams, A., Arlt, V.M., Philips, D.H., White, P.A., Halappanavar, S., 2012. Subchronic oral exposure to benzo(*a*)pyrene leads to distinct transcriptomic changes in the lungs that are related to carcinogenesis. Toxicol. Sci. 129, 213–224.

Leeruff, E., Kazarianmoghaddam, H., Katz, M., 1986. Controlled oxidations of benzo[*a*]pyrene. Can. J. Chem. 64, 1297–1303.

McLaughin, L.A., Ronseaux, S., Finn, R.D., Henderson, C.J., Wolf, C.R., 2010. Deletion of microsomal cytochrome b_5 profoundly affects hepatic and extrahepatic drug metabolism. Mol. Pharmacol. 75, 269–278.

Mrázová, B., Kotrbová, V., Kořínková, M., Svobodová, L., Hudeček, J., Hodek, P., Kizek, R., Frei, E., Stiborová, M., 2007. Kinetics of ellipticine oxidation by cytochromes P450 1A1 and 1A2 reconstituted with NADPH: cytochrome P450 reductase. Chem. Listy 101, s237–s239.

Nesnow, S., Ross, J., Nelson, G., Holden, K., Erexson, G., Kligerman, A., Gupta, R.C., 1993. Quantitative and temporal relationships between DNA adduct formation in target and surrogate tissues: implications for biomonitoring. Environ. Health Perspect. 101 (Suppl. 3), 37–42.

Phillips, D.H., 2005. Macromolecular adducts as biomarkers of human exposure to polycyclic aromatic hydrocarbons. In: The Carcinogenic Effects of Polycyclic Aromatic Hydrocarbons. Imperial College Press, London, pp. 137–169.

Phillips, D.H., Arlt, V.M., 2007. The ^{32}P-postlabeling assay for DNA adducts. Nat. Protoc. 2, 2772–2781.

Phillips, D.H., Castegnaro, M., 1999. Standardization and validation of DNA adduct postlabelling methods: report of interlaboratory trials and production of recommended protocols. Mutagenesis 14, 301–315.

Phillips, D.H., Venitt, S., 2012. DNA and protein adducts in human tissues resulting from exposure to tobacco smoke. Int. J. Cancer 131, 2733–2753.

Platt, K.L., Oesch, F., 1983. Efficient synthesis of non-K-region *trans*-dihydrodiols of polycyclic aromatic-hydrocarbons from *ortho*-quinones and catechols. J. Org. Chem. 48, 265–268.

Porter, T.D., 2002. The roles of cytochrome b_5 in cytochrome P450 reactions. J. Biochem. Mol. Toxicol. 16, 311–316.
Prinzbach, H., Freudenberger, V., Scheidegger, U., 1967. Cyclische gekreuzt-konjugierte bindungssysteme. 13. NMR-untersuchungen am phenafulvensyste. Helv. Chim. Acta 50, 1087–1107.
Schenkman, J.B., Jansson, I., 2003. The many roles of cytochrome b_5. Pharmacol. Ther. 97, 139–152.
Rendic, S., DiCarlo, F.J., 1997. Human cytochrome P450 enzymes: a status report summarizing their reactions, substrates, inducers, and inhibitors. Drug Metab. Rev. 29, 413–480.
Riddick, D.S., Ding, X., Wolf, C.R., Porter, T.D., Pandey, A.V., Zhang, Q.Y., Gu, J., Finn, R.D., Ronseaux, S., McLaughlin, L.A., Anderson, C.J., Zou, L., Flück, C.E., 2013. NADPH-cytochrome P450 oxidoreductase: roles in physiology, pharmacology, and toxicology. Drug Metab. Dispos. 41, 12–23.
Roos, P.H., 1996. Chromatographic separation and behavior of microsomal cytochrome P450 and cytochrome b_5. J. Chromatogr. B 684, 107–131.
Schoket, B., Lévay, K., Philips, D.H., Vincze, I., 1989. ^{32}P-postlabelling analysis of DNA adducts of benzo[*a*]pyrene formed in complex metabolic activation systems *in vitro*. Cancer Lett. 48, 67–75.
Schwarz, D., Kisselev, P., Honeck, H., Cascorbi, I., Schunck, W.H., Roots, I., 2001. Co-expression of human cytochrome P4501A1 (CYP1A1) variants and human NADPH-cytochrome P450 reductase in the baculovirus/insect cell system. Xenobiotica 31, 345–356.
Shimada, T., Fujii-Kuriyama, Y., 2004. Metabolic activation of polycyclic aromatic hydrocarbons to carcinogens by cytochrome P450 1A1 and 1B1. Cancer Sci. 95, 1–6.
Shimada, T., Gillam, E.M., Oda, Y., Tsumura, F., Sutter, T.R., Guengerich, F.P., Inoue, K., 1999. Metabolism of benzo[*a*]pyrene to *trans*-7,8-dihydroxy-7, 8-dihydrobenzo[*a*]pyrene by recombinant human cytochrome P450 1B1 and purified liver epoxide hydrolase. Chem. Res. Toxicol. 12, 623–629.
Shimada, T., Oda, Y., Gillam, E.M., Guengerich, F.P., Inouye, K., 2001. Metabolic activation of polycyclic aromatic hydrocarbons and other procarcinogens by cytochromes P450 1A1 and P450 1B1 allelic variants and other human cytochromes P450 in *Salmonella typhimurium* NM2009. Drug Metab. Dispos. 29, 1176–1182.
Siddens, L.K., Larkin, A., Krueger, S.K., Bradfield, C.A., Waters, K.M., Tigon, S.C., Perena, C.B., Löhr, C.V., Arlt, V.M., Philips, D.H., Williams, D.E., Baird, W.M., 2012. Polycyclic aromatic hydrocarbons as skin carcinogens: comparison of benzo[*a*]pyrene, dibenzo[*def,p*]chrysene and three environmental mixtures in the FVB/N mouse. Toxicol. Appl. Pharmacol. 264, 377–386.
Stiborová, M., Indra, R., Moserová, M., Černá, V., Rupertová, M., Martínek, V., Eckschlager, T., Kizek, R., Frei, E., 2012. Cytochrome b_5 increases cytochrome P450 3A4-mediated activation of anticancer drug ellipticine to 13-hydroxyellipticine whose covalent binding to DNA is elevated by sulfotransferases and *N*-acetyltransferases. Chem. Res. Toxicol. 25, 1075–1085.
Stiborová, M., Martínek, V., Schmeiser, H.H., Frei, E., 2006. Modulation of CYP1A1-mediated oxidation of carcinogenic azo dye Sudan I and its binding to DNA by cytochrome b_5. Neuro Endocrinol. Lett. 27 (Suppl 2), 35–39.
Stiborová, M., Martínek, V., Rýdlová, H., Hodek, P., Frei, E., 2002. Sudan I is a potential carcinogen for humans: evidence for its metabolic activation and detoxication by human recombinant cytochrome P450 1A1 and liver microsomes. Cancer Res. 62, 567856–567884.
Stiborová, M., Sejbal, J., Bořek-Dohalská, L., Poljaková, J., Forsterová, K., Rupertová, M., Wiesner, J., Hudeček, J., Wiessler, M., Frei, E., 2004. The anticancer drug ellipticine forms covalent DNA adducts, mediated by human cytochromes P450, through metabolism to 13-hydroxyellipticine and ellipticine N^2-oxide. Cancer Res. 64, 8374–8380.
Uno, S., Dalton, T.P., Derkenne, S., Curran, C.P., Miller, M.L., Shertzer, H.G., Nebert, D.W., 2004. Oral exposure to benzo [*a*] pyrene in the mouse: detoxication by inducible cytochrome P450 is more important than metabolic activation. Mol. Pharmacol. 65, 1225–1237.
Uno, S., Dalton, T.P., Dragin, N., Curran, C.P., Derkenne, S., Miller, M.L., Shertzer, H.G., Gonzalez, F.J., Nebert, D.W., 2006. Oral benzo[*a*]pyrene in Cyp1 knockout mouse lines: CYP1A1 important in detoxication, CYP1B1 metabolism required for immune damage independent of total-body burden and clearance rate. Mol. Pharmacol. 69, 1103–1114.
Wang, X.J., Chamberlain, M., Vassieva, O., Henderson, C.J., Wolf, C.R., 2005. Relationship between hepatic phenotype and changes in gene expression in cytochrome P450 reductase (POR) null mice. Biochem. J. 388, 857–867.
Wiechelman, K.J., Braun, R.D., Fitzpatrick, J.D., 1988. Investigation of the bicinchoninic acid protein assay: identification of the groups responsible for color formation. Anal. Biochem. 175, 231–237.
Xu, D.W., Penning, T.M., Blair, I.A., Harvey, R.G., 2009. Synthesis of phenol and quinone metabolites of benzo[*a*]pyrene, a carcinogenic component of tobacco smoke implicated in lung cancer. J. Org. Chem. 74, 597–604.
Yamazaki, H., Shimada, T., Martin, M.V., Guengerich, F.P., 2001. Stimulation of cytochrome P450 reactions by apo-cytochrome b_5: evidence against transfer of heme from cytochrome P450 3A4 to apo-cytochrome b_5 or heme oxygenase. J. Biol. Chem. 276, 30885–30891.
Zhu, S., Li, L., Thornton, C., Carvalho, P., Avery, B.A., Willett, K.L., 2008. Simultaneous determination of benzo[*a*]pyrene and eight of its metabolites in *Fundulus heteroclitus* bile using ultra-performance liquid chromatography with mass spectrometry. J. Chromatogr. B 863, 141–149.

Chemical Research in Toxicology

Article

pubs.acs.org/crt

Cytochrome b_5 Increases Cytochrome P450 3A4-Mediated Activation of Anticancer Drug Ellipticine to 13-Hydroxyellipticine Whose Covalent Binding to DNA Is Elevated by Sulfotransferases and *N,O*-Acetyltransferases

Marie Stiborová,*[,†] Radek Indra,[†] Michaela Moserová,[†] Věra Černá,[†] Martina Rupertová,[†] Václav Martínek,[†] Tomáš Eckschlager,[‡] René Kizek,[§] and Eva Frei[∥]

[†]Department of Biochemistry, Faculty of Science, Charles University, Albertov 2030, 128 40 Prague 2, Czech Republic

[‡]Department of Pediatric Hematology and Oncology, Charles University and University Hospital Motol, Prague, Czech Republic

[§]Department of Chemistry and Biochemistry, Faculty of Agronomy, Mendel University, Brno, Czech Republic

[∥]Division of Preventive Oncology, National Center for Tumor Diseases, German Cancer Research Center (DKFZ), 69120 Heidelberg, Germany

Supporting Information

ABSTRACT: The antineoplastic alkaloid ellipticine is a prodrug, whose pharmacological efficiency is dependent on its cytochrome P450 (P450)- and/or peroxidase-mediated activation in target tissues. The P450 3A4 enzyme oxidizes ellipticine to five metabolites, mainly to 13-hydroxy- and 12-hydroxyellipticine, the metabolites responsible for the formation of ellipticine-13-ylium and ellipticine-12-ylium ions that generate covalent DNA adducts. Cytochrome b_5 alters the ratio of ellipticine metabolites formed by P450 3A4. While the amounts of the detoxication metabolites (7-hydroxy- and 9-hydroxyellipticine) were not changed with added cytochrome b_5, 12-hydroxy- and 13-hydroxyellipticine, and ellipticine N^2-oxide increased considerably. The P450 3A4-mediated oxidation of ellipticine was significantly changed only by holo-cytochrome b_5, while apo-cytochrome b_5 without heme or Mn-cytochrome b_5 had no such effect. The change in amounts of metabolites resulted in an increased formation of covalent ellipticine-DNA adducts, one of the DNA-damaging mechanisms of ellipticine antitumor action. The amounts of 13-hydroxy- and 12-hydroxyellipticine formed by P450 3A4 were similar, but more than 7-fold higher levels of the adduct were formed by 13-hydroxyellipticine than by 12-hydroxyellipticine. The higher susceptibility of 13-hydroxyellipticine toward heterolytic dissociation to ellipticine-13-ylium in comparison to dissociation of 12-hydroxyellipticine to ellipticine-12-ylium, determined by quantum chemical calculations, explains this phenomenon. The amounts of the 13-hydroxyellipticine-derived DNA adduct significantly increased upon reaction of 13-hydroxyellipticine with either 3′-phosphoadenosine-5′-phosphosulfate or acetyl-CoA catalyzed by human sulfotransferases 1A1, 1A2, 1A3, and 2A1, or *N,O*-acetyltransferases 1 and 2. The calculated reaction free energies of heterolysis of the sulfate and acetate esters are by 10−17 kcal/mol more favorable than the energy of hydrolysis of 13-hydroxyellipticine, which could explain the experimental data.

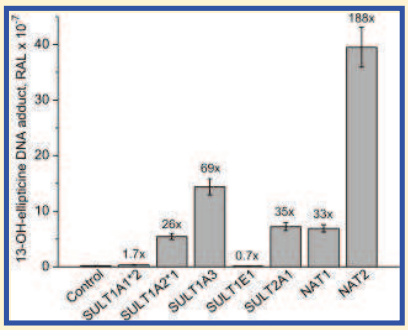

INTRODUCTION

Ellipticine (5,11-dimethyl-6*H*-pyrido[4,3-*b*]carbazole, Scheme 1), an alkaloid isolated from Apocynaceae plants, exhibits significant antitumor and anti-HIV activities [for a summary see refs 1−3]. The main reasons for the interest in ellipticine and its derivatives for clinical purposes are their high efficiencies against several types of cancer, their limited toxic side effects, and their lack of hematological toxicity.[4] Nevertheless, ellipticine is a potent mutagen. Many ellipticine derivatives are mutagenic to *Salmonella typhimurium* Ames tester strains, bacteriophage T4, *Neurospora crassa*, and mammalian cells and induce prophage lambda in *Escherichia coli* [for an overview, see refs 1−3].

It was suggested that the major mechanisms of antitumor, mutagenic, and cytotoxic activities of ellipticine are (i) intercalation into DNA[4,5] and (ii) inhibition of DNA topoisomerase II activity.[2−7] We have demonstrated that ellipticine also covalently binds to DNA after being enzymatically activated by cytochromes P450 (P450) or peroxidases,[1−3,8−13] suggesting a third DNA-damaging mechanism of action. Two major DNA adducts generated from ellipticine-13-ylium and ellipticine-12-ylium (Scheme 1), by P450- and peroxidase-mediated metabolism, are formed *in vitro* and *in vivo* in DNA of healthy organs of rats and mice treated with this anticancer drug.[1,3,8−13]

The same DNA adducts were also detected in human cancer cells in culture, such as breast adenocarcinoma MCF-7,[14] the

Received: January 24, 2012
Published: March 5, 2012

dx.doi.org/10.1021/tx3000335 | *Chem. Res. Toxicol.* 2012, 25, 1075−1085

Scheme 1. Scheme of Ellipticine Metabolism by P450s and Peroxidases Showing the Identified Metabolites and Those Proposed to Form DNA Adducts[a]

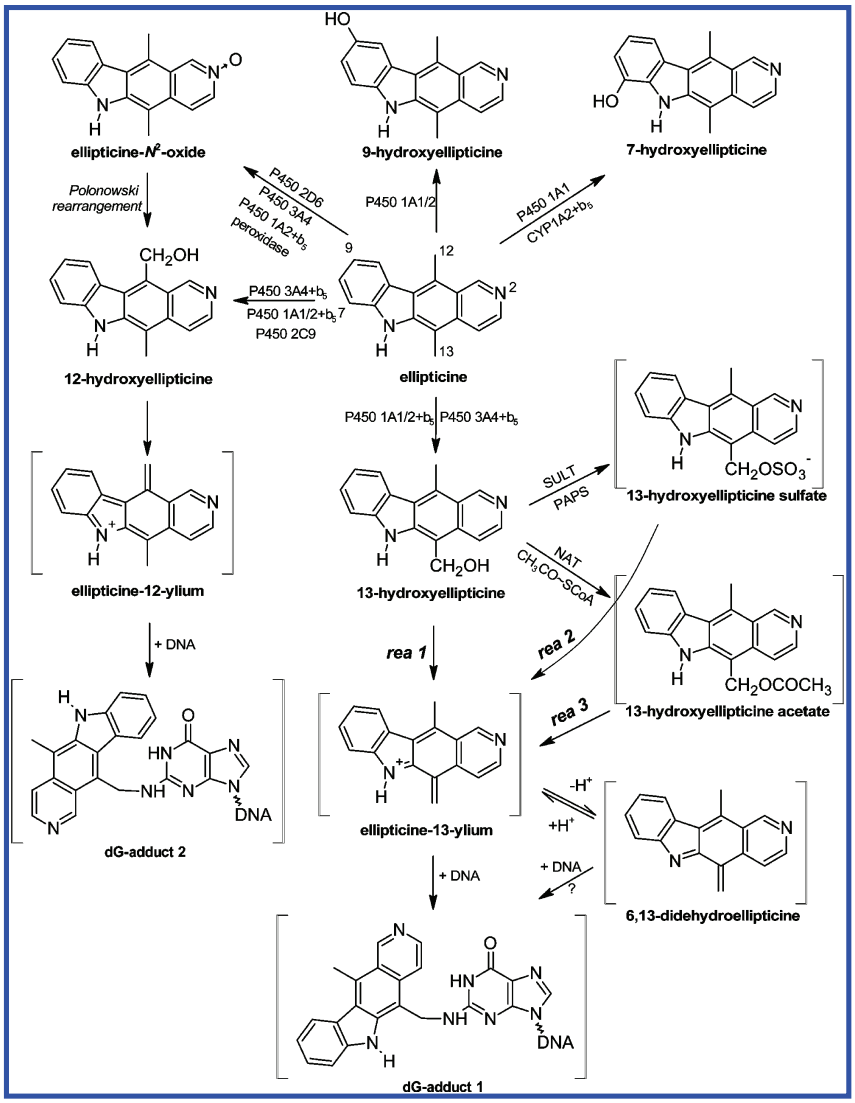

[a]The compounds shown in brackets were not detected under the experimental conditions and/or not structurally characterized. The P450 enzymes predominantly oxidizing ellipticine shown in the figure were identified in this work and/or in our previous studies.[10,11,18,19]

leukemias HL-60 and CCRF-CEM,[15] neuroblastoma[16] and glioblastoma cells,[17] and in rat mammary adenocarcinoma *in vivo*.[3] Toxic effects of ellipticine in these cancer cells correlated with levels of ellipticine-derived DNA adducts and were dependent on the expression of P450 1A1, 1B1, 3A4, lactoperoxidase, cyclooxygenase, or myeloperoxidase in these cells.[14−17] On the basis of these data, ellipticine might be considered a drug, whose pharmacological efficiency and/or genotoxic side effects are dependent on its activation by P450s and peroxidases in target tissues.

Because of the ellipticine-derived DNA adducts we found in healthy organs of rats, the risk of treating patients with this compound has to be considered. Our *in vivo* studies, however, demonstrated that ellipticine-DNA adducts did not persist in healthy tissues of rats, the experimental model mimicking the fate of ellipticine in humans[8,12] treated with ellipticine.[12] Therefore, these results suggest a relatively low risk of the genotoxic side effects to humans by ellipticine during the cancer treatment.

Of the P450s investigated, human P450 3A4 and rat P450 3A1 are the most active enzymes oxidizing ellipticine to 13-hydroxy- and 12-hydroxyellipticine, the reactive metabolites that dissociate to ellipticine-13-ylium and ellipticine-12-ylium which bind to DNA,[3,9,10] while the P450 1A isoforms preferentially form the other ellipticine metabolites, 9-hydroxy- and 7-hydroxyellipticine, which are the detoxication products (Scheme 1). As a consequence, ellipticine-DNA adduct levels formed by P450 1A are very low.[10,18,19] Recently, we found that cytochrome b_5 alters the ratio of ellipticine metabolites formed by isolated P450 1A1 and 1A2 reconstituted with NADPH:P450 reductase, favoring the formation of 12-hydroxy- and 13-hydroxyellipticine at the expense of 9-hydroxy- and 7-hydroxyellipticine. The change in metabolite ratio resulted in an increased formation of covalent ellipticine-DNA adducts.[19] This finding explained the previous apparent discrepancies we

dx.doi.org/10.1021/tx3000335 | *Chem. Res. Toxicol.* 2012, 25, 1075−1085

found between isolated enzymes and *in vivo* studies, where P450 1A enzymatic activity correlated with ellipticine-DNA-adduct levels,[8] while isolated P450 1A1 or 1A2 in reconstituted systems was much less effective than P450 3A4.[1,10] This effect of cytochrome b_5 might be even more pronounced *in vivo* since, as we showed previously, ellipticine induces levels of both P450 1A[20] and cytochrome b_5 in rat liver[19] and in several cancer cell lines (i.e., glioblastoma and neuroblastoma cells).[16,17,21] In glioblastoma and neuroblastoma cells, ellipticine also induces P450 3A4,[17,21,22] the enzyme whose efficiency to oxidize several substrates including ellipticine is extensively influenced by cytochrome b_5.[10,23−25] Because P450 3A4 is so important for ellipticine activation, modulation of P450 3A4-catalyzed activation of ellipticine to 12-hydroxy- and 13-hydroxyellipticine by cytochrome b_5 is investigated here in detail. Mechanistic studies of the action of cytochrome b_5 on the catalysis of P450 3A4 were performed using the holoprotein of cytochrome b_5, its apo-form (devoid of heme) or apo-cytochrome b_5 reconstituted with manganese protoporphyrin IX (Mn-cytochrome b_5).

The *N*,*O*-acetyltransferase (NAT) and sulfotransferase (SULT) enzymes, which are expressed in several cancer cells,[26−33] can detoxify but also further activate the products of metabolism of xenobiotics. We therefore also examined whether these enzymes modify the DNA-adduct levels resulting from covalent binding of 13-hydroxyellipticine to DNA.

EXPERIMENTAL PROCEDURES

Caution: *Ellipticine is a potent mutagen and should be handled with care. Exposure to ^{32}P should be avoided, by working in a confined laboratory area, with protective clothing, plexiglass shielding, Geiger counters, and body dosimeters. Waste must be discarded according to appropriate safety procedures.*

Chemicals and Enzymes. $NADP^+$, NADPH, ellipticine, D-glucose 6-phosphate, D-glucose 6-phosphate dehydrogenase, hemin, acetyl-CoA, 3′-phosphoadenosine-5′-phosphosulfate (PAPS) and calf thymus DNA were obtained from Sigma Chemical Co. (St Louis, MO, USA); 9-hydroxyellipticine (5,11-dimethyl-9-hydroxy-6*H*-pyrido[4,3-*b*]-carbazole) was from Calbiochem (San Diego, CA, USA). All of these and other chemicals from commercial sources used in the experiments were of reagent grade or better. 7-Hydroxyellipticine and the N^2-oxide of ellipticine were synthesized as described[10] by J. Kučka (Charles University, Prague, Czech Republic); their purity was >99.5% as estimated by high-performance liquid chromatography (HPLC). Enzymatically prepared 12-hydroxy- and 13-hydroxyellipticine were obtained from multiple HPLC runs of ethyl acetate extracts of incubations of ellipticine with human and/or rat hepatic microsomes as described.[10] Their authenticity was confirmed by UV spectroscopy, electrospray mass spectrometry, and high field ^1H NMR spectroscopy. The purity as analyzed by HPLC was >99.9%.[10] Supersomes isolated from insect cells transfected with baculovirus constructs containing cDNA of human P450 3A4 and expressing NADPH:P450 reductase were obtained from Gentest Corp. (Woburn, MI, USA) and tested for their efficiencies to oxidize ellipticine. Cytosolic extracts, isolated from insect cells transfected with baculovirus constructs containing human cDNA of SULT1A1*2, 1A2*1, 1A3, 1E, or 2A1 were obtained from Oxford Biomedical Research Inc. (Oxford, MA, USA), and those containing cDNA of human NAT1*4 or NAT2*4 were from Gentest (Woburn, MA, USA). Cytosolic extracts expressing SULT1A1 and SULT1A2 conjugated *p*-nitrophenol at rates of 124 and 5.5 nmol/min/mg protein, respectively; SULT1A3 conjugated dopamine at the rate of 8 nmol/min/mg protein; SULT1E conjugated estrone at the rate of 266 pmol/min/mg protein; and SULT2A1 conjugated dehydroepiandrosterone at the rate of 584 pmol/min/mg protein. Cytosolic extracts expressing NAT1 and NAT2 had a catalytic activity of 1,300 nmol/min/mg protein (substrate *p*-aminosalicylic acid) and 290 nmol/min/mg protein (substrate sulfamethazine), respectively. Enzyme activities in control cytosol were less than 10 pmol/min/mg protein. Enzymes and chemicals for the ^{32}P-postlabeling assay were obtained from the sources described.[1,10] All of these and other chemicals were of reagent grade or better.

Isolation of Cytochrome b_5 and Apo-cytochrome b_5. Cytochrome b_5 was isolated from rabbit liver microsomes by the procedure described by Roos.[34] The apo-cytochrome b_5 protein was prepared using heterologous expression in *Escherichia coli* as described in our earlier work.[35]

Incorporation of Heme into Apo-cytochrome b_5. The preparation of hemin chloride solution and its incorporation into apo-cytochrome b_5 were performed by the procedure described elsewhere and in our previous paper.[35,36] Absorbance spectra of reconstituted cytochrome b_5 (from 350 to 500 nm) were recorded on a Hewlett-Packard 8453 UV spectrophotometer. The reconstitution of cytochrome b_5 was considered to be complete when the Soret peak of cytochrome b_5 shifted from 413 to 409 nm and an increase in absorbance at 385 nm, caused by an excess of free Tris-ligated hemin, was observed in the spectrum.

Analogous procedures were utilized to incorporate manganese protoporphyrin IX (Frontier Scientific, USA) into apo-cytochrome b_5 (Mn-cytochrome b_5).[35,37]

Determination of Reconstituted Cytochrome b_5 Content. The concentration of apo-cytochrome b_5 reconstituted with heme was determined spectrophotometrically (the absolute absorbance spectrum), using the molar extinction coefficient ε_{413} = 117 $mM^{-1}\cdot cm^{-1}$,[38,39] or from the difference spectrum of reduced minus oxidized form, using molar extinction coefficient $\varepsilon_{424-409}$ = 185 $mM^{-1}\cdot cm^{-1}$.[39] The concentration of Mn-cytochrome b_5 was determined using an extinction coefficient of 57 $mM^{-1}\cdot cm^{-1}$ at 469 nm.[40]

Incubations. Unless stated otherwise, incubation mixtures used to study ellipticine metabolism contained the following in a final volume of 500 μL: 100 mM potassium phosphate buffer (pH 7.4), 1 mM NADPH of NADPH-generating system (1 mM $NADP^+$, 10 mM D-glucose 6-phosphate, and 1 U/mL D-glucose 6-phosphate dehydrogenase, to generate NADPH), human P450 3A4 in Supersomes (100 pmol) reconstituted with or without rabbit hepatic cytochrome b_5, apo-cytochrome b_5, or Mn-cytochrome b_5 (500 pmol), and 20 μM ellipticine dissolved in 5 μL methanol. In the control incubation, either P450 or ellipticine was omitted. The reaction was initiated by adding ellipticine. After incubation at 37 °C for 20 min in open glass tubes (ellipticine oxidation was linear up to 30 min of incubation[18,41]), the reaction was stopped, phenacetin added as internal standard, and metabolites extracted, separated, and quantified by HPLC as described.[10,18,41]

Incubation mixtures used to analyze DNA-adduct formation by ellipticine were as described above but contained 100 μM ellipticine dissolved in 5 μL of methanol, 1 mM NADPH instead of the NADPH generating system, and 1 mg of calf thymus DNA in a final volume of 750 μL. The reaction was initiated by adding ellipticine. Incubations were carried out at 37 °C for 30 min; ellipticine-DNA adduct formation was linear up to 30 min.[1] Control incubations were carried out without (i) P450, (ii) NADPH, or (iii) ellipticine. After the incubation, DNA was isolated from the residual water phase by the phenol/chloroform extraction method as described.[1] The extracted DNA was then dissolved in 200 μL of distilled water and the DNA content determined spectrophotometrically. The 260/280 nm ratios of DNA were 1.8. The isolated DNA was used to detect and quantify DNA adducts by the ^{32}P-postlabeling assay (see below).

Incubations in which 13-hydroxyellipticine was used instead of ellipticine, contained in a final volume of 500 μL: 50 mM potassium phosphate buffer (pH 5.0, 6.0, 7.0, 7.4, 8.0 and 8.4), 100 μM 13-hydroxyellipticine dissolved in 5 μL of methanol, and 1 mg of calf thymus DNA. After the 90 min incubations (37 °C) and ethyl acetate extraction, DNA was isolated from the residual water phase by the phenol/chloroform extraction method as described.[1] Incubation mixtures used to analyze the effect of SULTs and NATs on the 13-hydroxyellipticine-derived DNA adducts contained in a final volume of 500 μL, 50 mM potassium phosphate buffer (pH 7.4), 1 mg of calf

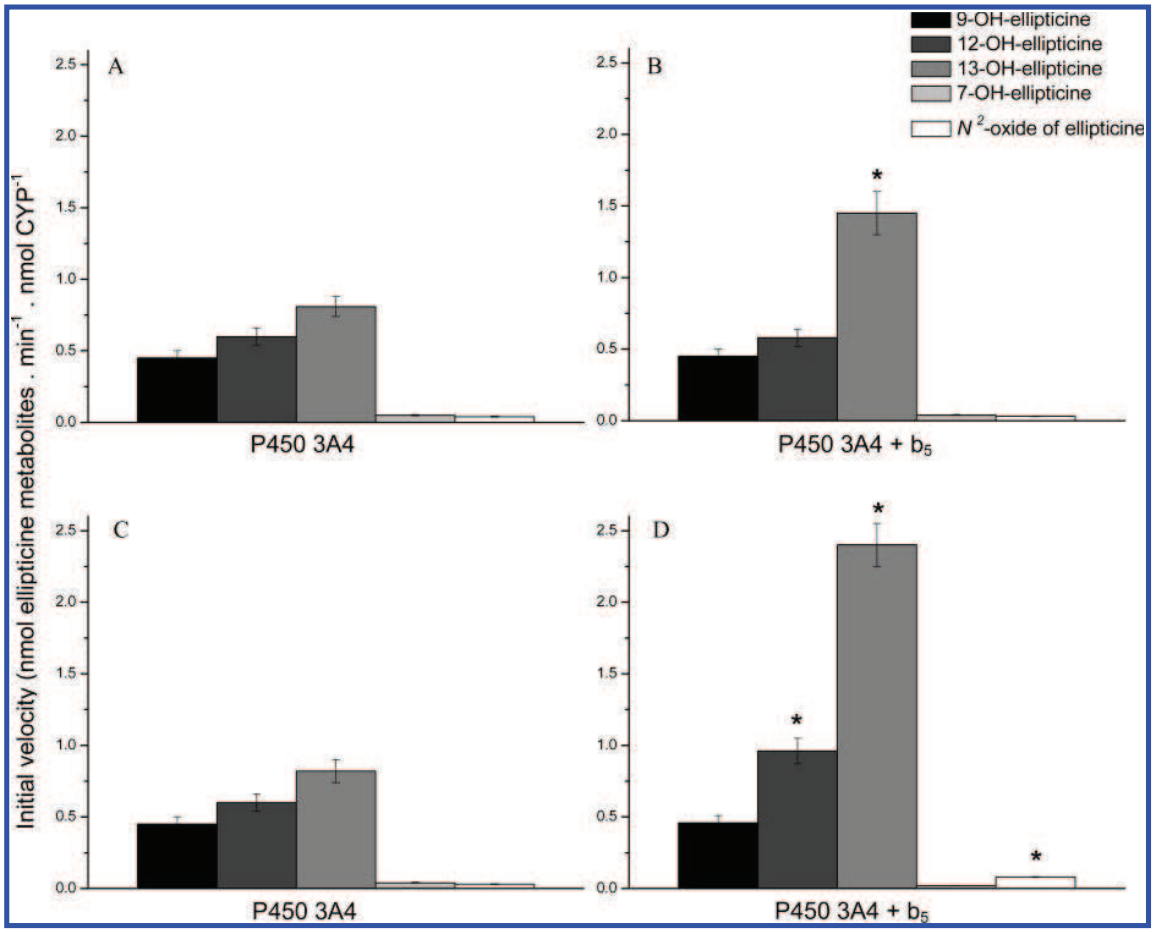

Figure 1. Effect of cytochrome b_5 (B and D) on the initial velocity of ellipticine oxidation to 9-hydroxyellipticine, 12-hydroxyellipticine, 13-hydroxyellipticine, 7-hydroxyellipticine, and ellipticine N^2-oxide by P450 3A4 in the presence of the NADPH-generating system (B) and the same enzyme in the presence of NADPH (D) compared to incubations without cytochrome b_5 (A, NADPH regenerating system; C, NADPH added). Assays were performed as described under Experimental Procedures. Average values ± SD are shown ($N = 3$). Values significantly different from the control (without cytochrome b_5); $*p < 0.001$ (Student's *t*-test).

thymus DNA, and 1 μM 13-hydroxyellipticine either in the presence or absence of 39 nmol human SULT1A1*2, 1A2*1, 1A3, 1E, or 2A1 and 100 μM PAPS or NAT1 or NAT2, and 2 mM acetyl-CoA. After the 90 min incubations (37 °C) and ethyl acetate extraction, DNA was isolated from the residual water phase by the phenol/chloroform extraction method as described.[1] The isolated DNA was used to detect and quantify DNA adducts by the ^{32}P-postlabeling assay (see below).

^{32}P-Postlabeling Analysis and HPLC Analysis of ^{32}P-Labeled 3′,5′-Deoxyribonucleoside Bisphosphate Adducts. The ^{32}P-postlabeling of nucleotides using the nuclease P1 enrichment procedure, found previously to be appropriate to detect and quantify ellipticine-derived DNA adducts formed *in vitro* and *in vivo*,[1,3,8−13] was employed in the experiments. The TLC and HPLC analyses were done as reported recently.[1,3,8−13]

Quantum Chemical Calculations. Reaction free energies for heterolytic dissociation of 13-hydroxyellipticine and its conjugates [reactions 1−3 (rea 1, rea 2, and rea 3) in Scheme 1] and for an analogous reaction of 12-hydroxyellipticine were calculated by an *ab initio* quantum chemical approach. The accuracy of absolute reaction free energies is better, if electron correlation effects are considered during the calculation. In the present study, we evaluated the heterolytic dissociation of 12-/13-hydroxyellipticine and the 13-hydroxyellipticine conjugates, which are reactions conserving the number of paired electrons (isogyric reactions). This fact facilitates the calculation of thermochemical data even at relatively low levels of theory, lacking the electron correlation effects, Hartree−Fock (HF). The heterolytic dissociation, however, involves charged species that are best modeled with basis sets containing polarization functions since the charge distorts the electron distribution. In addition, anions require inclusion of diffuse functions. Therefore, the geometry optimizations and frequency calculations of all reactants and products studied here were performed on the HF level of theory in conjunction with the 6-31++G(d,p) basis set using the Gaussian 09 package.[42]

Accurate computation of solvation energies of charged species is still a challenge. Therefore, several approaches to estimate solvent effects were evaluated. Initially, the solvent effect was estimated by performing energy optimizations using the Conductor-like Polarizable Continuum Model (C-PCM) with default atomic radii.[43] The thermal corrected Gibbs free energies (at 298 K) were obtained from electronic calculations and harmonic vibration frequencies of these optimized structures. The resulting free energies were also corrected to represent the biochemically relevant reference state: pH 7 and 1 M concentration for all reactants except for water, for which the reference concentration was 55.3 M.[44] The reaction Gibbs free energies of individual reaction steps ($\Delta G^{0\prime}_{rea}$) evaluated here were calculated as the total energies of products minus the total energies of reactants.

Solvation free energies of all reactants and products were also calculated with the Langevin dipole solvation model (LD).[45] Merz−Kollman partial atomic charges obtained from *ab initio* calculations served as input for the LD model built in the ChemSol program, v2.1.[46] The standard (biochemical) free energy changes of individual

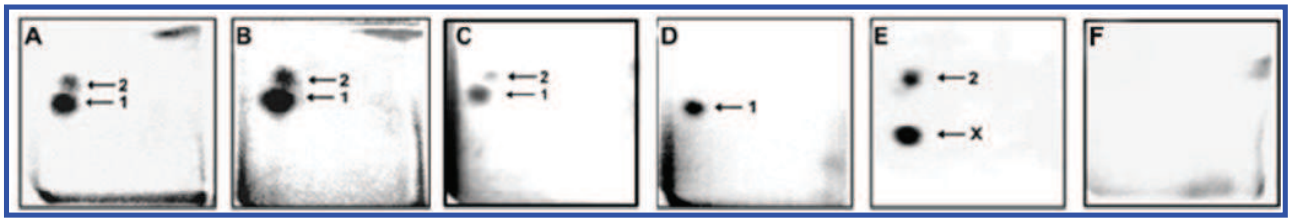

Figure 2. Autoradiographic profile of ^{32}P-labeled DNA adducts generated in calf thymus DNA by ellipticine after its activation with P450 3A4 without (A) and with cytochrome b_5 (P450 3A4/cytochrome b_5 1:5) (B); of ^{32}P-labeled digests of DNA of mammary adenocarcinoma of Wistar rats treated i.p. with 4 mg of ellipticine per kilogram body weight (C); and from calf thymus DNA reacted with 13-hydroxyellipticine (D) or 12-hydroxyelipticine (E). Autoradiographic profile of calf thymus DNA incubated with ellipticine after its activation with P450 3A4 without NADPH (control incubation) (F). Analyses were performed by the nuclease P1 version of the ^{32}P-postlabeling assay. Adduct spots 1 and 2 correspond to the ellipticine-derived DNA adducts. Besides adduct 2 formed by 12-hydroxyellipticine, another strong adduct (spot X in panel E), which was not found in any other activation systems or *in vivo*,[3,63] was generated.

reaction steps were then calculated according to a formula used previously:[47,48]

$$\Delta G_{\mathrm{rea}}^{0'wat(LD)} = \sum \Delta G_{\mathrm{products}}^{0'gas} - \sum \Delta G_{\mathrm{reactants}}^{0'gas} + \sum \Delta G_{\mathrm{products}}^{solvLD} - \sum \Delta G_{\mathrm{reactants}}^{solvLD}$$

where $\Sigma\Delta G^{0gas}$ denotes the sum of corrected Gibbs free energies of products or reactants in gas phase, and $\Sigma\Delta G^{solvLD}$ refers to the sum of solvation free energies of the products or reactants calculated with the LD method. The similar combination of the *ab initio* (HF) gas phase free energy and LD solvation energy was successfully employed in free energy calculations of other carcinogens (aflatoxin B1, vinyl chloride, and acrylamide) and well reproduced the experimentally determined energies.[49−51]

Finally, we combined LD solvation energies with experimental solvation energies for H_2O, H_3O^+, and OH^-. A similar approach has been previously employed for the calculation of pK_a for carboxylic acids.[52]

RESULTS

Cytochrome b_5 Modulates Ellipticine Oxidation Catalyzed by Cytochromes P450 3A4. The human P450 3A4 enzyme in the presence of NADPH:P450 reductase and its cofactor NADPH oxidizes ellipticine to five metabolites, 7-hydroxy-, 9-hydroxy-, 12-hydroxy-, and 13-hydroxyellipticine and the N^2-oxide of ellipticine (Figure 1A and C and Supporting Information, Table 1), which are also formed by human, rat, rabbit, and mouse hepatic microsomes.[10,13,18,41] 13-Hydroxy- and 12-hydroxyellipticine, two reactive ellipticine metabolites forming DNA adducts,[10,11] and 9-hydroxyellipticine, a detoxication product of ellipticine,[10,18] were the predominant metabolites formed by P450 3A4. Another activation metabolite, ellipticine N^2-oxide, a precursor of 12-hydroxyellipticine,[10,11] and a further detoxication product, 7-hydroxyellipticine, were formed to a much lower extent.

The patterns and amounts of ellipticine metabolites generated by P450 3A4 changed significantly when cytochrome b_5 was present in the P450 3A4 enzymatic system (Figure 1B and D, and Supporting Information, Table 1). While the amounts of the detoxication products of ellipticine (7-hydroxy- and 9-hydroxyellipticine) were not changed with added cytochrome b_5, 12-hydroxy- and 13-hydroxyellipticine, and ellipticine N^2-oxide increased considerably. Up to a 1.6-, 2.9-, and 2.7-fold more 12-hydroxy- and 13-hydroxyellipticine and ellipticine N^2-oxide, respectively, were found with added cytochrome b_5 and NADPH (Figure 1D). A lower increase in these metabolites was, however, found when the NADPH-generating system was used instead of NADPH (Figure 1B). Glucose 6-phosphate dehydrogenase of the NADPH-generating system added to the incubation mixtures might act as a protein scavenger binding the reactive species generated from these metabolites.

Cytochrome b_5 Increases the Ellipticine-Derived DNA Adduct Formation Mediated by Cytochrome P450 3A4. Using the nuclease P1 version of the ^{32}P-postlabeling assay, which was suitable to detect and quantify DNA adducts formed by ellipticine,[1,8−12] two ellipticine-derived DNA adducts (see Scheme 1 for the structures of two deoxyguanosine adducts 1 and 2) were detected in the calf thymus DNA incubated with this drug and P450 3A4 with NADPH:P450 reductase and NADPH (Figure 2A,B). The two adducts are identical to those found previously after *in vitro* incubation of calf thymus DNA with ellipticine, human, rat, rabbit, and mouse hepatic microsomes or human and rat P450s,[1,9,10] or peroxidases,[11] or after treatment of cells in culture with this anticancer drug,[14−17,22] or *in vivo* in several organs of rats including mammary adenocarcinoma[3,8,12] (Figure 2C), and mice[13] exposed to this agent. These adducts are generated from ellipticine-13-ylium and ellipticine-12-ylium (Scheme 1), the reactive species formed from the corresponding hydroxyellipticines (Figure 2D,E) as confirmed by cochromatographic analysis using TLC and HPLC.[10,11,53] More than 7-fold higher levels of adduct 1 than adduct 2 are formed by the P450 3A4 enzymatic system, whereas only 1.3-fold more 13-hydroxyellipticine (species responsible for formation of adduct 1) than 12-hydroxyellipticine generating adduct 2 (compare Figure 1 and Supporting Information, Table 1) was determined in incubations with P450 3A4.

The increased levels of 12-hydroxy- and 13-hydroxyellipticine formed by the P450 3A4 enzymatic system containing cytochrome b_5 and NADPH resulted in increased levels of these two ellipticine-derived DNA adducts (Table 1). The presence of cytochrome b_5 resulted in 2.9-fold higher levels of the ellipticine-DNA adduct 1, which correlated with a 2.9-fold increased formation of 13-hydroxyellipticine (Table 1 and Figure 1). The same was true for the parallel effects of cytochrome b_5 on ellipticine-DNA-adduct 2 levels and 12-hydroxyellipticine yields in incubations with P450 3A4 (Table 1, Figure 1, and Supporting Information, Table 1).

Modulation of Ellipticine Oxidation by Cytochromes P450 3A4 Is Dependent on Holo-cytochrome b_5. In order to investigate the mechanism of cytochrome b_5-mediated modulation of ellipticine oxidation by P450 3A4, we also examined the influence of apo-cytochrome b_5 and Mn-cytochrome b_5. As shown in Figure 3, the P450 3A4-mediated

dx.doi.org/10.1021/tx3000335 | *Chem. Res. Toxicol.* 2012, 25, 1075−1085

Table 1. Effect of Cytochrome b_5 on DNA Adduct Formation by Ellipticine Oxidized with Human P450 3A4 and NADPH[a]

activating system	relative adduct labeling (mean ± SD/ 10^7nucleotides)		
	adduct 1	adduct 2	total
P450 3A4 + NADPH:P450 reductase	3.6 ± 0.342	0.5 ± 0.1	4.1 ± 0.4
P450 3A4 + NADPH:P450 reductase + cytochrome b_5 (1:5)	10.5 ± 0.5*	0.9 ± 0.1*	11.4 ± 0.8*

[a]Values are given as means ± SD (N = 6). The total relative adduct labeling represents the sum of relative adduct labeling values of adducts 1 and 2. Values significantly different from the control (without cytochrome b_5): *p < 0.001 (Student's t-test).

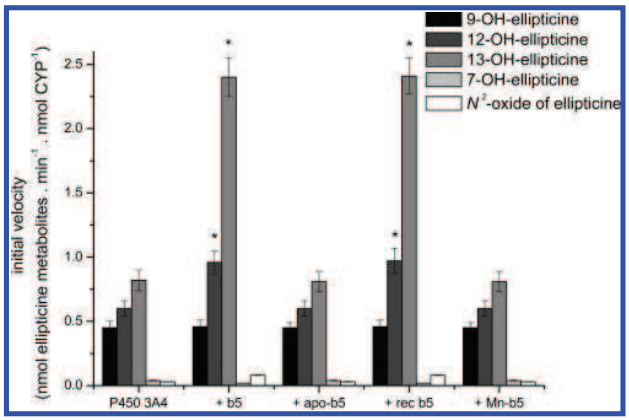

Figure 3. Effect of cytochrome b_5, apo-cytochrome b_5, apo-cytochrome b_5 reconstituted with heme, and Mn-cytochrome b_5 on the initial velocity of ellipticine oxidation to 9-hydroxyellipticine, 12-hydroxyellipticine, 13-hydroxyellipticine, 7-hydroxyellipticine, and ellipticine N^2-oxide by P450 3A4 in the presence of NADPH. Assays were performed as described under Experimental Procedures. Average values ± SD are shown (N = 3). Values significantly different from control (without cytochrome b_5); *p < 0.001 (Student's t-test).

oxidation of ellipticine was significantly changed only by holo-cytochrome b_5 or apo-cytochrome b_5 reconstituted with heme, while apo-cytochrome b_5 without the heme cofactor was without such effects (Figure 3 and Supporting Information, Table 2). We also employed a structurally similar analogue of cytochrome b_5, known to have limited electron transfer capability, Mn-cytochrome b_5.[37,54] The apo-cytochrome b_5 reconstituted with Mn-protoporphyrin IX should adopt the same 3D conformation as the native cytochrome b_5, but it lacks electron transfer capability.[22,54] Also in the case of Mn-cytochrome b_5, no changes in ellipticine oxidation were found (Figure 3 and Supporting Information, Table 2).

Modulation of Levels of DNA Adducts Formed by 13-Hydroxyellipticine by SULT and NAT Enzymes. Formation of the deoxyguanosine adduct generated from 13-hydroxyellipticine with DNA *in vitro* is pH-dependent; only low levels of this DNA adduct were detectable at pH 5.0, while increasing the pH resulted in a pronounced increase in the formation of this adduct (Table 2). Exposure of 13-hydroxyellipticine to either SULT or NAT enzymes in the presence of cofactors of these enzymes (PAPS, acetyl-CoA) greatly increases DNA adduction; the amount of 13-hydroxyellipticine-derived DNA adduct increased significantly. The different human SULTs showed vastly differing activities leading up to 68.5-fold more

Table 2. pH Effect on Adduct Levels Formed by Reaction of 13-Hydroxyellipticine with DNA[a], Detected by ^{32}P-Postlabeling[b]

pH	relative adduct labeling (mean ± SD/10^7 nucleotides)
5.0	0.01 ± 0.001
6.0	1.3 ± 0.3
7.0	17.0 ± 1.2
7.4	23.3 ± 2.0
8.0	41.0 ± 2.9
8.4	49.7 ± 3.2

[a]See adduct spot 1 in Figure 1. [b]Experimental conditions are as described in Experimental Procedures, except that 50 μM 13-hydroxyellipticine and 1 mg of calf thymus DNA (37 °C, 90 min) were used. Relative adduct labeling and standard deviations were obtained from triplicate determinations.

DNA adducts catalyzed by SULT1A3 than without a SULT enzyme (Figure 4). In contrast, 13-hydroxyellipticine seems not

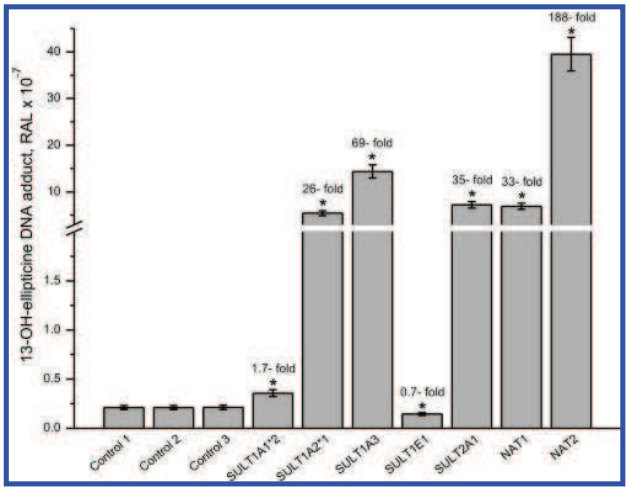

Figure 4. Effect of SULTs and NATs on DNA adduct formation by 13-hydroxyellipticine. Mean values ± standard deviations shown in the figure represent results obtained from three parallel incubations (N = 3). Controls 1, 2, and 3 represent the incubation without enzymes (control 1), the incubation with SULT1A3 without PAPS (control 2), and that with NAT2 without acetyl-CoA (control 3). Numbers above bars are fold increases over the control. Values significantly different from the control (without conjugation enzymes): *p < 0.001 (Student's t-test).

to be a substrate of SULT2E1 because this SULT did not stimulate the formation of the DNA adduct. NAT2 was by far the most active conjugation enzyme leading to 188-fold higher DNA adduct levels, while NAT1 increased these 33-fold. No increase in levels of the DNA adduct was found when enzyme cofactors PAPS or acetyl-CoA were not present in incubations (Figure 4), indicating that formation of the sulfate and acetate esters (conjugates) is responsible for the increase in levels of the 13-hydroxyellipticine-derived DNA adduct. In addition, these results suggest that sulfate and acetate esters of 13-hydroxyellipticine are more potent proximate mutagens than 13-hydroxyellipticine itself. This might be due to easier heterolytic dissociation of the conjugates in comparison to the heterolysis of parental 13-hydroxyellipticine.

Calculation of Heterolytic Cleavage of 12-Hydroxy- and 13-Hydroxyellipticine and Their Sulfate or Acetate

dx.doi.org/10.1021/tx3000335 | Chem. Res. Toxicol. 2012, 25, 1075–1085

Conjugates: Thermodynamic Approaches. First, the viability of heterolytic dissociation of 12-hydroxy- and 13-hydroxyellipticine was compared using quantum chemical calculations and three different approaches to solvation modeling. For these reactions, we initially considered two paths leading directly to ellipticine-12-ylium and ellipticine-13-ylium, paths A and B in Scheme 2, and one indirect path, denoted as path C in Scheme 2. This paths leads to the formation of 6,12-didehydroellipticine and 6,13-didehydroellipticine that represent deprotonated forms of ellipticine-12/13-ylium species. Regardless of the path, results indicated significantly higher susceptibility of 13-hydroxyellipticine toward heterolytic dissociation in comparison to 12-hydroxyellipticine (see difference in reaction free energies $\Delta\Delta G^{0\prime}_{\mathrm{rea}\ 12-13\mathrm{OH}}$ shown in Table 3). The major portion of the difference comes from the lower free energy (higher stability) of ellipticine-13-ylium over ellipticine-12-ylium, −10 and −12 kcal/mol for C-PCM and LD solvation models, respectively.

Scheme 2. Proposed Paths of Heterolytic Cleavage of 12/13-Hydroxyellipticine and Their Sulfate and Acetate Conjugates That Were Considered in the Theoretical Section

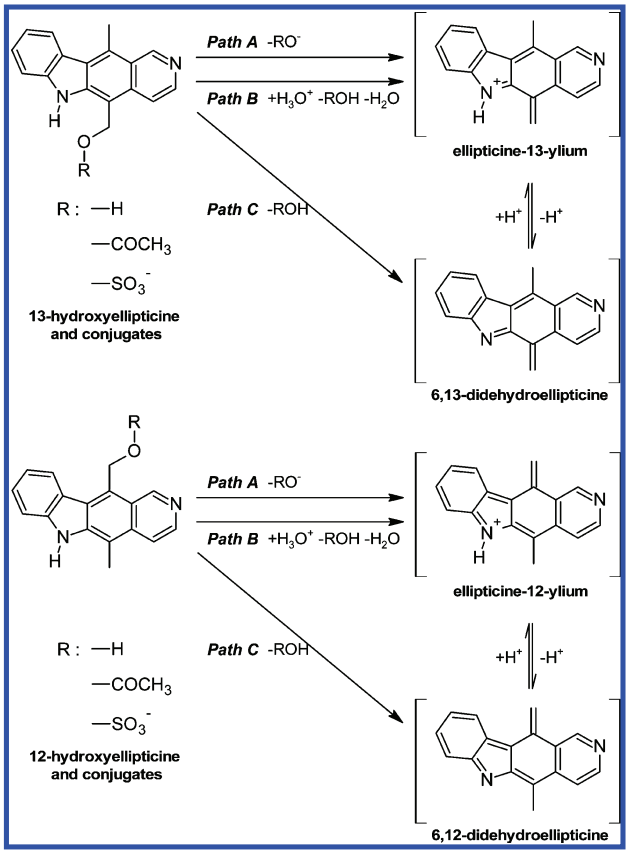

Paths A and B should in theory, after correction to pH 7, predict identical reaction free energies. They, however, vary significantly, although the discrepancy decreases when the solvation model is improved. We considered the average over paths A and B to make the best estimate of the actual reaction energy within estimated error (Table 3). The major error probably comes from the absence of electron correlation effects and from inaccuracies in the prediction of solvation free energies of charged species participating in these reactions: H_3O^+, OH^-, ellipticine-12-ylium, and ellipticine-13-ylium ions.

Reaction path C that represents the formation of 6,12- and 6,13-didehydroellipticines does not involve charged species. Thus, the absolute free energies of these reactions are almost independent of the solvation model (column *C* in Table 3). The small positive reaction free energy (5.9−9.3 kcal/mol) indicates that low amounts of the 6,13-didehydroellipticine metabolite in the incubation mixture are expected (0.01−0.0001% of 13-hydroxyellipticine), while the formation of 6,12-didehydroellipticine is not favored due to the high positive reaction free energy of its formation, 24−28 kcal/mol.

The results also support the generally accepted concept that proton-mediated hydrolysis of these compounds is the major mechanism leading to ellipticine-12-ylium and ellipticine-13-ylium (Scheme 2). The oxonium ion destabilizes the bond between carbon 12 or 13 and oxygen of the hydroxyl group, and two molecules of water (from the oxonium ion and the hydroxyl group) are formed. These findings indicate a preferential hydrolysis of 12-hydroxy- and 13-hydroxyellipticine under acidic conditions.

While 7-fold higher levels of adduct 1 than adduct 2 are formed by the P450 3A4 from ellipticine, levels of 13-hydroxyellipticine forming adduct 1 are only 1.3-fold higher than those of 12-hydroxyellipticine generating adduct 2 (Figure 1 and Supporting Information, Table 1). Several reasons might be responsible for the different potency of 13-hydroxyellipticine and 12-hydroxyellipticine to form DNA adducts. The dissociation (hydrolysis) of both hydroxyellipticines to the cationic yllium might be one of the reasons (Scheme 1). Indeed, as shown in Table 3, showing differences in standard reaction free energies calculated by quantum chemical approach, hydrolysis of 13-hydroxyellipticine is more favorable than that of 12-hydroxyellipticine.

In addition, the experimental data showed that reactions of 13-hydroxyellipticine with either PAPS or acetyl-CoA catalyzed by several SULTs or NATs enhanced DNA adduct 1 levels. Calculated reaction free energies of heterolysis of the sulfate

Table 3. Reaction Free Energies of Heterolytic Dissociation of 12-Hydroxy- and 13-Hydroxyellipticine Calculated by *ab Initio* Quantum Chemical Approaches in Combination with Different Solvation Models

solvation model	C-PCM		LD (ChemSol)		LD with exp. solv. for H_2O, H_3O^+ and OH^-	
reaction path (Scheme 2)	A and B average ± error	*C*	A and B average ± error	*C*	A and B average ± error	*C*
$\Delta G^{0\prime}_{\mathrm{rea}\ 12\mathrm{OH}}$ [a]	21 ± 40	26	9 ± 11	25	22 ± 3	28
$\Delta G^{0\prime}_{\mathrm{rea}\ 13\mathrm{OH}}$ [a]	10 ± 40	7.1	−5 ± 11	5.9	8 ± 3	9.3
$\Delta\Delta G^{0\prime}_{\mathrm{rea}\ 12-13\mathrm{OH}}$	11	19	14	19	14	19
$\Delta pK'_{\mathrm{eq}\ 12-13\mathrm{OH}}$ [b]	8	14	10	14	10	14

[a]Standard biochemical reaction free energies in kcal/mol. [b]Difference in equilibrium constants (12-OH- minus 13-OH-ellipticine).

dx.doi.org/10.1021/tx3000335 | *Chem. Res. Toxicol.* 2012, 25, 1075−1085

Table 4. Comparison of Reaction Free Energies of Heterolytic Dissociation of 12/13-Hydroxyellipticine, 12/13-Hydroxyellipticine Sulfate, and Acetate Conjugates Calculated by *ab Initio* Quantum Chemical Approaches in Combination with Different Solvation Models [13-Hydroxyellipticine and Its Esters (A), and 12-Hydroxyellipticine and Its Esters (B)]

(A)

solvation model	*C-PCM*		LD (ChemSol)		LD with exp. solv. for H_2O, H_3O^+ and OH^-	
reaction path (Scheme 2)	A and B average ± error	*C*	A and B average ± error	*C*	A and B average ± error	*C*
$\Delta G^{0\prime}_{rea\ 13OH}$ [a]	9.7 ± 40	7.1	−5.0 ± 11	5.9	8 ± 3	9.3
$\Delta G^{0\prime a}_{rea\ 13OSO_3^-}$	−3.8 ± 30	−1.9	−16 ± 5	−1.3	−9 ± 6	−1.3
$\Delta G^{0\prime a}_{rea\ 13OAc}$	−0.5 ± 30	3.7	−15 ± 3	1.1	−8 ± 8	1.1

(B)

solvation model	C-PCM		LD (ChemSol)		LD with exp. solv. for H_2O, H_3O^+ and OH^-	
reaction path (Scheme 2)	A and B average ± error	*C*	A and B average ± error	*C*	A and B average ± error	*C*
$\Delta G^{0\prime a}_{rea\ 12OH}$	21 ± 40	26	9 ± 11	25	22 ± 3	29
$\Delta G^{0\prime}_{rea\ 12OSO_3^-}$ [a]	4.4 ± 30	16	−1.1 ± 5	21	6.5 ± 6	21
$\Delta G^{0\prime}_{rea\ 12OAc}$ [a]	−8.8 ± 30	21	−4.2 ± 3	19	3.4 ± 8	19

[a] Standard biochemical reaction free energies in kcal/mol.

and acetate esters that should be formed during these reactions are by 11−17 kcal/mol more favorable than for hydrolysis of 13-hydroxyellipticine (Table 4A). Therefore, while only a small portion of 13-hydroxyellipticine could be present in the form of ellipticine-13-ylium at pH 7, the negative free energy of heterolysis indicates that under the equilibrium conditions at pH 7 the major portion of sulfate or acetate esters (more than 99%) is dissociated to ellipticine-13-ylium that forms the DNA adduct. This is consistent with the experimental finding that whereas high levels of the 13-hydroxyellipticine-derived DNA adduct were found in experimental animals exposed to ellipticine,[3,8,12,13] no 13-hydroxyellipticine sulfates and acetate conjugates were detected in these animals.[55,56]

Reaction free energies calculated for elimination (path C) of the sulfate and acetate esters are predicted to be 7−10 and 5−8 kcal/mol, respectively, lower than that of the OH group, indicating that a significant portion (10 to 90%) of these conjugates could be present as 6,13-didehydroellipticine. Although path C is less preferred at pH 7, it is virtually pH independent and could contribute to DNA adduct formation under alkaline conditions.

Heterolytic dissociation of the 12-hydroxyellipticine sulfate or acetate esters is favored by 10−30 kcal/mol in comparison to their parental compound 12-hydroxyellipticine (Table 4B). Therefore, while heterolysis of 12-hydroxyellipticine is unfavored, the dissociation of its conjugates is feasible. Free energy for the corresponding hydrolytic reaction is predicted to be around zero, indicating the presence of significant amounts of the reactive species (ellipticine-12-ylium) (Table 4B). The 12-hydroxyellipticine sulfate and acetate conjugates are, however, less prone to hydrolysis (represented by paths A and B) than 13-hydroxyellipticine conjugates, with differences ranging from 8−16 kcal/mol.

Free energy for the formation of 6,12-didehydroellipticine from the 12-hydroxyellipticine sulfate and acetate esters, reaction path C, is predicted to be unfavored (16−21 kcal/mol, Table 4B), indicating the absence of 6,12-didehydroellipticine under the conditions considered here.

DISCUSSION

The results of the present work show that P450 3A4 preferentially oxidizes ellipticine to 13-hydroxy- and 12-hydroxyellipticine, the metabolites responsible for the formation of DNA adducts.[10,11] In this study, we suggest three possible reaction paths leading to the formation of the reactive species from these metabolites; direct heterolytic dissociation (hydrolysis), heterolytic dissociation (hydrolysis) after attack by the oxonium ion; and formation of 6,12- and 6,13-didehydroellipticines (see reaction paths A−C in Scheme 2). The oxonium ion-mediated hydrolysis of these compounds is probably the favorable mechanism responsible for the formation of ellipticine-12-ylium and ellipticine-13-ylium (path B in Scheme 2).

If this path were the rate limiting step of DNA adduct formation from 13-hydroxyellipticine, then DNA adduct levels should be higher under acidic conditions. This is not the case since only low levels of this DNA adduct were detectable at pH 5.0, while under alkaline conditions considerably higher amounts of this adduct were formed. Not only the hydrolysis of 13-hydroxyellipticine but also the reactivity of ellipticine-13-ylium toward the amino group of guanine in DNA seems to be important. This finding supports the suggested structure of 13-hydroxyellipticine-mediated deoxyguanosine adduct, where ellipticine-13-ylium is bound to the amino group in position 2 of guanine (Scheme 1). A decrease in pH leads to changes in nucleobase protonation in the DNA chain, causing a decrease in its nucleophilicity, essential for binding of ellipticine-13-ylium.

In the system containing only P450 3A4 with NADPH:P450 reductase, approximately the same levels of 13-hydroxy- and 12-hydroxyellipticine metabolites were found. However, more than 7-fold higher levels of adduct 1 than adduct 2 are formed in this enzymatic system. This finding might be explained by the preference in the dissociation (hydrolysis) of 13-hydroxyellipticine to ellipticine-13-ylium in comparison to that of 12-hydroxyellipticine to ellipticine-12-ylium. The major part of the difference comes from lower (10−12 kcal/mol) free energy of carbo-cation derived from 13-hydroxyellipticine (ellipticine-13-ylium).

The results of this study also demonstrate that the presence of cytochrome b_5 leads to more DNA-adducts, predominantly the adduct with 13-hydroxyellipticine. Therefore, besides the stimulating effect of cytochrome b_5 on P450 1A1-mediated oxidation of ellipticine to 12-hydroxy- and 13-hydroxyellipticine

that was found previously,[19] this heme protein also seems to play a key role in the P450 3A4-mediated DNA-damage caused by ellipticine. In both cases, addition of cytochrome b_5 to the P450s shifts ellipticine oxidation to activation at the expense of detoxication. To further confirm these *in vitro* results, a cytochrome b_5-knockout cell model is planned to be used to analyze the oxidation products of ellipticine and ellipticine-derived DNA adducts.

The effect of cytochrome b_5 upon ellipticine activation may be even more pronounced *in vivo* because as we found previously,[19] ellipticine induces levels of cytochrome b_5 in the liver of rats treated with this drug. Moreover, ellipticine also induces expression of *P450 3A4* mRNA and P450 3A4 protein in several cancer cell lines,[17,21] and as a ligand of aryl hydrocarbon receptor,[57] it also induces P450 1A1/2,[17,20−22] the enzyme that in the presence of cytochrome b_5 also activates ellipticine.[19] Hence, all these ellipticine-mediated induction effects produce concerted regulatory effects of this drug on its own metabolism. To quantify the involvement of cytochrome b_5 in ellipticine metabolism *in vivo*, we plan to use cytochrome b_5-knockout mice.[58,59]

Generally, two mechanisms of cytochrome b_5-mediated modulation of P450 catalysis have been suggested by several authors; it can affect the P450 catalytic activities by donating the second electron to P450 in a P450 catalytic cycle and/or by acting as an allosteric modifier of the oxygenase (for reviews, see refs 23−25 and 60). The mechanism(s) underlying such allosteric effects, based on reports that apo-cytochrome b_5 can stimulate P450 catalysis, remains uncertain. It does seem clear, however, that cytochrome b_5 binding can cause conformational changes to the substrate access channel and binding pocket in the P450 enzyme.[23−25,60−62] The results found in this study show that modulation of ellipticine oxidation by P450 3A4 is induced only by the holo-cytochrome b_5. These findings indicate a high specificity of interaction of P450 3A4 with holo-cytochrome b_5 containing heme, which is necessary not only for electron transfer but also for the natural conformation of the cytochrome b_5 protein. The lack of effect of apo-cytochrome b_5 on P450 3A4 catalysis might hence be the result of not only the loss of the electron transfer activity but may also result from changes in 3D structure of its protein. We described the properties and configurations of cytochrome b_5 and its apo-form extensively in our earlier paper.[19] While the holo-cytochrome b_5 contains four helixes and three loops, forming the heme binding pocket, apo-cytochrome b_5 has only one structural element, a helix of amino acids 39−42 (see Figure 7 in our previous study[19]). This structural change results in significant alterations in surface geometry and electrostatic properties of apo-cytochrome b_5, preventing adequate protein−protein interactions of cytochrome b_5 with P450 3A4. Moreover, no changes in ellipticine oxidation were also produced by cytochrome b_5 containing manganese protoporphyrin IX (Mn-cytochrome b_5), a structural analogue of cytochrome b_5 without electron transfer ability. These findings are similar to the ones with P450 1A1/2, where also the holo-cytochrome b_5 was the only active species, and neither apo-cytochrome b_5 nor the enzyme with Mn-protoporphyrin IX was active. All these results demonstrate that both the natural 3D structure of the cytochrome b_5 protein, dictating optimal conformational states of the P450-cytochrome b_5 complex, and the presence of the protoporphyrin IX bonded-Fe ions as an electron transfer agent are necessary for the observed effects.[19]

Reactions of 13-hydroxyellipticine with either PAPS or acetyl-CoA catalyzed by several SULTs and NAT1 and NAT2 leads to higher 13-hydroellipticine-DNA adduct levels. As follows from calculated reaction free energies of heterolysis of the sulfate and acetate esters of 13-hydroxyellipticine that should be formed during such reactions, this finding might be explained by substantially easier hydrolysis of these esters than 13-hydroxyellipticine itself (compare Table 4A). The human conjugation enzymes used show widely varying substrate specificities. NAT2 was the most active enzyme, while 13-hydroxyellipticine was no substrate for SULT1E1. The amount of protein added to the incubations was always the same, but the specific activities of the individual enzymes varied greatly. This variation of substrate specificity is also reflected with 13-hydroxyellipticine as substrate.

The data shown here, together with our earlier work with reconstituted P450 1A1 and 1A2,[19] emphasize the importance of investigating enzyme complexes in xenobiotic metabolism to evaluate the role of the different components in the balance between activation and detoxication. In addition, as was seen by us and others earlier,[26,28,29,47,48] the role of conjugation enzymes in activation of not only aromatic hydroxylamines but also hydroxylated methyl derivatives of aromatics has to be carefully investigated. Computational chemistry in conjunction with detailed experiments is a very valuable tool to determine thermodynamic equilibriums to explain differences in reactivity also in biological systems.

■ ASSOCIATED CONTENT

Ⓢ Supporting Information

Effect of cytochrome b_5 on initial velocity of ellipticine oxidation and effect of cytochrome b_5, apo-cytochrome b_5, apo-cytochrome b_5 reconstituted with heme and Mn-cytochrome b_5 on initial velocity of ellipticine oxidation. This material is available free of charge via the Internet at http://pubs.acs.org.

■ AUTHOR INFORMATION

Corresponding Author

*Tel: +420 221951285. Fax: +420 221951283. E-mail: stiborov@natur.cuni.cz.

Funding

This work was supported by the Grant Agency of the Czech Republic (grants P301/10/0356 and 203/09/0812) and Charles University in Prague (grant UNCE #42). The access to the MetaCentrum computing facilities provided under the program LM2010005 funded by the Ministry of Education of the Czech Republic is highly appreciated.

Notes

The authors declare no competing financial interest.

■ ACKNOWLEDGMENTS

V.M. thanks Professor Jan Florian (Loyola University Chicago, Chicago, USA) for introducing him to the field of computational chemistry.

■ DEDICATION

This work is dedicated to Professor Gustav Entlicher on the occasion of his 70th birthday.

■ ABBREVIATIONS

HPLC, high-performance liquid chromatography; i.p., intraperitoneal; P450, cytochrome P450; PAPS, 3′-phosphoadenosine-5′-phosphosulfate; PEI-cellulose, polyethylenimine-cellulose; RAL, relative adduct labeling; r.t., retention time; TLC, thin layer chromatography

■ REFERENCES

(1) Stiborová, M., Bieler, C. A., Wiessler, M., and Frei, E. (2001) The anticancer agent ellipticine on activation by cytochrome P450 forms covalent DNA adducts. *Biochem. Pharmacol. 62*, 1675−84.

(2) Stiborová, M., Rupertová, M., Schmeiser, H. H., and Frei, E. (2006) Molecular mechanism of antineoplastic action of an anticancer drug ellipticine. *Biomed. Pap. Med. Fac. Univ. Palacky Olomouc Czech Repub. 150*, 13−23.

(3) Stiborová, M., Rupertová, M., and Frei, E. (2011) Cytochrome P450- and peroxidase-mediated oxidation of anticancer alkaloid ellipticine dictates its anti-tumor efficiency. *Biochim. Biophys. Acta 1814*, 175−185.

(4) Auclair, C. (1987) Multimodal action of antitumor agents on DNA: The ellipticine series. *Arch. Biochem. Biophys. 259*, 1−14.

(5) Garbett, N. C., and Graves, D. E. (2004) Extenting nature's leads: the anticancer agent ellipticine. *Curr. Med. Chem. Anti-Cancer Agents 4*, 149−172.

(6) Fossé, P., René, B., Charra, M., Paoletti, C., and Saucier, J. M. (1992) Stimulation of topoisomerase II-mediated DNA cleavage by ellipticine derivatives: structure-activity relationships. *Mol. Pharmacol. 42*, 590−595.

(7) Froelich-Ammon, S. J., Patchan, M. W., Osheroff, N., and Thompson, R. B. (1995) Topoisomerase II binds to ellipticine in the absence or presence of DNA. Characterization of enzyme-drug interactions by fluorescence spectroscopy. *J. Biol. Chem. 270*, 14998−5004.

(8) Stiborová, M., Breuer, A., Aimová, D., Stiborová-Rupertová, M., Wiessler, M., and Frei, E. (2003) DNA adduct formation by the anticancer drug ellipticine in rats determined by ^{32}P-postlabeling. *Int. J. Cancer 107*, 885−890.

(9) Stiborová, M., Stiborová-Rupertová, M., Bořek-Dohalská, L., Wiessler, M., and Frei, E. (2003) Rat microsomes activating the anticancer drug ellipticine to species covalently binding to deoxyguanosine in DNA are a suitable model mimicking ellipticine bioactivation in humans. *Chem. Res. Toxicol. 16*, 38−47.

(10) Stiborová, M., Sejbal, J., Bořek-Dohalská, L., Aimová, D., Poljaková, J., Forsterová, K., Rupertová, M., Wiesner, J., Hudeček, J., Wiessler, M., and Frei, E. (2004) The anticancer drug ellipticine forms covalent DNA adducts, mediated by human cytochromes P450, through metabolism to 13-hydroxyellipticine and ellipticine N^2-oxide. *Cancer Res. 64*, 8374−8380.

(11) Stiborová, M., Poljaková, J.., Ryšlavá, H., Dračínský, M., Eckschlager, T., and Frei, E. (2007) Mammalian peroxidases activate anticancer drug ellipticine to intermediates forming deoxyguanosine adducts in DNA identical to those found *in vivo* and generated from 12-hydroxyellipticine and 13-hydroxyellipticine. *Int. J. Cancer 120*, 243−251.

(12) Stiborová, M., Rupertová, M., Aimová, D., Ryšlavá, H., and Frei, E. (2007) Formation and persistence of DNA adducts of anticancer drug ellipticine in rats. *Toxicology 236*, 50−60.

(13) Stiborová, M., Arlt, V. M., Henderson, C. J., Wolf, C. R., Kotrbová, V., Moserová, M., Hudeček, J., Phillips, D. H., and Frei, E. (2008) Role of hepatic cytochromes P450 in bioactivation of the anticancer drug ellipticine: studies with the hepatic NADPH:cytochrome P450 reductase null mouse. *Toxicol. Appl. Pharmacol. 226*, 318−327.

(14) Bořek-Dohalská, L., Frei, E., and Stiborová, M. (2004) DNA adduct formation by the anticancer drug ellipticine and its hydroxy derivatives in human breast adenocarcinoma MCF-7 cells. *Collect. Czech. Chem. Commun. 69*, 603−615.

(15) Poljaková, J., Frei, E., Gomez, J. E., Aimová, D., Eckschlager, T., Hraběta, J., and Stiborová, M. (2007) DNA adduct formation by the anticancer drug ellipticine in human leukemia HL-60 and CCRF-CEM cells. *Cancer Lett. 252*, 270−279.

(16) Poljaková, J., Eckschlager, T., Hraběta, J., Hřebačková, J., Smutný, S., Frei, E., Martínek, V., Kizek, R., and Stiborová, M. (2009) The mechanism of cytotoxicity and DNA adduct formation by the anticancer drug ellipticine in human neuroblastoma cells. *Biochem. Pharmacol. 77*, 1466−1479.

(17) Martínková, E., Dontenwill, M., Frei, E., and Stiborová, M. (2009) Cytotoxicity of and DNA adduct formation by ellipticine in human U87MG glioblastoma cancer cells. *Neuro Endocrinol. Lett . 30* (Suppl. 1), 60−66.

(18) Kotrbová, V., Aimová, D., Březinová, A., Janouchová, K., Poljaková, J., Hodek, P., Frei, E., and Stiborová, M. (2006) Cytochromes P450 reconstituted with NADPH:P450 reductase mimic the activating and detoxicating metabolism of the anticancer drug ellipticine in microsomes. *Neuro Endocrinol. Lett. 27* (Suppl. 2), 18−20.

(19) Kotrbová, V., Mrázová, B., Moserová, M., Martínek, V., Hodek, P., Hudeček, J., Frei, E., and Stiborová, M. (2011) Cytochrome b_5 shifts oxidation of the anticancer drug ellipticine by cytochromes P450 1A1 and 1A2 from its detoxication to activation, thereby modulating its pharmacological efficacy. *Biochem. Pharmacol. 82*, 669−680.

(20) Aimová, D., Svobodová, L., Kotrbová, V., Mrazová, B., Hodek, P., Hudeček, J., Vaclavikova, R., Frei, E., and Stiborová, M. (2007) The anticancer drug ellipticine is a potent inducer of rat cytochromes P450 1A1 and 1A2, thereby modulating its own metabolism. *Drug Metab. Dispos. 35*, 1926−1934.

(21) Martinkova, E., Maglott, A., Leger, D. Y., Bonnet, D., Stiborova, M., Takeda, K., Martin, S., and Dontenwill, M. (2010) alpha5beta1 integrin antagonists reduce chemotherapy-induced premature senescence and facilitate apoptosis in human glioblastoma cells. *Int. J. Cancer 127*, 1240−1248.

(22) Poljakova, J., Hrebackova, J., Dvorakova, M., Moserova, M., Eckschlager, T., Hrabeta, J., Göttlicherova, M., Kopečkova, B., Frei, E., Kizek, R., and Stiborova, M. (2011) Anticancer agent ellipticine combined with histone deacetylase inhibitors, valproic acid and trichostatin A, is an effective DNA damage strategy in human neuroblastoma. *Neuro Endocrinol. Lett. 32* (Suppl 1), 101−116.

(23) Schenkman, J. B. Jansson, I. The many roles of cytochrome b_5. *Pharmacol. Ther. 9*, 139-152.

(24) Yamazaki, H., Gillam, E. M., Dong, M. S., Johnson, W. W., Guengerich, F. P., and Shimada, T. (1997) Reconstitution of recombinant cytochrome P450 2C10(2C9) and comparison with cytochrome P450 3A4 and other forms: effects of cytochrome P450-P450 and cytochrome P450-b_5 interactions. *Arch. Biochem. Biophys. 342*, 329−337.

(25) Yamazaki, H., Shimada, T., Martin, M. V., and Guengerich, F. P. (2001) Stimulation of cytochrome P450 reactions by apo-cytochrome b_5: evidence against transfer of heme from cytochrome P450 3A4 to apo-cytochrome b_5 or heme oxygenase. *J. Biol. Chem. 276*, 30885−30891.

(26) Glatt, H., Boeing, H., Engelke, C. E., Ma, L., Kuhlow, A., Pabel, U., Pomplun, D., Teubner, W., and Meinl, W. (2001) Human cytosolic sulphotransferases: genetics, characteristics, toxicological aspects. *Mutat. Res. 482*, 27−40.

(27) Aust, S., Obrist, P., Klimpfinger, M., Tucek, G., Jäger, W., and Thalhammer, T. (2005) Altered expression of the hormone- and xenobiotic-metabolizing sulfotransferase enzymes 1A2 and 1C1 in malignant breast tissue. *Int. J. Oncol. 26*, 1079−1085.

(28) Lin, S. S., Chung, J. G., Lin, J. P., Chuang, J. Y., Chang, W. C., Wu, J. Y., and Tyan, Y. S. (2005) Berberine inhibits arylamine *N*-acetyltransferase activity and gene expression in mouse leukemia L 1210 cells. *Phytomedicine 12*, 351−358.

(29) Sim, E., Westwood, I., and Fullam, E. (2007) Arylamine *N*-acetyltransferases. *Expert Opin. Drug Metab. Toxicol. 3*, 169−184.

(30) Butcher, N. J., Tetlow, N. L., Cheung, C., Broadhurst, G. M., and Minchin, R. F. (2007) Induction of human arylamine *N*-

acetyltransferase type I by androgens in human prostate cancer cells. *Cancer Res. 67*, 85−92.
(31) Murias, M., Miksits, M., Aust, S., Spatzenegger, M., Thalhammer, T., Szekeres, T., and Jaeger, W. (2008) Metabolism of resveratrol in breast cancer cell lines: impact of sulfotransferase 1A1 expression on cell growth inhibition. *Cancer Lett. 261*, 172−182.
(32) Meinl, W., Ebert, B., Glatt, H., and Lampen, A. (2008) Sulfotransferase forms expressed in human intestinal Caco-2 and TC7 cells at varying stages of differentiation and role in benzo[a]pyrene metabolism. *Drug Metab. Dispos. 36*, 276−283.
(33) Shu, X. H., Li, H., Sun, X. X., Wang, Q., Sun, Z., Wu, M. L., Chen, X. Y., Li, C., Kong, Q. Y., and Liu, J. (2011) Metabolic patterns and biotransformation activities of resveratrol in human glioblastoma cells: relevance with therapeutic efficacies. *PLoS One 6*, e27484.
(34) Roos, P. H. (1996) Chromatographic separation and behavior of microsomal cytochrome P450 and cytochrome b_5. *J. Chromatogr., B 684*, 107−131.
(35) Kotrbová, V., Aimová, D., Ingr, M., Bořek-Dohalská, L., Martínek, V., and Stiborová, M. (2009) Preparation of a biologically active apo-cytochrome b_5 *via* heterologous expression in *Escherichia coli*. *Protein Expression Purif. 66*, 203−209.
(36) Mulrooney, S. B., and Waskell, L. (2000) High-level expression in *Escherichia coli* and purification of the membrane-bound form of cytochrome b_5. *Protein Expression Purif. 19*, 173−178.
(37) Zhang, H., Hamdane, D., Im, S. C., and Waskell, L. (2008) Cytochrome b_5 inhibits electron transfer from NADPH-cytochrome P450 reductase to ferric cytochrome P450 2B4. *J. Biol. Chem. 283*, 5217−5225.
(38) Strittmatter, P., and Velick, S. F. (1956) The isolation and properties of microsomal cytochrome. *J. Biol. Chem. 221*, 253−264.
(39) Estabrook, R. W., and Werringloer, J. (1978) The measurement of difference spectra: application to the cytochromes of microsomes. *Methods Enzymol. 52*, 212−220.
(40) Gruenke, L. D., Sun, J., Loehr, T. M., and Waskell, L. (1997) Resonance Raman spectral properties and stability of manganese protoporphyrin IX cytochrome b_5. *Biochemistry 36*, 7114−7125.
(41) Stiborová, M., Bořek-Dohalská, L., Aimová, D., Kotrbová, V., Kukacková, K., Janouchová, K., Rupertová, M., Ryšlavá, H., Hudeček, J., and Frei, E. (2006) Oxidation pattern of the anticancer drug ellipticine by hepatic microsomes − Similarity between human and rat systems. *Gen. Physiol. Biophys. 25*, 245−621.
(42) Frisch, M. J., Trucks, G. W., Schlegel, H. B., Scuseria, G. E., Robb, M. A., Cheeseman, J. R., Scalmani, G., Barone, V., Mennucci, B., Petersson, G. A., Nakatsuji, H., Caricato, M., Li, X., Hratchian, H. P., Izmaylov, A. F., Bloino, J., Zheng, G., Sonnenberg, J. L., Hada, M., Ehara, M., Toyota, K., Fukuda, K., Hasegawa, J., Ishida, M., Nakajima, T., Honda, Y., Kitao, O., Nakai, H., Vreven, T., Montgomery, J. A., Jr., Peralta, J. E., Ogliaro, F., Bearpark, M., Heyd, J. J., Brothers, E., Kudin, K. N., Staroverov, V. N., Kobayashi, R., Normand, J., Raghavachari, K., Rendell, A., Burant, J. C., Iyengar, S. S., Tomasi, J., Cossi, M., Rega, N., Millam, J. M., Klene, M., Knox, J. E., Cross, J. B., Bakken, V., Adamo, C., Jaramillo, J., Gomperts, R., Stratmann, R. E., Yazyev, O., Austin, A. J., Cammi, R., Pomelli, C., Ochterski, J. W., Martin, R. L., Morokuma, K., Zakrzewski, V. G., Voth, G. A., Salvador, P., Dannenberg, J. J., Dapprich, S., Daniels, A. D., Farkas, O., Foresman, J. B., Ortiz, J. V., Cioslowski, J., and Fox, D. J. (2009) *Gaussian 09*, Gaussian, Inc., Wallingford, CT.
(43) Cossi, M., Rega, N., and Scalmani, G. (2003) Energies, structures, and electronic properties of molecules in solution with the C-PCM solvation model. *J. Comput. Chem. 24*, 669−681.
(44) Camaioni, D. M., and Schwerdtfeger, C. A. (2005) Comment on "accurate experimental values for the free energies of hydration of H+, OH-, and H3O+. *J. Phys. Chem. A 109*, 10795−10797.
(45) Florian, J., and Warshel, A. (1997) Langevin dipoles model for *ab initio* calculations of chemical processes in solution: Parametrization and application to hydration free energies of neutral and ionic solutes and conformational analysis in aqueous solution. *J. Phys. Chem. B 101*, 5583−5595.
(46) Florian, J., and Warshel, A. (1999) Calculations of hydration entropies of hydrophobic, polar, and ionic solutes in the framework of the Langevin dipoles solvation model. *J. Phys. Chem. B 103*, 10282−10288.
(47) Stiborová, M., Martínek, V., Svobodová, M., Šístková, J., Dvorák, Z., Ulrichová, J., Šimánek, V., Frei, E., Schmeiser, H. H., Phillips, D. H., and Arlt, V .M. (2010) Mechanisms of the different DNA adduct forming potentials of the urban air pollutants 2-nitrobenzanthrone and carcinogenic 3-nitrobenzanthrone. *Chem. Res. Toxicol. 23*, 1192−1201.
(48) Stiborová, M., Mareš, J., Frei, E., Arlt, V. M., Martínek, V., and Schmeiser, H. H. (2011) The human carcinogen aristolochic acid I is activated to form DNA adducts by human NAD(P)H:quinone oxidoreductase without the contribution of acetyltransferases or sulfotransferases. *Environ. Mol. Mutagen. 52*, 448−459.
(49) Bren, U., Guengerich, F. P., and Mavri, J. (2007) Guanine alkylation by the potent carcinogen Aflatoxin B1: quantum chemical calculations. *Chem. Res. Toxicol. 20*, 1134−1140.
(50) Bren, U., Zupan, M., Guengerich, F. P., and Mavri, J. (2006) Chemical eeactivity as a tool to study carcinogenicity: reaction between chloroethylene oxide and guanine. *J. Org. Chem. 71*, 4078−4084.
(51) Galeša, K., Bren, U., Kranjc, A., and Mavri, J. (2008) Carcinogenicity of acrylamide: A computational study. *J. Agric. Food Chem. 56*, 8720−8727.
(52) Liptak, M. D., and Shields, G. C. (2001) Accurate pKa calculations for carboxylic acids using complete basis set and Gaussian-n models combined with CPCM continuum solvation methods. *J. Am. Chem. Soc. 123*, 7314−7319.
(53) Moserová, M., Kotrbová, V., Rupertová, M., Naiman, K., Hudeček, J., Hodek, P, Frei, E., and Stiborová, M. (2008) Isolation and partial characterization of the adduct formed by 13-hydroxyellipticine with deoxyguanosine in DNA. *Neuro Endocrinol. Lett. 29*, 728−732.
(54) Zhang, H., Im, S. C., and Waskell, L. (2007) Cytochrome b_5 increases the rate of product formation by cytochrome P450 2B4 and competes with cytochrome P450 reductase for a binding site on cytochrome P450 2B4. *J. Biol. Chem. 282*, 29766−19776.
(55) Chadwick, M., Silveira, D. M., Platz, B. R., and Hayes, D. (1978) Comparative physiological disposition of ellipticine in several animal species after intravenous administration. *Drug Metab. Dispos. 6*, 528−541.
(56) Branfam, A. R., Bruni, R J., Reihold, V. N., Silveira, D. M., Chadwick, M., and Yesair, D. W. (1978) Characterization of metabolites of ellipticine in rat bile. *Drug Metab. Dispos. 6*, 542−548.
(57) Gasiewicz, T. A., Kende, R. S., Rucci, G., Whitney, B., and Willey, J. J. (1996) Analysis of structural requirements for Ah receptor antagonist activity: Ellipticines, flavones, and related compounds. *Biochem. Pharmacol. 52*, 787−830.
(58) Finn, R. D., McLaughlin, L. A., Ronseaux, S., Rosewell, I., Houston, J. B., Henderson, C. J., and Wolf, C. R. (2008) Defining the *in vivo* role for cytochrome b_5 in cytochrome P450 function through the conditional hepatic deletion of microsomal cytochrome b_5. *J. Biol. Chem. 283*, 31385−31393.
(59) McLaughin, L. A., Ronseaux, S., Finn, R. D., Henderson, C. J., and Wolf, C. R. (2010) Deletion of microsomal cytochrome b_5 profoundly affects hepatic and extrahepatic drug metabolism. *Mol. Pharmacol. 75*, 269−278.
(60) Zhang, H., Myshkin, E., and Waskell, L. (2005) Role of cytochrome b_5 in catalysis by cytochrome P450 2B4. *Biochem. Biophys. Res. Commun. 338*, 499−506.
(61) Porter, T. D. (2002) The roles of cytochrome b_5 in cytochrome P450 reactions. *J. Biochem. Mol. Toxicol. 16*, 311−316.
(62) Loughran, P. A., Roman, L. J., Miller, R. T., and Masters, B. S. (2001) The kinetic and spectral characterization of the *E. coli*-expressed mammalian CYP4A7: cytochrome b_5 effects vary with substrate. *Arch. Biochem. Biophys. 385*, 311−321.
(63) Kizek, R., Adam, V., Hrabeta, J., Eckschlager, T., Smutny, S., Burda, J. V., Frei, E., and Stiborova, M. (2012) Anthracyclines and ellipticines as DNA-damaging anticancer drugs: Recent advances. *Pharmacol. Ther. 133*, 26−39.